



UNIFORMED SERVICES UNIVERSITY OF THE HEALTH SCIENCES

4301 JONES BRIDGE ROAD
BETHESDA, MARYLAND 20814-4799



APPROVAL SHEET

Title of Dissertation: "Characterization of Yeast Aspartic Protease 3 (*A novel basic-residue specific prohormone processing enzyme*)"

Name of Candidate: Niamh X. Cawley
Doctor of Philosophy Degree
16 May 1995

Dissertation and Abstract Approved:

Sue Yun Chung
Committee Chairperson

May 16, 1995
Date

A. M. Hohen
Committee Member

5/16/95
Date

H. P. P. P.
Committee Member

5/16/95
Date

R. M. L. A.
Committee Member

16 May 1995
Date

Michael G. Brown
Committee Member

May 16, 1995
Date

V. H. H. H.
Committee Member

May 18, 1995
Date



UNIFORMED SERVICES UNIVERSITY OF THE HEALTH SCIENCES

4301 JONES BRIDGE ROAD
BETHESDA, MARYLAND 20814-4799



GRADUATE EDUCATION
(301) 295-3913

FINAL EXAMINATION FOR THE DEGREE OF DOCTOR OF PHILOSOPHY

Name of Student: Niamh X. Cawley

Date of Examination: 16 May 1995

Time: 9:00 a.m.

Place: Lecture Room B

DECISION OF EXAMINATION COMMITTEE MEMBERS:

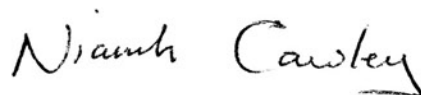
	PASS	FAIL
<u>Su Yun Chung</u> Dr. Su Yun Chung Chairperson	<u>✓</u>	<u> </u>
<u>Y. Peng Loh</u> Dr. Y. Peng Loh Major Advisor	<u>✓</u>	<u> </u>
<u>A. M. Holmes</u> Dr. Andrew M. Holmes Member	<u>✓</u>	<u> </u>
<u>Brian Cox</u> Dr. Brian Cox Member	<u>✓</u>	<u> </u>
<u>Michael Brownstein</u> Dr. Michael Brownstein Member	<u>✓</u>	<u> </u>
<u>Vivian Y.H. Hook</u> Dr. Vivian Y.H. Hook Member	<u>✓</u>	<u> </u>

COPYRIGHT STATEMENT

The author hereby certifies that the use of any copyrighted material in the dissertation entitled:

“Characterization of Yeast Aspartic Protease 3: *A novel basic-residue specific prohormone processing enzyme*”

beyond brief excerpts is with the permission of the copyrighted owner, and will save and hold harmless the Uniformed Services University of the Health Sciences from any damage which may arise from such copyright violations.

A handwritten signature in black ink, reading "Niamh Cawley". The signature is written in a cursive, flowing style.

Niamh X. Cawley

Department of Biochemistry

Uniformed Services University of the Health Sciences

ABSTRACT

Title of Thesis: Characterization of Yeast Aspartic Protease 3: *A novel basic-residue specific prohormone processing enzyme.*

Niamh X. Cawley, Doctor of Philosophy, 1995.

Thesis directed by: Dr. Y. Peng Loh, Ph.D.
Chief, Section on Cellular Neurobiology,
Laboratory of Developmental Neurobiology,
National Institute of Child Health and Human Development,
National Institutes of Health.

and

Professor (Adjunct),
Department of Biochemistry,
Uniformed Services University of the Helath Sciences.

Yeast aspartic protease 3 (YAP3p), was first cloned, based on its ability to correctly process pro- α -mating factor at specific paired-basic residue cleavage sites. The specificity of this aspartic protease for basic residue cleavage sites of prohormones renders it a member of a novel sub-class of aspartic proteases that may be involved in prohormone and proneuropeptide processing in general. YAP3p was first overexpressed, purified and

characterized from the cellular extract of induced yeast. The cellular form of YAP3p was characterized as a ~70kDa glycoprotein and was shown to cleave pro-opiomelanocortin and its fragments at specific paired-basic residue cleavage sites *in vitro*. Deletion of 0.2kb fragment from the 3' end of the *YAP3* cDNA resulted in the expression of a carboxy-terminally truncated protein which had a hydrophobic domain and a putative glycoprophosphatidylinositol membrane anchor removed. This truncated YAP3p was secreted into the growth media, purified and characterized as ~150-180kDa and ~90kDa hyperglycosylated glycoproteins with optimum enzymatic activity between pH 4.0-4.5. Removal of the N-linked sugars from the hyperglycosylated YAP3p by endoglycosidase H resulted in the reduction in size of both forms to a single ~65kDa protein. In comparison to the calculated isoelectric point (pI) of the truncated YAP3p of 4.0, a pI value of ~4.5 was determined experimentally by isoelectric focussing gel electrophoresis. A Q_{10} of 1.95 for YAP3p was calculated when the dependence of YAP3p activity on temperature was determined. Secreted YAP3p was shown to cleave at mono-, paired- and tetra-basic residue cleavage sites of many prohormone substrates. Analysis of the kinetic parameters for the cleavage of these substrates demonstrated that YAP3p preferred paired- versus mono-basic sites, with the most efficient cleavage being at the tetra-basic residue site of ACTH¹⁻³⁹. The inhibitor constant, K_i , of YAP3p for pepstatin A was determined to be ~0.4 μ M. An antibody to YAP3p was generated and characterized and was found to be useful for the analysis of YAP3p in a number of immunoassays. The antibody showed specific YAP3p-like immunoreactivity in mammalian brain and pituitary cells by

immunocytochemistry and specific bands of ~90kDa and ~70kDa in soluble protein extracts of these tissues by western blot analysis.

TITLE

**CHARACTERIZATION OF YEAST ASPARTIC PROTEASE 3: A
NOVEL BASIC-RESIDUE SPECIFIC PROHORMONE
PROCESSING ENZYME.**

by

Niamh X. Cawley

Thesis submitted to the Department of Biochemistry Graduate Program of the
Uniformed Services University of the Health Sciences, in partial fulfillment of the
requirement for the degree of Doctor of Philosophy, 1995.

DEDICATION

To my wife,
Helen,
for her encouragement and patience throughout.

ACKNOWLEDGMENTS

For those of you who know me, I take great personal satisfaction in a job well done. I am very proud to be able to present my work in this thesis. The quality of the work presented here is a testimony to the many people who helped me throughout my graduate years. First and foremost is my advisor, Dr. Peng Loh. You embody all the qualities of a great advisor and good person, I will always be your student and will always cherish your friendship. Secondly, I thank the members of Dr. Loh's laboratory, both past and present which include Dr. Nigel Birch, Ms Winnie Tam, Dr. David Cool, Dr. Ted Friedman and Dr. Le-Ping Pu. It was fun working with you all and sharing both the successes and failures. I would also like to pay tribute to the faculty of the Biochemistry Department at the Uniformed Services University of the Health Sciences. I always felt welcome in a place where good science is taught by visionary scientists.

I am indebted to the National Institute of Child Health and Human Development who gave me the opportunity to work in the Laboratory of Developmental Neurobiology under the guidance of Dr. Loh and who supported me with a pre-Intramural Research Training Award.

TABLE OF CONTENTS

APPROVAL SHEETS	i
COPYRIGHT STATEMENT.....	iii
ABSTRACT.....	iv
TITLE	vii
DEDICATION.....	viii
ACKNOWLEDGMENTS.....	ix
TABLE OF CONTENTS	x
TABLE OF FIGURES	xvi
ABBREVIATIONS	xviii
 CHAPTER 1.....	 xx
GENERAL INTRODUCTION	xx
CELL BIOLOGY	xx
PROHORMONE PROCESSING	xxii
ASPARTIC PROTEASES.....	xxvii
 CHAPTER 2.....	 35
OVEREXPRESSION, PURIFICATION AND CHARACTERIZATION OF CELLULAR YEAST ASPARTIC PROTEASE 3.....	35
INTRODUCTION.....	35
METHODS	36
Purification of cellular YAP3p.....	37
RESULTS	37

CONCLUSION	40
CHAPTER 3.....	41
GENERATION AND CHARACTERIZATION OF ANTISERUM TO YEAST	
ASPARTIC PROTEASE 3.....	41
INTRODUCTION.....	41
METHODS	41
Generation of MW283 Antiserum to YAP3p	41
Immunodepletion of YAP3p activity.....	44
Western blot analysis of cellular YAP3p	46
Radioimmunoassay of YAP3p.....	46
Immunocytochemistry of induced yeast	48
CONCLUSION	51
CHAPTER 4.....	52
CARBOXY TERMINALLY TRUNCATED YAP3p IS SECRETED INTO THE GROWTH MEDIA: CHARACTERIZATION OF SECRETED YEAST	
ASPARTIC PROTEASE 3.....	52
SUMMARY	52
INTRODUCTION.....	53
METHODS	54
Subcellular distribution of full length and truncated YAP3p.....	54
Time course of secretion	56
Phospholipase C treatment of yeast membranes	56
Cleavage of ACTH ¹⁻³⁹ and mouse POMC by secreted YAP3p.....	57
pH and temperature studies of secreted YAP3p activity	58
Calculation of Q ₁₀	58
Western blot analysis of secreted YAP3p	58
Sephadex G-75 gel filtration of secreted YAP3p.....	59
Isoelectric point determination of secreted YAP3p	59
RESULTS	60

Distribution and secretion of YAP3p	60
Release of full length YAP3p from yeast membranes by phospholipase C	63
Cleavage of ACTH ¹⁻³⁹ and mouse POMC by secreted YAP3p.....	63
pH and temperature studies of secreted YAP3p activity	66
Characterization of the physical properties of secreted YAP3p.....	66
DISCUSSION	74
 CHAPTER 5.....	80
 CHARACTERIZATION OF THE ENZYMATIC ACTIVITY OF SECRETED	
YEAST ASPARTIC PROTEASE 3.....	80
 PART 1. PROCESSING OF ANGLERFISH PROSOMATOSTATIN I AND II BY YAP3p80	
SUMMARY	80
INTRODUCTION.....	81
PROCEDURES	81
Preparation of [³⁵ S]Cys labeled anglerfish pro-somatostatin I and II.....	81
Preparation of Yeast Aspartic Protease 3.....	83
Incubation of aPSS-I and aPSS-II with YAP3p and analysis of products.....	83
RESULTS	84
DISCUSSION	86
 PART 2. PROCESSING OF PROHORMONE SUBSTRATES CONTAINING MONO-	
AND/OR PAIRED-BASIC RESIDUE CLEAVAGE SITES BY SECRETED YAP3P	90
SUMMARY	90
INTRODUCTION.....	91
METHODS	91
Prohormone substrates	91
Preparation of Yeast Aspartic Protease 3.....	92
Assay and analysis of products generated by YAP3p.....	92
Cholecystokinin 33	92
Proinsulin, cholecystokinin 13-33, dynorphin A, dynorphin B, amidorphin and ACTH ¹⁻	
³⁹	93
Determination of Km and Vmax.....	93
Determination of kcat	94

RESULTS	95
Proteolytic Processing of Proinsulin by YAP3p	95
Proteolytic Processing of CCK33 by YAP3p	97
Proteolytic Processing of Dynorphin A, Dynorphin B and Amidorphin by YAP3p.....	102
Proteolytic Processing of ACTH ¹⁻³⁹ by YAP3p	103
DISCUSSION	108
 CHAPTER 6.....	115
PURIFICATION OF SECRETED YEAST ASPARTIC PROTEASE 3	115
SUMMARY	115
INTRODUCTION.....	116
PROCEDURES.....	117
YAP3p and Protein assays	117
Yeast enzyme source.....	117
Procedure for the purification of glycosylated YAP3p.....	118
Procedure for the purification of deglycosylated YAP3p	121
N-terminal amino-acid analysis of purified YAP3p.....	123
DISCUSSION	127
 CHAPTER 7.....	133
CHARACTERIZATION OF PURIFIED SECRETED YAP3p	133
SUMMARY	133
PART 1: DETERMINATION OF THE K _i OF YAP3p FOR THE ACTIVE SITE	
INHIBITOR, PEPSTATIN A.	133
Assay of the synthetic substrate, Boc-RVRR-MCA.....	133
Introduction-Method 1	134
Assay procedures.....	135
Calculations: Method 1	135
Introduction-Method 2	136
Assay procedures.....	136
Calculations: Method 2	136

PART 2: ANALYSIS OF THE SPECIFICITY OF PURIFIED YAP3p.....	141
Assay procedures.....	141
DISCUSSION	141
CHAPTER 8.....	143
ANALYSIS OF IMMUNOLOGICALLY RELATED MAMMALIAN	
HOMOLOGUES OF YEAST ASPARTIC PROTEASE 3.....	143
SUMMARY	143
INTRODUCTION.....	144
PROCEDURES	147
Immunocytochemistry on mammalian brain and pituitary sections.....	147
Western blot analysis of mammalian brain and pituitary proteins	148
DISCUSSION	155
CHAPTER 9.....	156
CONCLUSIONS	156
CHAPTER 10.....	159
MATERIALS AND METHODS	159
Concanavalin A chromatography.....	159
Protein desalting and lyophilization.....	159
YAP3p assay procedures.....	160
Polyacrylamide gel electrophoresis	161
Sample preparation.....	161
Preparation of polyacrylamide gels.....	162
Precast polyacrylamide electrophoresis gels.....	162
Protein staining procedures	163
Coomassie blue	163
Silver stain	163
Western blotting procedures	164
Transfer of the proteins.....	164

Antigen detection by Vectastain ABC kit.....	164
Antigen detection by Amersham enhanced chemiluminescence kit.....	165
Immunodepletion/immunoprecipitation	165
Indirect Immunofluorescence of Yeast.....	166
Determination of Km and Vmax	167
Calculations of Km, Vmax, kcat and kcat/Km	168
1. Amidorphin	168
2. ACTH ¹⁻³⁹	169
3. Dynorphin A.....	169
4. Dynorphin B.....	169
5. Proinsulin.....	170
6. CCK13-33.....	170
Protein assay.....	178
Sectioning and indirect immunofluorescence of mouse and bovine tissue	178
PUBLICATIONS.....	180
REFERENCES	183

TABLE OF FIGURES

FIGURE 1. SCHEMATIC DIAGRAM OF FULL LENGTH YAP3P.	xxxiii
FIGURE 2. AMINO ACID SEQUENCE ALIGNMENT OF ASPARTIC PROTEASE ACTIVE SITE TRIADS.	xxxiv
FIGURE 3. SCHEMATIC DIAGRAM OF BOVINE PRO-OPIOMELANOCORTIN.	39
FIGURE 4. PURIFICATION OF THE MALTOSE BINDING PROTEIN-YEAST ASPARTIC PROTEASE 3 FUSION PROTEIN (MBP-YAP3P).	43
FIGURE 5. IMMUNODEPLETION OF YAP3P ACTIVITY.	45
FIGURE 6. WESTERN BLOT ANALYSIS OF PURIFIED CELLULAR YAP3P.	47
FIGURE 7. YAP3P RADIOIMMUNOASSAY.	49
FIGURE 8. IMMUNOCYTOCHEMISTRY OF INDUCED YEAST EXPRESSING YAP3P.	50
FIGURE 9. SCHEMATIC DIAGRAM OF FULL LENGTH (A) AND C-TERMINALLY TRUNCATED YAP3P (B) PROTEIN.	55
FIGURE 10. DISTRIBUTION AND SECRETION TIME COURSE OF FULL LENGTH AND TRUNCATED YAP3P.	61
FIGURE 11. TIME COURSE OF SECRETION FOR TRUNCATED YAP3P.	62
FIGURE 12. ACTH ¹⁻³⁹ CLEAVING ACTIVITY FROM INDUCED GROWTH MEDIA.	64
FIGURE 13. CLEAVAGE OF MOUSE POMC BY SECRETED YAP3P.	65
FIGURE 14. pH PROFILE FOR SECRETED YAP3P ACTIVITY.	67
FIGURE 15. ANALYSIS OF STABILITY AND DEPENDENCE OF SECRETED YAP3P ACTIVITY ON TEMPERATURE.	69
FIGURE 16. WESTERN BLOT ANALYSIS OF SECRETED YAP3P USING ANTISERUM MW283.	70
FIGURE 17. SEPHADEX G-75 GEL FILTRATION OF SECRETED YAP3P.	72
FIGURE 18. ISOELECTRIC POINT (PI) DETERMINATION OF YAP3P.	73
FIGURE 19. SCHEMATIC DIAGRAM OF ANGLERFISH PROSOMATOSTATIN I AND II.	82
FIGURE 20. CLEAVAGE OF ANGLERFISH PROSOMATOSTATIN I AND II BY YAP3P.	85
FIGURE 21. TIME COURSE FOR THE CLEAVAGE OF APSS I AND APSS II BY YAP3P.	88
FIGURE 22. PROTEOLYTIC PROCESSING OF PROINSULIN.	96
FIGURE 23. PRIMARY AMINO-ACID SEQUENCE OF CCK33.	98
FIGURE 24. TIME COURSE OF GENERATION OF CCK8-IMMUNOREACTIVE PRODUCTS FROM CCK33 BY YAP3P.	99
FIGURE 25. PROTEOLYTIC PROCESSING OF CHOLECYSTOKININ 33.	100
FIGURE 26. PROTEOLYTIC PROCESSING OF CHOLECYSTOKININ 13-33.	101
FIGURE 27. PROTEOLYTIC PROCESSING OF DYNORPHIN A(1-11).	104
FIGURE 28. PROTEOLYTIC PROCESSING OF DYNORPHIN B(1-13).	105
FIGURE 29. PROTEOLYTIC PROCESSING OF AMIDORPHIN.	106
FIGURE 30. PURIFICATION PROFILES OF GLYCOSYLATED YAP3P.	119
FIGURE 31. COOMASSIE BLUE STAINED GEL OF PURIFIED GLYCOSYLATED YAP3P.	120
FIGURE 32. ANALYSIS OF GLYCOSYLATED YAP3P BY ANION EXCHANGE CHROMATOGRAPHY.	122
FIGURE 33. ANALYSIS OF DEGLYCOSYLATED YAP3P BY ANION EXCHANGE CHROMATOGRAPHY.	124

FIGURE 34. COOMASSIE BLUE STAINED GEL OF PURIFIED DEGLYCOSYLATED YAP3P	125
FIGURE 35. N-TERMINAL SEQUENCE ANALYSIS OF PURIFIED YAP3P	126
FIGURE 36. EQUATIONS GOVERNING KINETICS OF ENZYME REACTIONS.....	138
FIGURE 37. DETERMINATION OF K_i OF YAP3P FOR PEPSTATIN A: METHOD 1.....	139
FIGURE 38. DETERMINATION OF K_i OF YAP3P FOR PEPSTATIN A: METHOD 2.....	140
FIGURE 39. SCHEMATIC DIAGRAM OF BOVINE PRO-OPIOMELANOCORTIN.	145
FIGURE 40. IMMUNOCYTOCHEMISTRY OF MOUSE BRAIN SECTIONS WITH YAP3P ANTISERUM.	149
FIGURE 41. IMMUNOCYTOCHEMISTRY OF BOVINE AND MOUSE PITUITARY SECTIONS WITH YAP3P ANTISERUM.	150
FIGURE 42. WESTERN BLOT ANALYSIS OF BOVINE INTERMEDIATE AND NEURAL LOBE SECRETORY VESICLE SOLUBLE EXTRACT.	152
FIGURE 43. WESTERN BLOT ANALYSIS OF THE SOLUBLE EXTRACT OF MOUSE HYPOTHALAMUS AND MOUSE ANTERIOR PITUITARY	154
FIGURE 44. INITIAL RATE (A) AND LINEWEAVER-BURK (B) PLOTS FOR THE CLEAVAGE OF AMIDORPHIN BY YAP3P	172
FIGURE 45. INITIAL RATE (A) AND LINEWEAVER-BURK (B) PLOTS FOR THE CLEAVAGE OF ACTH ¹⁻³⁹ BY YAP3P	173
FIGURE 46. INITIAL RATE (A) AND LINEWEAVER-BURK (B) PLOTS FOR THE CLEAVAGE OF DYNORPHIN A BY YAP3P	174
FIGURE 47. INITIAL RATE (A) AND LINEWEAVER-BURK (B) PLOTS FOR THE CLEAVAGE OF DYNORPHIN B BY YAP3P	175
FIGURE 48. INITIAL RATE (A) AND LINEWEAVER-BURK (B) PLOTS FOR THE CLEAVAGE OF PROINSULIN BY YAP3P	176
FIGURE 49. INITIAL RATE (A) AND LINEWEAVER-BURK (B) PLOTS FOR THE CLEAVAGE OF CHOLECYSTOKININ 13-33 BY YAP3P	177

ABBREVIATIONS

ACE	Angiotensin I converting enzyme
ACTH	Adrenocorticotropin hormone
AESBF	4-(2-Aminoethyl)-benzenesulfonyl fluoride
AL	Anterior lobe
AMC	7-amino-4-methyl-coumarin
aPSS	Anglerfish prosomatostatin
aSS-	Anglerfish somatostatin
β_h -LPH	Human β -lipotropin hormone
Boc	<i>t</i> -butyloxycarbonyl
BSA	Bovine serum albumin
C-, N-	Carboxy-, amino-
CCK	Cholecystokinin
CLIP	Corticotropin-like intermediate lobe peptide
ConA	Concanavlin A
DEAE	Diethyl-amino-ethyl
DTT	Dithiothreitol
ECL	Enhanced chemiluminescence
dynA	Dynorphin A
dynB	Dynorphin B
EDTA	Ethylene-diamine-tetra acetic acid
enk	Enkephalin
ER	Endoplasmic reticulum
FPLC	Fast protein liquid chromatography
GlcNAC ₂	N-acetylglucosamine
Glu	Glucose
GPI	Glycophosphatidylinositol
HPLC	High pressure liquid chromatography
IgG	Immunoglobulin G
IL	Intermediate lobe
IPTG	Isopropyl- β -D-thiogalactopyranoside
kDa	Kilo daltons
Man	Mannose
MBP	Maltose binding protein
MCA	Methylcoumarin amide
MF	Mating factor
MSH	Melanocyte stimulating hormone
N-linked	Asparagine-linked
NL	Neural lobe
O-linked	Ser/Thr-linked
OD	Optical density
PBS	Phosphate buffered saline
PC	Prohormone convertase
PCE	Pro-opiomelanocortin converting enzyme

PCR	Polymerase chain reaction
PepA	Pepstatin A
pI	Isoelectric point
PLC	Phospholipase C
PMSF	Phenylmethylsulphonylfluoride
POMC	Pro-opiomelanocortin
PTH	Phenylthiohydantoin
PTP	Prohormone thiol protease
RIA	Radioimmunoassay
SDS-PAGE	Sodium dodecyl sulphate-polyacrylamide gel electrophoresis
SEM	Standard error of the mean
SPC	Signal peptidase complex
SRP	Signal recognition particle
TCA	Trichloroacetic acid
TGN	Trans golgi network
Tris	Tris-(hydroxymethyl)-aminomethane
YAP3p	yeast aspartic protease 3 protein

CHAPTER 1

GENERAL INTRODUCTION

CELL BIOLOGY

One of the major events in cellular biology is the process by which proteins are directed to their correct cellular compartments and how they are post-translationally modified *en route*. Much work has been done in the past fifteen years to attempt to delineate the mechanisms and components of these processes.

Proteins that are destined to be secreted must proceed through the cell's secretory pathway, consisting of the endoplasmic reticulum (ER), golgi apparatus and secretory vesicles, while undergoing post-translational modifications in these distinct cellular compartments. The presence of a hydrophobic signal peptide or pre-sequence (1) (usually ~20-30 amino acids in length) at or close to the amino-terminal of the nascent protein, directs it to the ER membrane by association with a signal recognition particle (SRP) (2, 3) that halts translation and associates with a receptor on the membrane, the SRP receptor. Once associated with the membrane, the nascent protein is co-translationally translocated (4) through the membrane where upon the pre-sequence is removed by a signal peptidase complex (SPC) (5, 6) of 2 to 5 integral membrane proteins. Having been inserted correctly, modifications to the protein as it traverses the ER, such as glycosylation, disulfide bond formation, isomerization and folding, occur. Core

asparagine-linked or N-linked glycosylation occurs in the ER at consensus sites on the protein identified by the sequence Asn-X-Ser/Thr, where X is any amino acid except proline. The enzyme, oligosaccharyltransferase, is responsible for the transfer of the oligosaccharide moiety $\text{Glu}_3\text{Man}_9\text{GlcNAc}_2$ from its lipid-associated precursor, $\text{Glu}_3\text{Man}_9\text{GlcNAc}_2$ -pyrophosphate-dolichol, to these asparagine residues (7). Core O-linked glycosylation also occurs in the ER by attachment of mannose residues to the hydroxyl side chains of serine and/or threonine residues, however, no consensus amino acid sequence for the recognition of O-linked sites on the protein has yet been discovered. In the golgi apparatus, which consists of three distinct domains termed cis-, medial-, and trans-golgi, additional modifications to the new proteins occur. These events include primarily, phosphorylation, elongation of N- and O-linked oligosaccharides and proteolytic processing by specific endoproteolytic processing enzymes. This last event occurs in the trans golgi network (TGN). Immature secretory vesicles containing the proteins that are destined to be secreted via the regulated secretory pathway, e.g. peptide hormones and neuropeptides, bud off from the TGN. Further proteolytic processing of these proteins occur in these vesicles as they mature. The pH and Ca^{++} ion concentrations appear to play an important role in the processing and possibly the trafficking/signalling events in the secretory pathway. For example the concentration of total Ca^{++} in the TGN is in the 5-10 mM range while in the secretory vesicles it increases to ~20-50 mM concentration (8), however it is probable that the concentrations of free Ca^{++} are much lower due to the binding ability of secretory proteins, such as the chromogranins, for Ca^{++} (9). Similarly,

while the pH of the ER is ~7.4, the TGN and immature secretory vesicles are slightly more acidic at ~6.2 (10, 11) and the mature vesicles become acidified to pH 4.5-5.5 (10, 12).

PROHORMONE PROCESSING

Neuropeptides and peptide hormones are synthesized as large inactive precursors which are cleaved either in the TGN or the secretory vesicles by endoproteases at specific paired or single basic residue cleavage sites to release biologically active peptides (13-16). The cleaved peptides generally undergo further processing by exopeptidases to remove the C- and/or the N-terminally extended basic residues, depending on whether the endoprotease initially cleaved in between, on the amino or on the carboxyl side of the pair of basic residues. A carboxypeptidase B-like enzyme, known as carboxypeptidase E or H, which can cleave C-terminal basic residues (17), and an aminopeptidase B-like enzyme that can trim the N-terminal basic residues (18) from the neuropeptides after liberation from their precursors, have been isolated. The peptides can also be modified at the N-terminus, such as acetylation, and/or at the C-terminus by amidation.

A number of paired/single basic residue specific endoproteases which are potential neuropeptide precursor processing enzyme candidates *in vivo* have been described which include members from the serine, aspartic, thiol and metallo-protease classes (for reviews, see ref. (13,15,16,19,20)). The criteria by which an enzyme is judged to be a prohormone processing enzyme are its ability to cleave a prohormone substrate specifically; to be able to function adequately at the pH at which the prohormone is cleaved *in vivo*; and finally to be localized to the same compartment where the prohormone is processed *in vivo*. In the

past, the identification and characterization of these prohormone processing enzymes has been dependent primarily upon the ability to purify the protein from an enriched tissue source or tumor cell line and to assay its activity under conditions similar to those found *in vivo*. However, while the purification procedures appear to be effective, the small quantities of enzyme *in vivo* and the limitations of tissue source have directed the focus of investigation from conventional protein purification to the power of molecular biology. Ultimately, once a putative processing enzyme has been cloned, gene knockout experiments using transgenic mice or anti-sense RNA transfections will define the importance of these enzymes in any given prohormone processing system.

Members of two classes of processing endoproteases, the subtilisin-like serine proteases (13,16,19-22) and aspartic proteases (23) have been cloned, and/or purified, and their amino acid sequence partially or fully determined. Other endoprotease processing enzyme candidates have also been described including metallo-, thiol and serine proteases (15). However, while the activities of these enzymes have been purified and characterized, only one member from the metalloprotease class has recently been cloned (24,25).

The difficulty in identifying prohormone processing enzymes has been greatly facilitated by the manipulation of yeast genetics. An enzyme in yeast, named Kex2p, which is classified as a Ca^{++} dependent, subtilisin-like serine protease, has been characterized genetically and biochemically as the enzyme responsible for the paired-basic residue specific processing of pro- α -mating factor (MF) and pro-killer toxin (26,27). It was therefore the first enzyme to be characterized unambiguously as a prohormone processing enzyme. Kex2p functions, in conjunction with Kex1p, a carboxypeptidase B-like enzyme

in yeast, and a dipeptidyl aminopeptidase (28,29), to generate the mature mating pheromone, α -mating factor. *Kex2* was found to have homology to the human *fur* oncogene. The gene product, furin, was subsequently determined to be a proprotein processing enzyme (30,31). Recently, a family of mammalian homologues of *Kex2* have been cloned as a result of a polymerase chain reaction (PCR) strategy using active site directed primers designed from the *Kex2* gene. To date, six mammalian enzymes (prohormone convertases, PCs) belonging to this family have been cloned. These include PC1 (32-35) (also known as PC3) (36), PC2 (32,36), PACE4 (37), PC4 (38,39), PC5/6A (21,22), and PC6B (40). Notably, two of the members, PC1/3 and PC2 have been shown to be localized primarily to peptide-rich regions in the brain and endocrine tissues (32,33,41,42), while furin, PACE4, PC5/6A and PC6B are ubiquitously distributed (22,37,43). PC4 has been localized only to testicular tissue (39). These enzymes appear to be synthesized as zymogens and are activated by proteolytic cleavage of an N-terminal pro-segment (44). In addition, carboxy-terminal processing can also occur (45). PC1 was shown to process the prohormone, pro-opiomelanocortin (POMC), to generate primarily adrenocorticotropin hormone (ACTH) and β -lipotropin (β -LPH) when the cDNAs of both PC1 and POMC were co-transfected into PC12 cells (46) and BSC-40 cells (47). In similar co-transfection experiments of PC2 and POMC, the major products found were β -endorphin and α -melanocyte stimulating hormone (α -MSH) (46). While POMC was capable of being processed by both PCs it appears that PC1 generated products that are the predominant products found in the anterior pituitary and the products produced by PC2 are those that are found predominantly in the intermediate lobe. The distribution of

both PC1 and PC2 by immunocytochemistry and *in situ* hybridization show the presence of PC1 primarily in the anterior pituitary while that of PC2 is highly expressed in the intermediate lobe (33,42,48). These results support a role of these enzymes in the processing of POMC *in vivo*. Other experiments have demonstrated that the PCs can process a number of mammalian prohormones at specific paired and mono-basic residue sites (49-54).

It is unlikely that there is one specific processing enzyme for each neuropeptide precursor, but rather a small number of enzymes exist, each of which prefers the conformation of certain precursors. Some will have overlapping specificity for the same precursors. These enzymes have different co-factor requirements and pH optima ranging from 4.5-7.0, and may therefore function in different cellular compartments of the secretory pathway i.e. trans-Golgi network and secretory granules. Table 1 represents a summary of most of the the enzymes mentioned here, however for a thorough review of processing enzymes see the reference of Loh, 1993 (15).

Table 1

NAME	CLASS	TISSUE DISTRIBUTION	PROPROTEINS CLEAVED
Pro-piomelanocortin converting enzyme (PCE)	Aspartic	Bovine pituitary secretory vesicles	POMC, Provasopressin, Proinsulin
Yeast aspartic protease 3 (YAP3p)	Aspartic	Yeast plasma membrane	Pro- α -mating factor, Proinsulin, CCK33, POMC
SS-28 generating enzyme	Aspartic	Anglerfish islet cell granules	Prosomatostatin I
Prohormone thiol protease (PTP)	Thiol	Bovine adrenal medulla chromaffin granules	Proenkaphalin
Prohormone convertase 1 (PC1/3)	*Serine	(Neuro)endocrine tissues	POMC, Pro-TRH, Pro- enkaphalin, Proinsulin
Prohormone convertase 2 (PC2)	*Serine	(Neuro)endocrine tissues	POMC, Pro-TRH, Proinsulin, Proglucagon
Prohormone convertase 4 (PC4)	*Serine	Testes	Unknown
PACE4	*Serine	Ubiquitous	Factor IX, von Willebrand's factor, rProsomatostatin
Furin	*Serine	Ubiquitous	Proalbumin, Prorenin, Proinsulin receptor, Growth factors, Proparathyroid, Proendothelin
Prohormone convertase 5 (PC5/6A)	*Serine	Ubiquitous	Unknown
Prohormone convertase 6 (PC6B)	*Serine	Ubiquitous	Unknown

Summary table of processing enzymes showing type of enzyme, cellular localiztion and proprotein substrates cleaved. * Subtilisin-like serine protease.

ASPARTIC PROTEASES

Aspartic proteases (EC 3.4.23.) constitute a large class of proteases that are present across the evolutionary gap from vertebrates to retroviruses. They are characterized by an optimum activity in the acidic pH range, inhibition by the active site inhibitor hexapeptide, pepstatin, isolated from *Streptomyces*, and a catalytic mechanism that involves the side chains of two positionally symmetrical aspartic acid residues. Aspartic proteases are generally found to be involved in the non-specific degradation of proteins, both intra- and extracellularly. Cathepsin D, for example, is involved in the degradation pathway within the cell which occurs in the lysosome. However the gastric enzymes, pepsin, gastricin and chymosin (formerly rennin) are involved in digestion in the stomach. Some specialized functions have been discovered for a number of aspartic proteases. For example, renin generates angiotensin I from its precursor by a specific cleavage. This decapeptide, angiotensin I, is subsequently converted to the vasoactive peptide, angiotensin II, by angiotensin converting enzyme (ACE), a diaminopeptidase. Renin is active at neutral pH, since it functions in the blood, making it a unique exception to the rule that aspartic proteases have an acidic pH optimum, (i.e. pH 2-5). Another example of a specific function for an aspartic protease is that of yeast barrier protein (Bar1p) present in the yeast growth media as a secreted enzyme. This protease specifically degrades α -mating factor in the growth media and therefore in effect regulates mating (55). Additionally, in retroviruses, aspartic proteases play a role in releasing viral proteins from polyprotein translation products during viral activation (56).

In general, aspartic proteases have a molecular mass of ~42kDa representing a single polypeptide chain on SDS-PAGE. However, for the lysosomal cathepsin D, this single polypeptide chain can be cleaved into two subunits of ~30kDa and ~12kDa. This processing of cathepsin D appears to be tissue specific since, pituitary cathepsin D is composed of the ~42kDa form and an equal amount of the two subunits mentioned above, but liver cathepsin D is solely composed of the two subunits. Both subunits need to be associated for the enzyme to be active.

X-ray crystal structures for a number of aspartic proteases have been resolved (57-61) that have allowed analysis of the structure of the active site. The results demonstrate that two domains of the protein backbone, each containing the consensus sequence Asp-Thr-Gly (DTG) or to a lesser extent Asp-Ser-Gly (DSG), fold together to form a symmetrical active site where the substrate binding sites, S6-S4', have been identified as pockets with hydrophobic character, especially in the S1 site. It is therefore not surprising to see that the specificity exhibited by these proteases show an absolute requirement for a hydrophobic residue in the P1 position of the substrate. The amino acids in the cleavage site of a particular substrate are classified as P1, P2, P3.... and P1', P2', P3'....., where P1 and P1' are the amino acids situated immediately amino and carboxy to the scissile peptide bond, respectively. The other amino acids are numbered accordingly in both directions relative to this scissile bond. The corresponding sites in the active site pocket of the enzyme where the amino acids P_n....P_{n'} of the substrate bind are classified as S1, S2, S3.... and S1', S2', S3'.... subsites.

In contrast to the mammalian, plant and fungal aspartic proteases, the retroviral aspartic proteases are much smaller, having less than 130 amino acids in the whole molecule and containing only one DTG active site triad. It has been speculated that, similar to the subunits of mammalian aspartic proteases, the retroviral aspartic proteases are active as a dimer (62). The catalytic mechanism of action for aspartic proteases is believed to be by general base catalysis in which the carboxyl groups of the aspartic residues activate a water molecule (63,64).

In 1985, a member of the aspartic protease family, as determined by inhibition of enzymatic activity by pepstatin A and diazoacetylnorleucine methyl ester, both active site specific inhibitors of aspartic proteases, was characterized (65). It was purified from the soluble extract of bovine pituitary intermediate lobe secretory vesicles and found to exhibit a unique specificity for the paired-basic residues of the prohormones, pro-opiomelanocortin (POMC), proinsulin and provasopressin (65,66). The enzyme was characterized as a ~70kDa glycoprotein with an optimum enzymatic activity at pH 4.5. The localization in secretory vesicles, specificity for the paired-basic residues of POMC and the acidic pH optimum, a pH consistent with that of the internal pH of secretory vesicles where processing occurs *in vivo*, resulted in the classification of this POMC converting enzyme (PCE, EC. 3.4.23.17) as a putative prohormone processing enzyme. Subsequent attempts to purify PCE in quantities necessary for sequencing and/or antibody production have not been successful.

Since the initial characterization of PCE, a number of other mammalian aspartic proteases have been described that appear to show the similar unique specificity for the

basic residues of prohormones. These include the anglerfish somatostatin-28 (aSS-28) generating enzyme from anglerfish islet cells (67) and a cathepsin D-like enzyme from the chromaffin granules of the bovine adrenal medulla (68). Both of these enzymes have been N-terminally sequenced and found to share homology to lysosomal cathepsin D. Additionally, the sizes reported for both are similar to the sizes of aspartic proteases in general. The aSS-28 generating enzyme was shown to have specificity for the mono-basic residue, Arg⁷³, of anglerfish prosomatostatin II, while the cathepsin D-like enzyme cleaved protachykinin at paired and mono-basic residues.

In addition to Kex2p, *Saccharomyces cerevisiae* was recently shown to express an aspartic protease, yeast aspartic protease 3 (YAP3p), that was cloned, based on its ability to process pro- α -MF correctly at paired-basic residues, in a *Kex2* deficient mutant (23). Similarly, transfection of anglerfish prosomatostatin II (aPSS II) into yeast resulted in the cloning of *YAP3* based on the ability of its gene product to generate somatostatin-28 (SS-28) from transfected aPSS II by a cleavage at the mono-basic residue, Arg⁷³ (69). The ability of this enzyme to apparently act as an alternative processing enzyme for Kex2p has resulted in a growing interest in this sub-class of aspartic proteases that demonstrate specificity for basic residues of prohormones.

Analysis of the nucleotide sequence of the *YAP3* gene reveals that it encodes a 569 amino-acid aspartic protease (Fig.1), with a calculated molecular mass of ~60kDa and isoelectric point of 4.5. There are ten potential N-linked glycosylation sites and a putative zymogen activation site similar to that of prorenin (70). The presence of a serine/threonine rich domain in this enzyme indicates a potential for O-linked glycosylation and/or

phosphorylation. Additionally, a putative yeast glyco-phosphatidylinositol (GPI) membrane anchoring consensus sequence (TSTSSKRN) (71) is present in the carboxy-terminus (C-terminus) that may be responsible for the association of YAP3p with a membrane compartment of the yeast cell, which was recently observed by Olsen, 1994, (72) and Bourbonnais et al., 1994, (73). YAP3p shows highest overall homology to Bar1 and Pep1, both yeast aspartic proteases, however, there is a high degree of homology around both active site regions with a wide variety of mammalian, plant and fungal aspartic proteases (Fig.2).

Prohormone and proneuropeptide processing occurs in the regulated secretory pathway of endocrine and neuroendocrine cells, e.g. proinsulin and pro-opiomelanocortin, while processing of constitutively secreted proteins e.g. proalbumin and growth factors, occur in the constitutive secretory pathway, which is present in all cells. The enzymes required for correct processing of these precursors in both pathways therefore play a pivotal role in the regulation of bioactive molecules that are destined to be secreted. The importance of their role is predicted by the observation of the evolutionary conservation of function between yeast and higher order eukaryotes as demonstrated by the physical and functional homology exhibited between yeast Kex2p and the mammalian PCs. While YAP3p appears to behave as an alternate processing enzyme for Kex2p in yeast, it seems likely that mammalian homologues of YAP3p exist that may also behave as alternative or even backup processing enzymes for the PCs. If this is the case, the mechanism of proprotein processing would be under the control of multiple levels of regulation. It would be of great importance to be able to determine the physiologically relevant events that

govern this regulation in light of the discovery of a number of genetic defects that lead to abnormal or aberrant peptide hormone levels, e.g. (74). To address this question, research is needed to study the structure of prohormones, the regulation of pH and Ca^{++} in the secretory pathway, the targeting of prohormones to the regulated secretory pathway and the characterization of the enzymes involved in the specific processing events. The work presented in this thesis focusses on the characterization of the physical and catalytic properties of one of these enzymes, yeast aspartic protease 3, with the hope that the knowledge obtained will elucidate for us a clearer picture of the physiological role that this and its putative mammalian homologues play, as members of a novel sub-class of aspartic proteases, in the specific activation of biomolecules from inactive precursors.

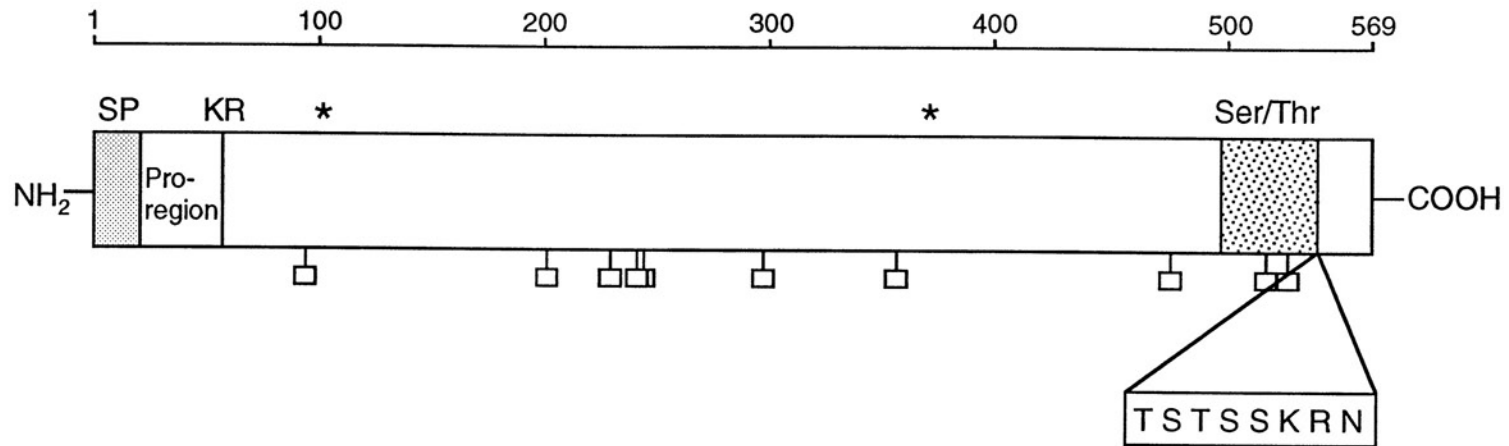


Figure 1. Schematic diagram of full length YAP3p protein

Ser/Thr= Serine/Threonine rich domain (aa503-545)

□ = Potential N-linked glycosylation sites

KR=Potential zymogen activation site (Lys⁶⁶-Arg⁶⁷)

SP= Signal peptide (aa1-21)

* = Active site aspartic residues (Asp¹⁰¹, Asp³⁷¹)

T⁵⁴¹STSSKRN⁵⁴⁸= Putative glycosyl phosphatidyl inositol membrane anchoring site (Asn⁵⁴⁸)

Enzyme	First active site triad																								
	*																								
Yeast YAP3p	G	T	P	P	Q	N	V	T	V	L	V	D	T	G	S	S	D	L	W	I	M	G	S	D	N
Yeast Bar1	G	T	P	S	Q	S	L	T	V	L	F	D	T	G	S	A	D	F	W	V	M	D	S	S	N
Yeast Pep1	G	T	P	G	Q	K	L	Q	V	D	V	D	T	G	S	S	D	L	W	V	P	G	Q	G	T
Fungal candidapepsin	G	S	N	N	Q	K	L	N	V	I	V	D	T	G	S	S	D	L	W	V	P	D	V	N	V
Mouse renin	G	T	P	P	Q	T	F	K	V	I	F	D	T	G	S	A	N	L	W	V	P	S	T	K	C
Human gastricin	G	T	P	P	Q	N	F	L	V	L	F	D	T	G	S	S	N	L	W	V	P	S	V	Y	C
Guinea pig cathepsin E	G	S	P	P	Q	N	F	T	V	I	F	D	T	G	S	S	N	L	W	V	P	S	V	Y	C
Bovine chymosin	G	T	P	P	Q	E	F	T	V	L	F	D	T	G	S	S	D	F	W	V	P	S	I	Y	C

Enzyme	Second active site triad																								
	*																								
Yeast YAP3p	T	L	T	T	T	K	I	P	A	L	L	D	S	G	T	T	L	T	Y	L	P	Q	T	V	V
Yeast Bar1	T	F	T	T	T	K	Y	P	V	L	L	D	S	G	T	S	L	L	N	A	P	K	V	I	A
Yeast Pep1	S	I	T	K	T	T	Y	P	A	L	L	D	S	G	T	T	L	I	Y	A	P	S	S	I	A
Fungal candidapepsin	T	I	N	T	D	N	V	D	V	L	L	D	S	G	T	T	I	T	Y	L	Q	Q	D	L	A
Mouse renin	L	L	C	E	E	G	C	A	V	V	V	D	T	G	S	S	F	I	S	A	P	T	S	S	L
Human gastricin	G	W	C	S	E	G	C	Q	A	I	V	D	T	G	T	S	L	L	T	V	P	Q	Q	Y	M
Guinea pig cathepsin E	M	F	C	S	E	G	C	Q	A	I	V	D	T	G	T	S	L	I	T	G	P	P	G	K	I
Bovine chymosin	V	A	C	E	G	G	C	Q	A	I	L	D	T	G	T	S	K	L	V	G	P	S	S	D	I

Figure 2. Amino acid sequence alignment of aspartic protease active sites

The conserved amino acids around the active site triads are indicated in bold. Amino acids are represented by their single letter codes. * = active site aspartic acid residues.

CHAPTER 2

OVEREXPRESSION, PURIFICATION AND CHARACTERIZATION OF CELLULAR YEAST ASPARTIC PROTEASE 3

Based on the published work entitled “Purification and Characterization of a Paired Basic Residue-Specific Yeast Aspartic Protease Encoded by the YAP3 Gene: Similarity to the mammalian pro-opiomelanocortin converting enzyme”. Azaryan, A.V., Wong, M., Friedman, T.C., Cawley, N.X., Estivariz, F.E., Chen, H-C. and Loh, Y.P. (1993) *J. Biol. Chem.* **268** 11968-11975.

The following chapter represents a summary of this published article.

INTRODUCTION

As already described in the main Introduction, the yeast aspartic protease 3 (*YAP3*) gene was first cloned based on its ability to partially suppress a Kex2 deficient mutant. It was shown that the *YAP3* gene product (YAP3p) was responsible for the paired-basic specific cleavage of pro- α -mating factor in this mutant yeast strain (23). Analysis of the primary sequence of YAP3p, translated from the nucleotide sequence, predicted an enzyme with a potential transmembrane domain in its carboxy terminus. There was also present a putative glyco-phosphatidylinositol binding site in its carboxy terminus similar to

that of Gasp1 (71), which predicted that this enzyme would be membrane associated. Other candidate prohormone processing enzymes contain either transmembrane domains or amphipathic alpha helical regions in their C-terminus that render these enzymes membrane associated (75-77). A carboxy-terminally truncated form of the enzyme was therefore engineered in order to express a soluble form of YAP3p. This would greatly facilitate purification of the enzyme.

METHODS

The plasmid containing the *YAP3* cDNA (a gift from Dr. Mogens T. Hansen, Novo Nordisk, Denmark), was first linearized by the restriction enzyme Nde II followed by a partial digest by Bst II to generate two *YAP3* inserts. Based on the restriction map of the plasmid and *YAP3* gene, the minor upper band (1.8 kb) encoded the full length of *YAP3* gene whereas the major lower band (1.6 kb) encoded a 3' truncated *YAP3* fragment. The 3' truncated *YAP3* fragment was subcloned into the yeast expression vector, pEMBLyex4 (78), under the control of the galactose inducible promoter. The yeast strain, BJ3501, deficient in the *Pep4* gene which encodes the major vacuolar aspartic protease in yeast, was used for transformation with the pEMBLyex4 vector carrying the *YAP3* fragment, using the lithium acetate method (79). Use of yeast strain BJ3501 lacking this aspartic protease greatly facilitated the purification of the overexpressed recombinant YAP3p.

Purification of cellular YAP3p

Yeast cells that were transformed with the pEMBLyex4-YAP3 construct were grown to an optical density (OD) at 600nm of ~1.5 in glucose selective media, centrifuged to harvest the cells and then resuspended and grown in galactose selective media for ~10hr to induce the expression of YAP3p. The cells were then harvested as before, resuspended in yeast lysis buffer (50 mM Hepes, 1 mM CaCl₂, pH 7.4) and subjected to six freeze-thaw cycles followed by sonication. The cell debris was centrifuged at 10,000 g for 20min and the supernatant collected for direct application to a concanavalin A (ConA) affinity chromatography column (see Materials and Methods). The ConA bound YAP3p was eluted with 0.5 M α -D-methyl-pyranomannoside and the eluate was dialysed overnight with 50 mM sodium citrate, pH 4.0. The dialysed sample was then applied to a pepstatin A (PepA) agarose inhibitor column (Pierce) that was pre-equilibrated in 50 mM sodium citrate, pH 4.0. After loading the protein sample, the column was washed with 3 volumes of the equilibration buffer containing 6 M urea and then with 5 volumes of equilibration buffer alone to remove the urea. The bound YAP3p was then eluted with 2 M LiBr, 50 mM Tris/Cl, pH 8.6 and immediately desalted with ammonium bicarbonate (see Materials and Methods). The desalted enzyme was either lyophilized and stored at 4°C or aliquoted and stored at -20°C until analysis. The yield of purified YAP3p was 100-150ng/g wet yeast (80).

RESULTS

Purified YAP3p was characterized with respect to its size, pH optimum, inhibitor profile and its ability to cleave the basic residues of mouse pro-opiomelanocortin (POMC)

and its fragments. The apparent molecular mass of YAP3p was determined to be ~70 kDa as demonstrated by SDS-PAGE followed by Coomassie blue staining of the purified protein. The inhibitor profile of YAP3p and the dependence of its enzymatic activity on pH was tested using ^{125}I labelled human β -lipotropin (^{125}I - β_{h} -LPH) as substrate (see Materials and Methods for YAP3p enzymatic assay procedures). YAP3p was found to be active in acidic pH's with a pH optimum at 4.0-4.5, while its inhibitor profile demonstrated that only pepstatin A, a specific inhibitor of aspartic proteases, inhibited the enzyme by 85-95%. All other class specific protease inhibitors had little or no effect on the YAP3p activity. The analysis of the products generated from POMC shows that YAP3p cleaved either between and/or on the carboxyl side of paired basic residues to yield adrenocorticotropin (ACTH) and β -LPH. In addition, human ACTH¹⁻³⁹ was shown to be cleaved at the tetrabasic residue site, Lys¹⁵-Lys¹⁶-Arg¹⁷-Arg¹⁸, primarily between Lys¹⁵-Lys¹⁶ to generate ACTH¹⁻¹⁵ and Lys¹⁶-Arg¹⁷-corticotropin-like intermediate lobe peptide (CLIP¹⁶⁻³⁹). Human β -LPH was also cleaved to yield β -melanocyte-stimulating hormone (β -MSH) and a mixture of β -endorphin^{1-31,1-29,1-28}. Bovine N-POMC¹⁻⁷⁷ was cleaved at the Arg-Lys cleavage site to yield γ_3 -MSH and Lys- γ_3 -MSH. A summary of the POMC sites cleaved by YAP3p is shown in Fig.3. When the substrate specificity of YAP3p was assessed with short model peptides, substrates with a single basic residue, e.g. Z-Gln-Gly-Arg-MCA, were not cleaved. However, a substrate with the R-X-R-R motif, Z-Arg-Val-Arg-Arg-MCA, was cleaved by YAP3p at the peptide bond between the two arginine residues releasing Arg-MCA which could be converted to AMC by treatment with aminopeptidase M.

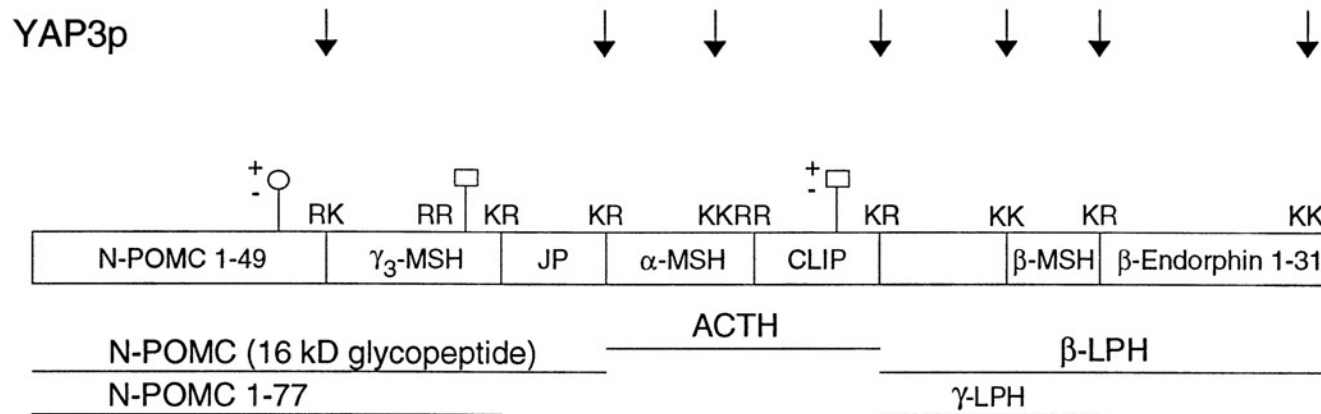


Figure 3. Schematic diagram of bovine pro-opiomelanocortin

POMC = pro-opiomelanocortin; ACTH = adrenocorticotropin hormone; MSH = melanocyte stimulating hormone; CLIP = corticotropin-like intermediate lobe peptide; LPH = lipotropin hormone. *Arrows* indicate the sites cleaved by YAP3p, *in vitro*.
 ○ = O-linked glycosylation site. □ = N-linked glycosylation sites.

CONCLUSION

The size, pH optimum, inhibitor profile and specificity of this enzyme renders YAP3p a member of the unique sub-class of aspartic protease processing enzymes. The results showed that YAP3p has a molecular mass considerably higher than other classical aspartic proteases, but similar to the mammalian aspartic protease, pro-opiomelanocortin converting enzyme, PCE (E.C. 3.4.23.17) previously purified and characterized from the intermediate lobe secretory vesicles of bovine pituitary, indicating that YAP3p may be the yeast homologue of PCE. The specificity exhibited by YAP3p supports the hypothesis that aspartic proteases may play an important role in the processing of prohormones *in vivo*.

CHAPTER 3

GENERATION AND CHARACTERIZATION OF ANTISERUM TO YEAST ASPARTIC PROTEASE 3

INTRODUCTION

In order to further characterize the physical properties of the novel aspartic protease from yeast (YAP3p), it was deemed that having an antibody to this enzyme would be very useful. Antiserum MW283 was generated by immunizing rabbits with a fusion protein constructed of maltose binding protein and YAP3p. This fusion protein was purified by two SDS-PAGE procedures, slab gel electrophoresis and continuous elution electrophoresis. Purified YAP3p was also used to boost the immunizations of the same rabbits once the procedure was worked out for its purification (80). The resultant antiserum was characterized by immunodepletion of YAP3p activity, Western blot, radioimmunoassay (RIA) and immunocytochemistry.

METHODS

Generation of MW283 Antiserum to YAP3p

The *YAP3* cDNA fragment (1.6 kb) was fused in frame at its 5' end with the maltose binding protein (MBP) cDNA. The resultant chimeric construct was transfected

into E.coli and induced to express the fusion protein (Fig.4.A) by IPTG induction. The procedure used was that of New England Biolabs, Inc., Protein Fusion and Expression Kit, and was engineered by Dr. May Wong, formerly of LDN, NICHD, NIH. The bacterial cells, expressing the fusion protein were solublized by boiling in 1% SDS for 10min. The boiled solution was then diluted with 0.33 volumes of a 4X SDS-PAGE sample buffer (see Materials and Methods) and then electrophoresed on either a vertical slab SDS-PAGE gel or a Biorad Continuous Elution Preparative Gel Electrophoresis Unit (Prep Cell). The polyacrylamide concentrations of the separating and stacking gels were 6% and 2.5%, respectively. For the slab gel, the ~110kDa sized fusion protein band was excised from the gel, minced and added to an equal volume of Freund's complete adjuvant. This mixture was used to immunize rabbits subcutaneously at Hazelton Biotechnologies, Inc., Vienna, Va, essentially as described previously (81). For the continuous elution Prep Cell, the protein sample was electrophoresed and the eluent was monitored by absorption at 280 nm while fractions of 3 mls were collected for analysis. An aliquot from every fifth fraction (#30-#65) was analysed by SDS-PAGE and the protein was stained by Coomassie brilliant blue (Fig.4.B). To further define the fractions that contained the pure fusion protein (~110kDa), aliquots from every fraction (#45-#64) around where the fusion protein was eluting from the prep cell (determined from the Coomassie blue stained gel) were analyzed by SDS-PAGE but this time the proteins were stained by the silver stain procedure (Fig.4.C, see Materials and Methods for staining procedures). Fractions #49-#67 were pooled and concentrated by centrifugation in a centricon 30 micro-concentrator.

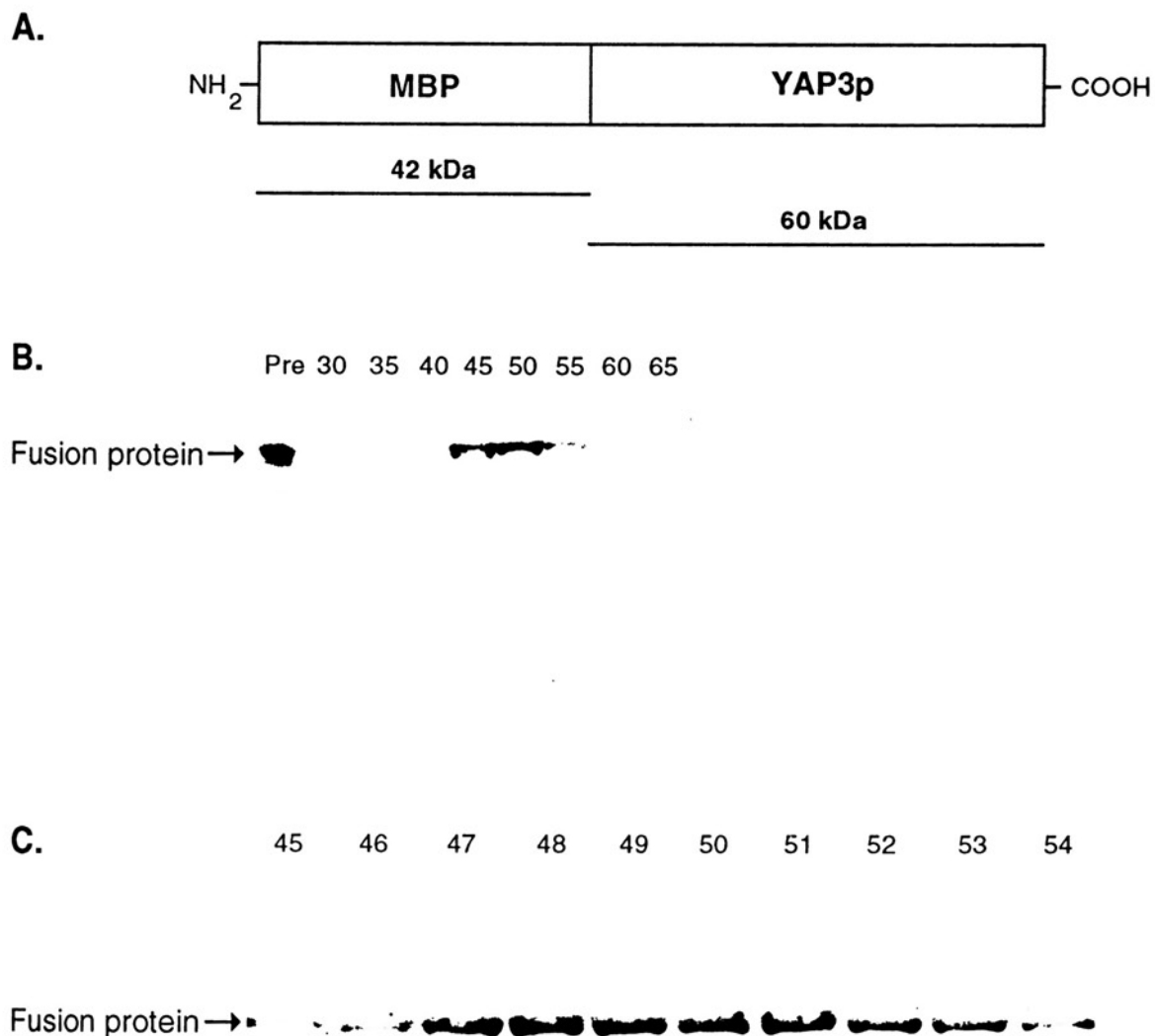


Figure 4. Purification of the maltose binding protein-yeast aspartic protease 3 fusion protein (MBP-YAP3p)

(A) Schematic diagram of MBP-YAP3p. (B) Coomassie blue stained gel of every fifth fraction from the continuous elution preparative SDS-PAGE unit (Prep cell). (C) Silver stained gel of every fraction from the Prep cell around where the fusion protein eluted. Pre = aliquot of solubilized bacteria expressing the fusion protein. Fraction numbers are indicated above each gel.

This purified fusion protein was also used to immunize the same rabbits at Hazelton Biotechnologies, Inc. In addition, for immunization boosts #6-#10, purified YAP3p was used, once the procedure for its purification from induced yeast cells was determined (see Chap.2 and (80)). Antiserum MW283 was generated by this procedure and was characterized by a number of immunological methodologies.

CHARACTERIZATION OF ANTISERUM MW283

Immunodepletion of YAP3p activity

As described in Chap.2, YAP3p was shown to cleave human ACTH¹⁻³⁹ into two major products, ACTH¹⁻¹⁵ and CLIP¹⁶⁻³⁹, which are easily analysed by HPLC. The ability of MW283 antiserum to deplete this cleaving activity compared to MW283 pre-immune serum was tested. An aliquot of purified YAP3p from the cellular extract of induced yeast was incubated with either MW283 antiserum or MW283 pre-immune serum (see Materials and Methods). The antibody/antigen complexes were precipitated by protein A-Sepharose beads (Pharmacia) and after centrifugation at 2000 g for 10min, the resultant supernatant was assayed by the ACTH¹⁻³⁹ assay. This experiment was done in triplicate. Analysis of the products, ACTH¹⁻¹⁵ and CLIP¹⁶⁻³⁹, demonstrated that overnight preincubation of YAP3p preparations with MW283 antiserum resulted in the depletion of the YAP3p cleaving activity (Fig.5.B) in the supernatant by 63% when compared to the activity of similar YAP3p preparations that were preincubated with MW283 preimmune serum (Fig.5.A).

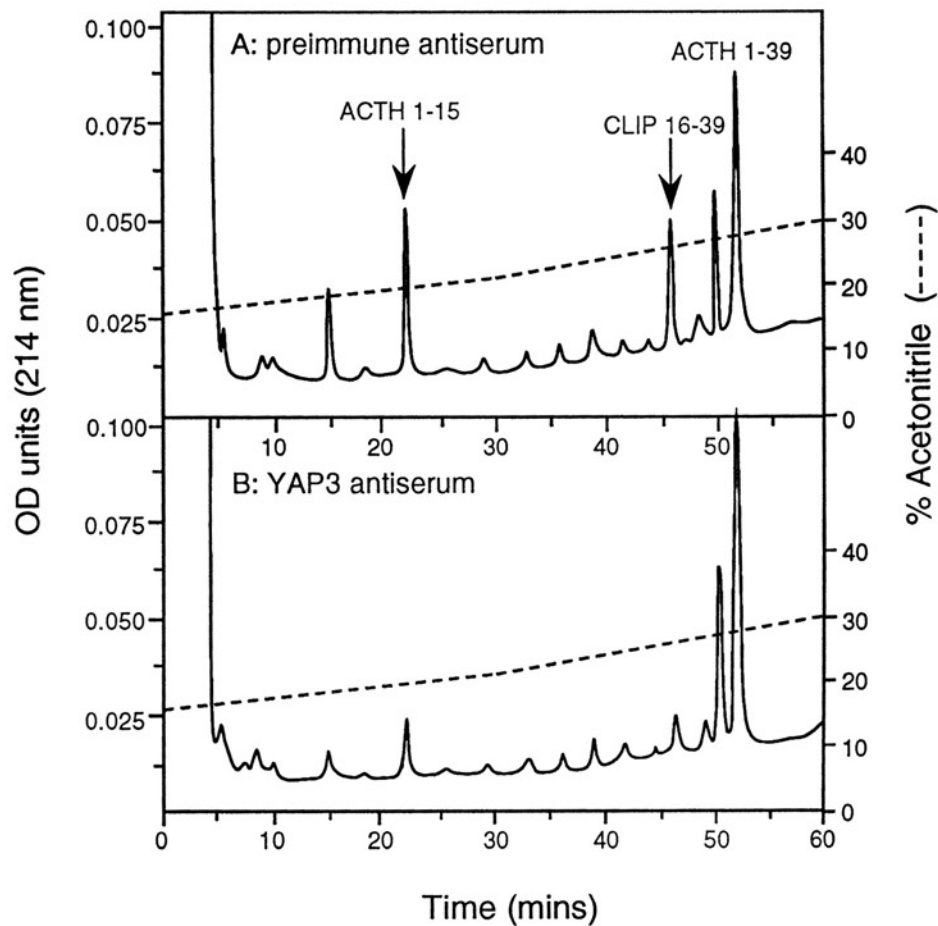


Figure 5. Immunodepletion of YAP3p activity

Equal aliquots of YAP3p activity were incubated with either preimmune serum or MW283 antiserum for 16hrs at 4°C. After removal of antibody-antigen complexes by protein-A sepharose beads, the supernatants were assayed for residual YAP3p activity.

(A) The generation of ACTH¹⁻¹⁵ and CLIP¹⁶⁻³⁹ demonstrates that preimmune serum did not immunodeplete YAP3p activity. **(B)** The decrease in the formation of products from ACTH¹⁻³⁹ demonstrates the specific depletion of YAP3p activity by MW283

Western blot analysis of cellular YAP3p

Purified cellular YAP3p was run on an SDS-PAGE gel and transferred to nitrocellulose for immunostaining (see Materials and Methods). The blotted protein was probed with either MW283 antiserum, pre-immune serum or MW283 antiserum that had been pre-absorbed with MBP-YAP3p fusion protein. All sera were diluted to 1:10,000. Antibody/antigen complexes were detected by the alkaline phosphatase procedure of Vector Labs., Inc., using biotinylated goat anti-rabbit IgG's as the secondary probe and a pre-equilibrated mixture of biotinylated-alkaline phosphatase and avidin as the tertiary probe. The results of the Western blot confirmed the specificity of MW283 antiserum by immunostaining the YAP3p protein (Fig.6, lane 1) while the preimmune and pre-absorption control lanes showed no apparent immunostaining (Fig.6, lanes 2 and 3, respectively).

Radioimmunoassay of YAP3p

Two μ g of purified MBP-YAP3p fusion protein were custom iodinated by the chloramine T procedure at Hazelton Biotechnologies, Inc. The iodinated protein was separated from the free iodine by a Sephadex G-50 gel filtration column and aliquoted for storage at -80°C . The titre of MW283 antiserum for the binding of fusion protein was determined by incubating fixed amounts of radiolabelled fusion protein ($\sim 15,000$ cpm) with serial dilutions of MW283 antiserum, overnight at 4°C . The buffer used was 1X Phosphate Buffered Saline (PBS) with 0.1% BSA and 0.1 mg/ml Aprotinin. The antibody/antigen complexes that formed were then precipitated by the sequential addition of normal rabbit serum (Peninsula) as a carrier protein followed by the addition of goat

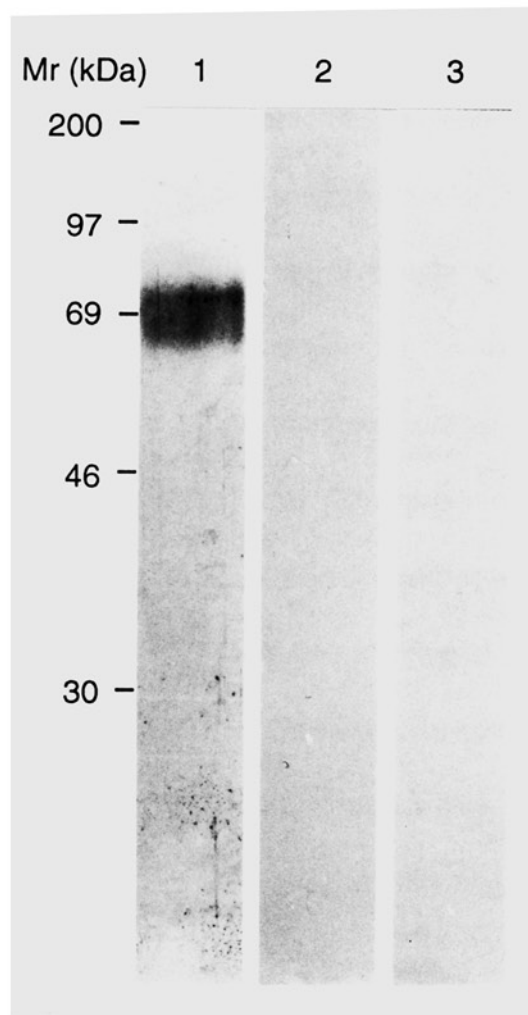


Figure 6. Western blot analysis of purified cellular YAP3p

Equal aliquots of purified YAP3p were loaded into each lane. Lane 1 probed with MW283, lane 2 probed with preimmune serum and lane 3 probed with MW283 that had been preabsorbed with purified fusion protein.

anti-rabbit IgG's (Peninsula) for 45min at room temperature. After centrifugation at 3000 g for 20min, the supernatant was aspirated and the pellet was counted in a γ -counter for the determination of immunoprecipitated fusion protein. A standard curve was also generated by determining the ability of unlabelled (cold) fusion protein to compete for the labelled (hot) fusion protein during the overnight incubation at a given antiserum concentration. The ability of MBP to compete for the hot fusion protein was also tested. The titre of MW283 to be used for the radioimmunoassay (RIA) was determined to be at a final dilution of 1:30,000 (Fig.7.A). Using the antiserum at this final dilution, a standard curve was generated by using fusion protein or maltose binding protein as the competing antigen. Maltose binding protein was unable to compete with the hot fusionprotein even up to a concentration of 4 μ g/ml while fusion protein itself generated a competition curve in the range of 2.5 ng/ml to 250 ng/ml fusion protein (Fig.7.B).

Immunocytochemistry of induced yeast

This work was done in collaboration with Dr. Le-Ping Pu, LDN, NICHD, NIH. Immunolabelling procedures were performed according to the indirect immunofluorescence method as previously described (82) and explained in detail in the Materials and Methods section. The results show that MW283 antiserum immunostained transformed/induced yeast cells, where the immunoreactivity was most evident surrounding the periphery of the yeast cell (Fig.8.A and C). This staining pattern, described as a doughnut shaped pattern is characteristic of staining in the yeast periplasm which has an acidic pH appropriate for YAP3p function. Substitution of primary antiserum with pre-immune serum (Fig.8.E) or omission of primary or secondary antibody (data

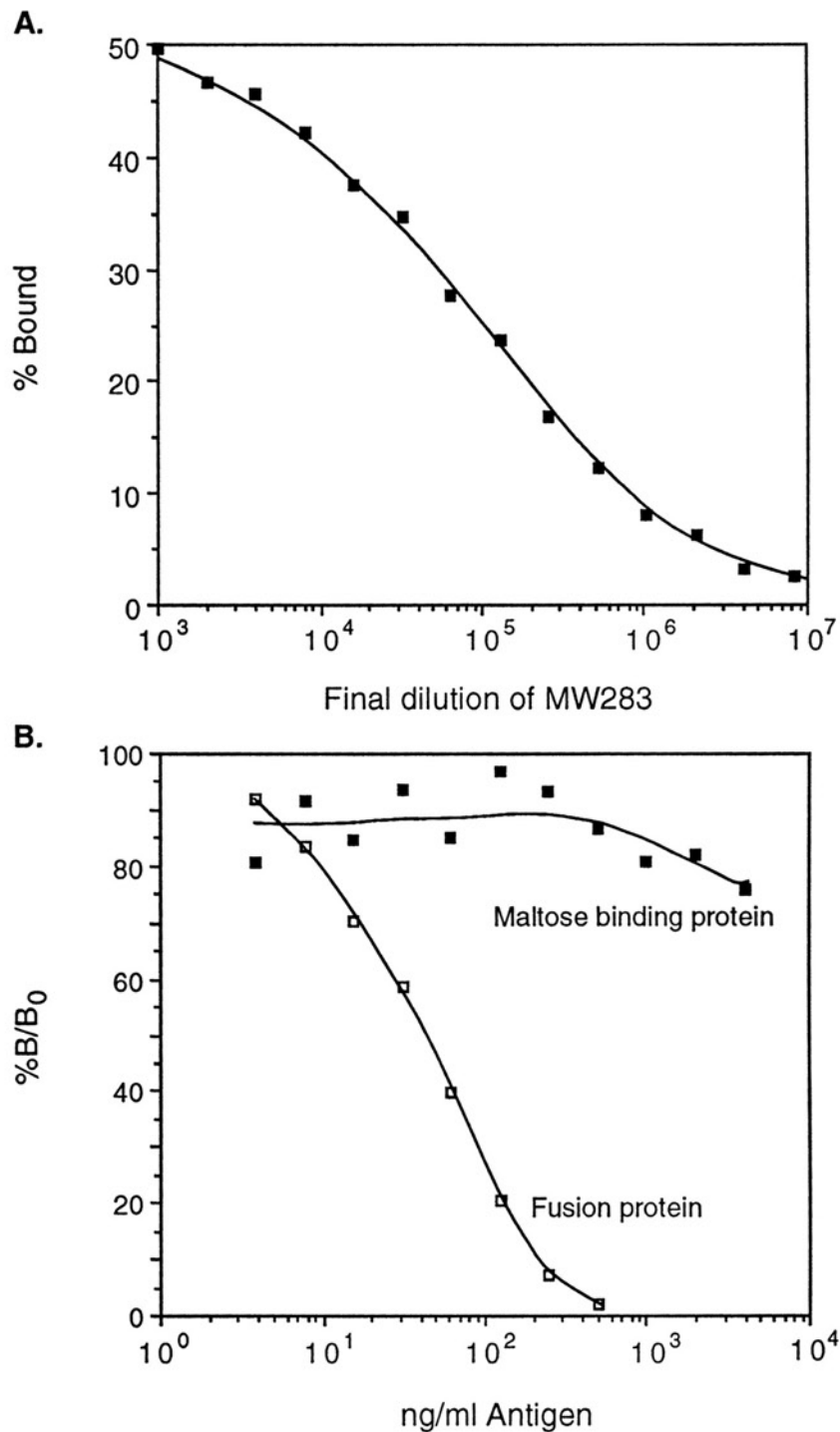


Figure 7. YAP3p radioimmunoassay

(A) Titration curve of MW283 for iodinated fusion protein. **(B)** Standard RIA curve for MW283 at 1:30,000 final dilution using fusion protein or MBP as competing antigen. MBP showed no significant competition up to 4 μ g/ml, while fusion protein competed in the range 2.5ng/ml to 250ng/ml.

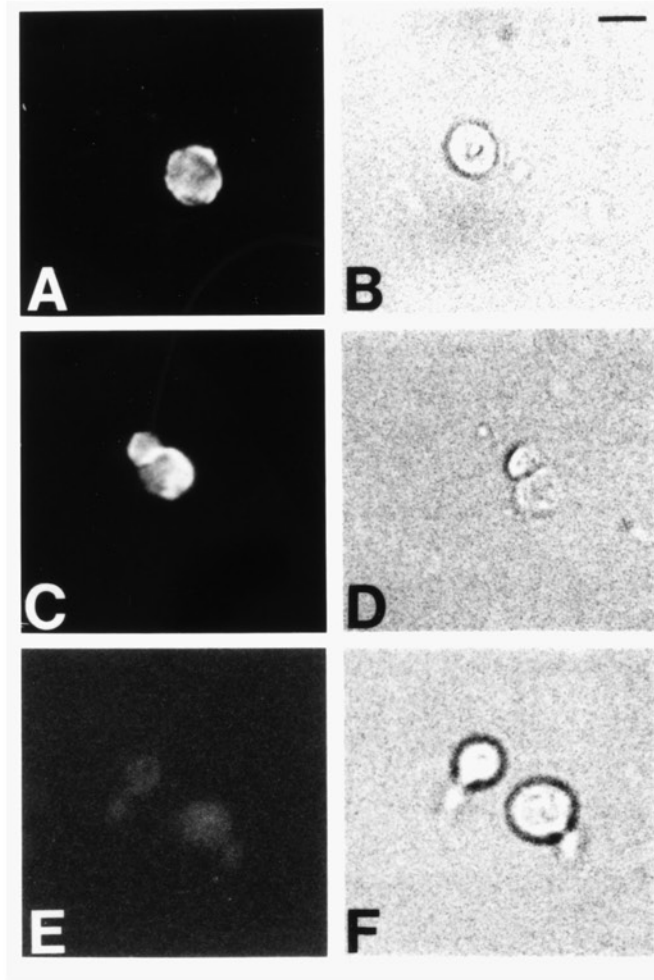


Figure 8. Immunocytochemistry of induced yeast expressing YAP3p

The indirect immunofluorescent method was used to stain yeast cells that had been induced to express YAP3p. **(A,C)** Immunopositive yeast cells showing staining at the periphery of both normal (A) and budding (B) cells indicative of periplasmic staining. **(E)** No apparent immunostaining when preimmune serum was used. **(B, D, F)** Bright field images of **A, C** and **E**. Bar 10 μ m.

not shown) all resulted in no apparent immunostaining. The bright field images of the immunostained yeast cells can be seen in panel B, D and F of Fig.8.

CONCLUSION

An antiserum was generated to YAP3p and characterized. The ability of MW283 to deplete YAP3p activity by 63% indicates an antiserum specific for the YAP3p protein in its active form. Western blot analysis confirmed the specificity of the antiserum by immunostaining purified YAP3p, while immunocytochemical studies showed a distinct localization of the induced YAP3p to the edges of the yeast cells. The periplasmic staining pattern observed in the induced yeast cells supports the hypothesis that YAP3p is a component of the yeast secretory pathway, as observed by Bourbonnais, (1993). It was demonstrated that this antiserum was also useful for RIA to specifically quantitate YAP3p antigen in a given sample, where YAP3p would be expressed as fusion protein equivalents. The studies shown here demonstrate that MW283 antiserum can be used in a variety of different immunological assays for the analysis of YAP3p.

CHAPTER 4

CARBOXY TERMINALLY TRUNCATED YAP3p IS SECRETED INTO THE GROWTH MEDIA: CHARACTERIZATION OF SECRETED YEAST ASPARTIC PROTEASE 3

Based on the published work entitled “Secretion of Yeast Aspartic Protease 3 (YAP3p) is Regulated by its Carboxy-Terminus Tail: Characterization of Secreted YAP3p”. Niamh X. Cawley, May Wong, Le-Ping Pu, Winnie Tam and Y. Peng Loh. (1995) *Biochemistry*, **34** 7430-7437.

SUMMARY

Wild type yeast aspartic protease 3 (YAP3p), was shown to be a membrane associated protease. The membrane association of YAP3p was demonstrated to be through a glyco-phosphatidylinositol anchor situated in the carboxy-terminus of the enzyme. Carboxy terminal truncation of YAP3p by 37 amino acids resulted in secretion of YAP3p into the growth media. Secreted YAP3p cleaved ACTH¹⁻³⁹ to generate ACTH¹⁻¹⁵ and CLIP¹⁶⁻³⁹ and mouse POMC to generate ACTH, β -LPH and N-POMC (inferred from the fact that to get free ACTH, β -LPH and N-POMC must have been released, see Fig.3 in Chap.2), indicating that the secreted forms of YAP3p demonstrated a similar specificity to that of the cellular form of YAP3p for these substrates (see Chap.2). Western blot

analysis after SDS-PAGE showed two secreted forms of YAP3p with apparent molecular weights of ~150-180kDa and ~90kDa. Treatment of YAP3p with endoglycosidase H reduced the size of both forms of the protein to ~65kDa, consistent with the presence of ten potential N-linked glycosylation sites in the deduced amino acid sequence of this protein. Removal of the N-linked sugars did not affect the enzymatic activity of YAP3p.

Secreted YAP3p has an isoelectric point of ~4.5 as determined by Isoelectric focussing gel electrophoresis. Analysis of the effect of temperature on the stability and the rate of enzymatic activity of YAP3p showed that the enzyme retained 100% of its activity when incubated for one hour at 37°C, while incubation at 50°C for one hour resulted in ~80% loss of activity. The dependence of activity on temperature demonstrated a calculated Q_{10} of 1.95.

INTRODUCTION

A prediction was made in Chap.2, based on the amino acid sequence analysis of YAP3p which showed a C-terminal hydrophobic domain and a putative glycosylphosphatidylinositol binding site, that full length YAP3p would be membrane associated and that removing the C-terminal would result in the expression of a soluble form of the enzyme. To investigate this hypothesis further, it was necessary to transform the yeast strain BJ3501 with the pEMBLyex4 vector carrying the complete coding sequence (1.8kb) of YAP3p and characterize the distribution and specificity of the expressed enzyme in direct comparison to the C-terminally truncated form of the enzyme

encoded by the 1.6kb fragment of the *YAP3* gene.

METHODS

Since it was technically difficult to obtain the 1.8 kb insert by restriction digestion, the polymerase chain reaction (PCR) procedure was used to generate two constructs (1.8kb and 1.6kb *YAP3* fragments named *pYAP3* and *pYAP3LC*, respectively) from the plasmid containing the *YAP3* gene. Each fragment was engineered with a BamH I site and a Pst II site at the 5' and 3' ends, respectively, for the directional cloning into the pEMBLyex4 vector. The 1.6kb insert was engineered with a stop codon immediately upstream from its 3' Pst II site. A schematic of the full length and truncated forms of YAP3p is seen in Fig.9.

Subcellular distribution of full length and truncated YAP3p

Yeast cells transformed with either *pYAP3* or *pYAP3LC* were grown to an optical density (OD) at 600nm of ~1.6 in glucose selective media (80), at 30°C, harvested and resuspended in galactose selective media. The cells were allowed to continue to grow for 25hr in this induction media. The growth rates of each clone were monitored by OD at 600nm and found to have parallel growth curves (data not shown). A 0.9ml aliquot from each clone was centrifuged at 2,000 g for 10min to sediment the cells and 10µl of the supernatant (growth media) was assayed for YAP3p activity by the ACTH¹⁻³⁹ assay. The yeast cell pellets were resuspended in 100µl water and 2µl AEBSF (2 mg/ml), freeze-thawed six times followed by 3 x 1sec sonication bursts (Converter, Branson Sonic Power

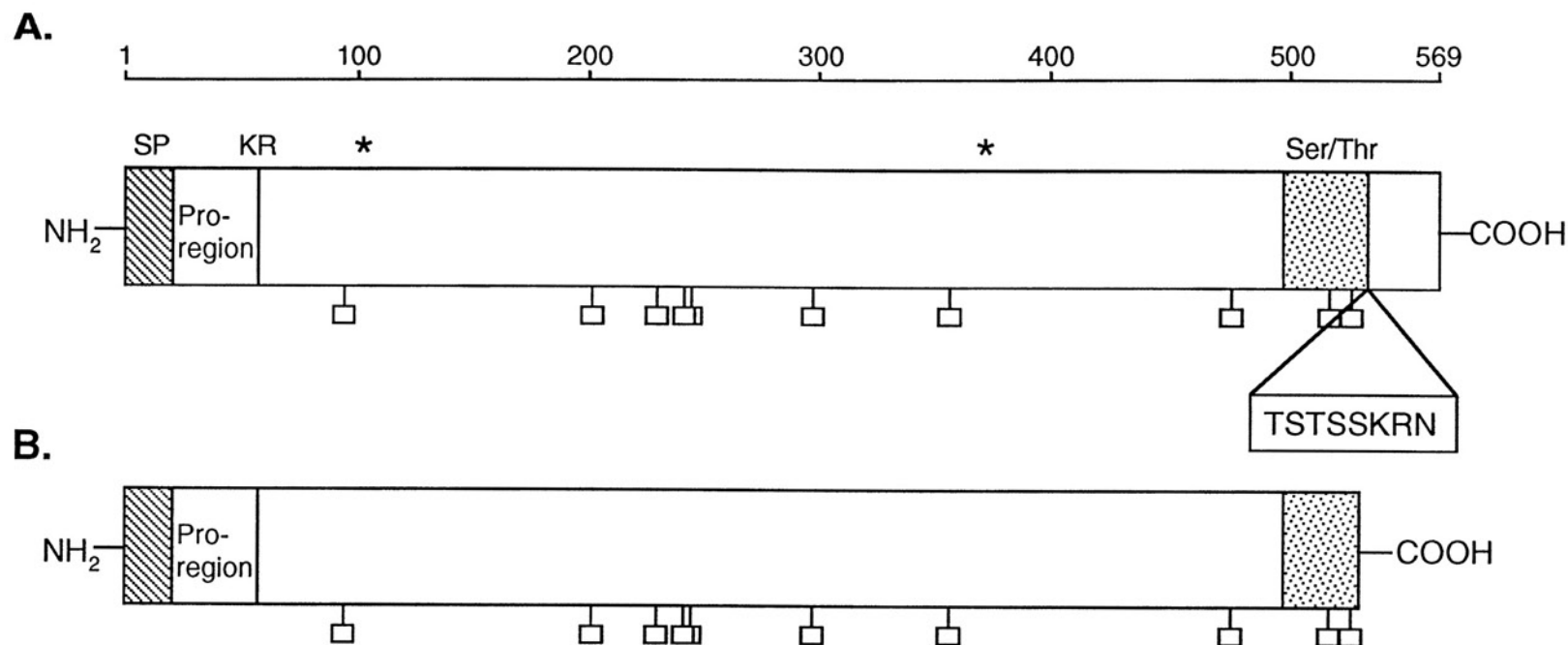


Figure 9. Schematic diagram of full length (A) and C-terminally truncated (B) YAP3p protein

Ser/Thr= Serine/Threonine rich domain (aa503-545) □ = Potential N-linked glycosylation sites
 $T^{541}STSSKRN^{548}$ = Putative glycosyl phosphatidyl inositol membrane anchoring site (Asn⁵⁴⁸)
 KR=Potential zymogen activation site (Lys⁶⁶-Arg⁶⁷) * = Active site aspartic residues (Asp¹⁰¹, Asp³⁷¹)
 SP= Signal peptide (aa1-21)

Co., Danbury, CT) on ice. The suspension was centrifuged at 10,000 g for 20min and the supernatant was saved. The membranes were washed with 50 μ l water and after centrifugation, this supernatant was added to the first and the combined soluble extract was saved for YAP3p activity determination. The membranes were resuspended in 100 μ l water. Ten μ l of the soluble extract and 0.17 μ l (5 μ l of 1:30 dilution) of the membrane suspension were assayed for YAP3p enzymatic activity by the ACTH¹⁻³⁹ assay. Total activity in the media, soluble extract and membrane extract of each clone was corrected for total volume and expressed as % activity of the overall total activity obtained from the 0.9ml aliquot. All extractions were carried out at 4°C.

Time course of secretion

During the induction period, 0.9ml aliquots were also removed from each suspension at 0, 0.5, 1, 2, 3, 5, 6, 7, 9, 11, and 12.5hr time points starting at the point of resuspension in galactose media. After centrifugation, 40 μ l of the supernatant (growth media) from the 1, 5, 7, 9, 11, and 12.5hr time points were assayed by the ACTH¹⁻³⁹ assay. A similar time course experiment was set up, where the media from either induced or uninduced yeast cells that were transformed with the truncated *YAP3* gene was assayed for enzymatic activity by the ¹²⁵I- β -LPH assay and for YAP3p immunoreactivity by RIA.

Phospholipase C treatment of yeast membranes

Membranes from yeast cells transformed with *pYAP3* (full length) and induced for 25hr were prepared as described above. Five μ l of the membranes were digested with phospholipase C (PLC, phosphatidylinositol specific, Sigma, St. Louis, MO.) as follows:

0.25 units of PLC in 0.1 M Tris/Cl, pH 7.4 containing 1 mM freshly prepared PMSF, overnight at 37°C. In a parallel control experiment, membranes were incubated with boiled PLC. After incubation, the reaction mixtures were microcentrifuged at 10,000 g for 20min and the supernatants were assayed by the ACTH¹⁻³⁹ assay. In a similar experiment, both the membranes and supernatant were assayed after PLC treatment to determine the percent of total YAP3p activity released from the membranes.

Cleavage of ACTH¹⁻³⁹ and mouse POMC by secreted YAP3p

Induced yeast (20hr), transformed with *pYAP3LC*, were harvested by centrifugation. The YAP3p present in the media was first assayed by the ACTH¹⁻³⁹ in the absence and presence of pepstatin A (3.0×10^{-6} M) to determine the specificity and degree of inhibition by pepstatin A of the secreted form. The YAP3p in the media was then partially purified by batch processing with Concanavalin A (ConA)-Sepharose beads described in Materials and Methods. The ConA eluate was desalted, lyophilized and reconstituted with water and stored in aliquots at -20°C until analysed.

Radiolabelled mouse POMC (³H]Arg-POMC) was generated from mouse pituitary neurointermediate lobes according to the procedure of Loh et al, 1984 (12). Ten thousand cpm of radiolabelled mouse POMC was incubated with an aliquot of the ConA purified YAP3p in 50µl, 0.1 M sodium citrate, pH 4.0 for 6hr. After the reaction, the products were immunoprecipitated (see Materials and Methods) by ACTH-specific antiserum, DP4, generated in Dr. Loh's laboratory. A negative control was performed by incubating POMC in the absence of YAP3p. The immunoprecipitated products were separated by 13% SDS-PAGE tube gels. Pre-stained molecular mass protein markers

(Amersham) were included in each gel as internal molecular mass standards. After the run, each gel was sliced into 1mm slices and after equilibrating in scintillation cocktail were counted in a β -counter. A graph of cpm against slice number resulted in the profile of ACTHir products generated from POMC.

pH and temperature studies of secreted YAP3p activity

The dependence of secreted YAP3p activity on pH was tested with the ^{125}I - β -LPH assay by incubating equal aliquots of YAP3p with substrate at different pH's. The buffer system used was citric acid/ Na_2HPO_4 giving a pH range of 2.3-7.6. Temperature stability of YAP3p was assessed by preincubating identical aliquots of partially purified secreted YAP3p for 1hr at 4°C-70°C in 0.1 *M* sodium citrate, pH 4.0 without substrate. Activity was then assayed by the ACTH¹⁻³⁹ assay at 37°C. The dependence of YAP3p activity on temperature was tested using the ACTH¹⁻³⁹ assay at 4, 23, 37, 50, 60 and 70°C.

Calculation of Q_{10}

The ACTH¹⁻¹⁵ product generated at 4, 23 and 37°C was plotted as a function of temperature. The exponential curve fit of these points, according to the Arrhenius relationship, ($\text{Rate} = Ae^{-E_a/RT}$) generated a line with $r^2=0.996$ and an equation which was used to calculate Q_{10} .

Western blot analysis of secreted YAP3p

Partially purified secreted YAP3p was divided into four equal aliquots. One aliquot was treated with endoglycosidase H, (endo H, Sigma, St. Louis, MO, 0.01 units in 0.05 *M* sodium phosphate buffer containing 2 *mM* PMSF, pH 6.0) at 37°C for ~12hr, and then all

samples were run on a 12% Tris/Glycine precast polyacrylamide gel (Novex, San Diego, CA) in denaturing/reducing conditions and transferred to nitrocellulose for immunostaining using standard SDS-PAGE and Western blotting techniques. The lanes were probed with primary antibody (MW283), preimmune antiserum or MW283 antiserum preabsorbed with 10µg MBP-YAP3p fusion protein. All antisera were at a dilution of 1:10,000 with 1X PBS containing 0.1% Tween 20 and 1.5% normal goat serum. Antigen detection was visualized using the alkaline phosphatase ABC kit and procedure from Vector Laboratories, Inc., Burlingame, CA.

Sephadex G-75 gel filtration of secreted YAP3p

ConA purified YAP3p was applied to a Sephadex G-75 gel filtration column coupled to an FPLC system (Pharmacia) equilibrated in 20mM sodium phosphate buffer, pH 7.0, 150mM NaCl, 1mM DTT and 0.01% Triton X-100. Half ml fractions were collected and assayed by the rapid ^{125}I - β_{h} -LPH assay. An identical aliquot of YAP3p was treated with endoglycosidase H (as described above) and analysed in the same manner.

Isoelectric point determination of secreted YAP3p

An aliquot of the partially purified YAP3p was run on a precast isoelectric focussing gel, pH range 3-7, according to the manufacturer (Novex, San Diego, CA). The protein was transferred to nitrocellulose and a Western blot was performed using YAP3p antiserum MW283. Isoelectric focussing protein standards (Bio-Rad Laboratories, Hercules, CA) were run in parallel, transferred to nitrocellulose and stained by Aurodye (Amersham Life Sciences, Arlington Heights, IL).

RESULTS

Distribution and secretion of YAP3p

Analysis of the enzymatic activity in the membrane, soluble extract and media revealed that most of the full length YAP3p activity (~83% of total activity, Fig.10.A, filled bars) was associated with the membranes, whereas the truncated YAP3p activity was primarily secreted (~76.5% of total activity, Fig.10.A, hatched bars) into the growth media. The time-course study of the secretion of YAP3p is shown in Fig.10.B. A comparison of the activity in the media between the full length (Fig.10.B, open squares) and the C-terminally truncated form (Fig.10.B, filled squares) of YAP3p shows that the truncated YAP3p was secreted into the growth media while the full length was not. In the analysis of the secretion of truncated YAP3p in uninduced and induced media, enzymatic activity was present only in the media of cells that were grown in the induction media, i.e galactose selective (Fig.11.A) and furthermore, pepstatin A inhibited the induced enzymatic activity (data not shown). Radioimmunoassay of the media showed the presence of fusion protein equivalents in the media of induced yeast cells and the absence in the media of uninduced yeast cells (Fig.11.B). The activity profile indicated that ~24hr was the optimum induction/secretion time point since activity in the media decreased after that probably due to some degradation or acid inactivation of the enzyme in the media. It has been observed that when the yeast grow to confluency and become overcrowded, the pH of the growth media can drop to below pH 3.0. In addition, YAP3p appears to be irreversibly inactivated when added to an acidic solution of less than pH 3.0 (unpublished observations).

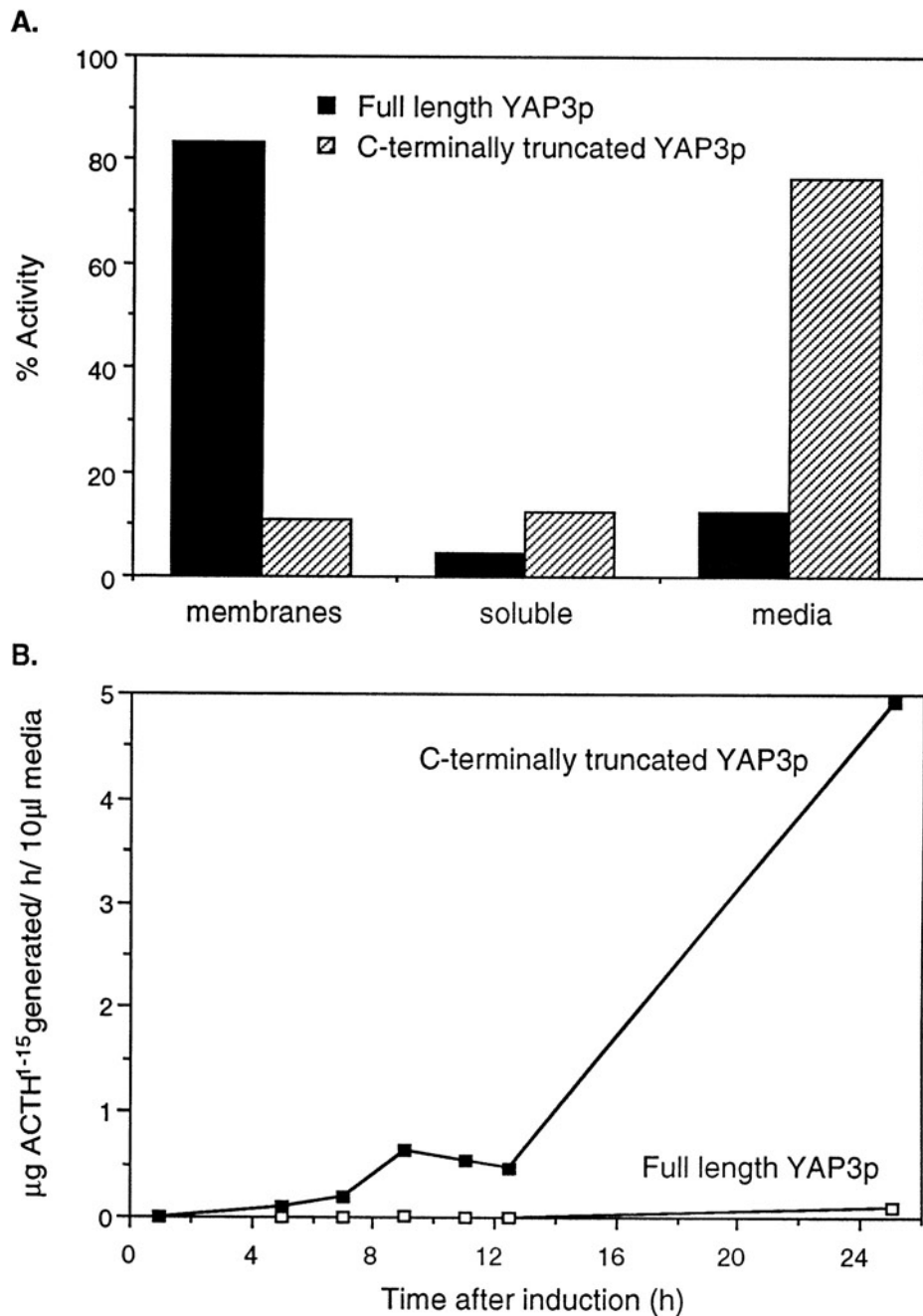


Figure 10. Distribution and secretion time course of full length and truncated YAP3p

(A) The distribution of YAP3p activity between cell membranes, soluble cellular extract and growth media for both YAP3p constructs was determined and expressed as % total activity. (B) Time course of YAP3p secretion. Aliquots of media from induced yeast that were transformed with either pYAP (full length) or pYAP3LC (truncated) were assayed by the ACTH¹⁻³⁹ assay. YAP3p activity is expressed as $\mu\text{g ACTH}^{1-15}$ generated/h/10 μl media. Filled squares (■) indicate the secretion profile of truncated YAP3p whereas open squares (□) indicate the secretion profile of full length YAP3p.

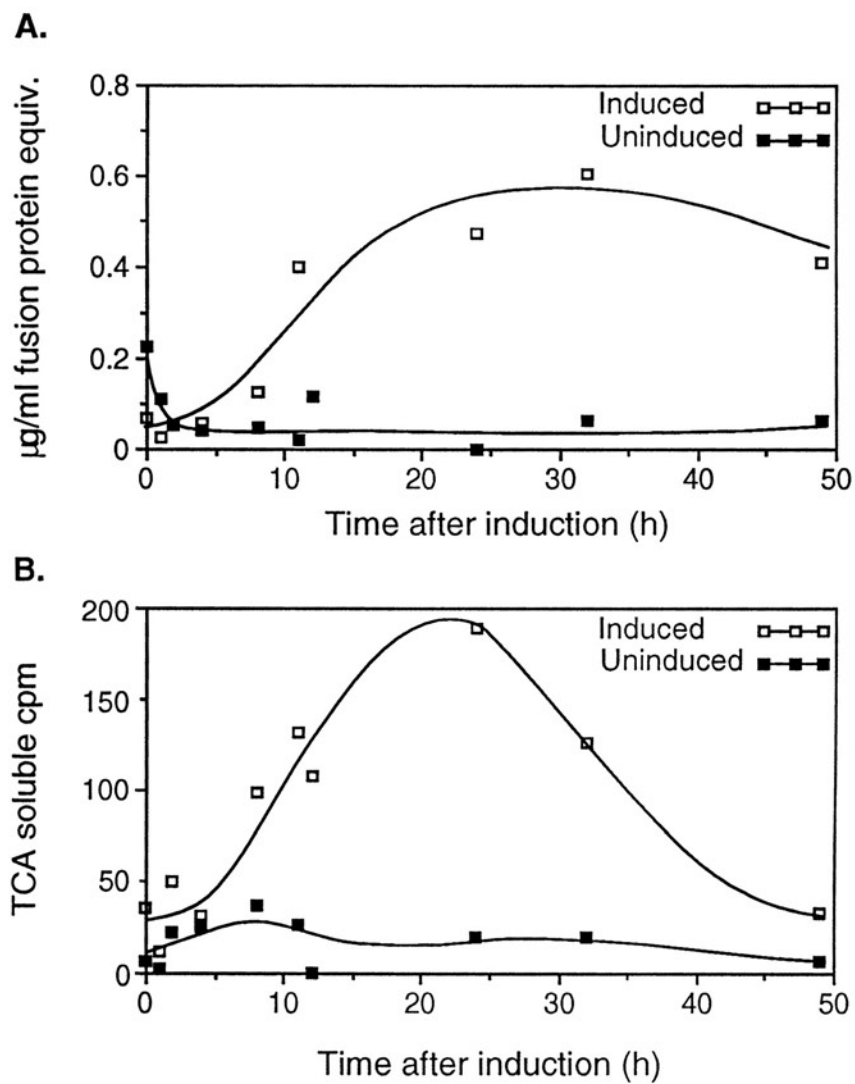


Figure 11. Time course of secretion for truncated YAP3p

(A) Analysis of uninduced and induced growth media for YAP3p immunoreactivity by RIA. **(B)** Analysis of uninduced and induced growth media for YAP3p enzymatic activity.

The presence of immunoreactive YAP3p even at the 50hr time point indicates that the antigen is still able to be recognized by the antibody suggesting that degradation of YAP3p is not primarily responsible for the loss of activity under longer induction periods, however the possibility that the antibody recognizes some degraded fragments of YAP3p still exist.

Release of full length YAP3p from yeast membranes by phospholipase C

Overnight incubation with phospholipase C of equal aliquots of membrane preparations from cells transformed with *pYAP3* resulted in the release of YAP3p activity which generated $3.7\mu\text{g} \pm 0.012$ (\pm SEM, $n=3$) of ACTH¹⁻¹⁵. In contrast, membranes treated with boiled PLC yielded YAP3p activity which generated $1.5\mu\text{g} \pm 0.024$ (\pm SEM, $n=3$) of ACTH¹⁻¹⁵. This ~2.5 fold increase of YAP3p activity in the supernatant after PLC treatment of the membranes over the negative control represents release of 54% of the total (membranes plus supernatant) YAP3p activity.

Cleavage of ACTH¹⁻³⁹ and mouse POMC by secreted YAP3p

The presence of YAP3p activity in the media was determined by the ACTH¹⁻³⁹ assay. Fig.12.A shows the generation of ACTH¹⁻¹⁵ and CLIP¹⁶⁻³⁹ from ACTH¹⁻³⁹ by secreted YAP3p activity. Addition of pepstatin A, an aspartic protease inhibitor, to the reaction mixture inhibited the generation of the products by >90% (Fig.12.B), indicating that the enzymatic activity in the media was due to YAP3p. Furthermore, no enzymatic activity was observed in the media of transformed uninduced yeast cells. Radiolabelled POMC was cleaved by YAP3p to generate primarily glycosylated ACTH¹⁻³⁹ (~13kDa) and ACTH¹⁻³⁹ (~4kDa), Fig.13.B and Fig.3. No immunoprecipitated POMC was detected

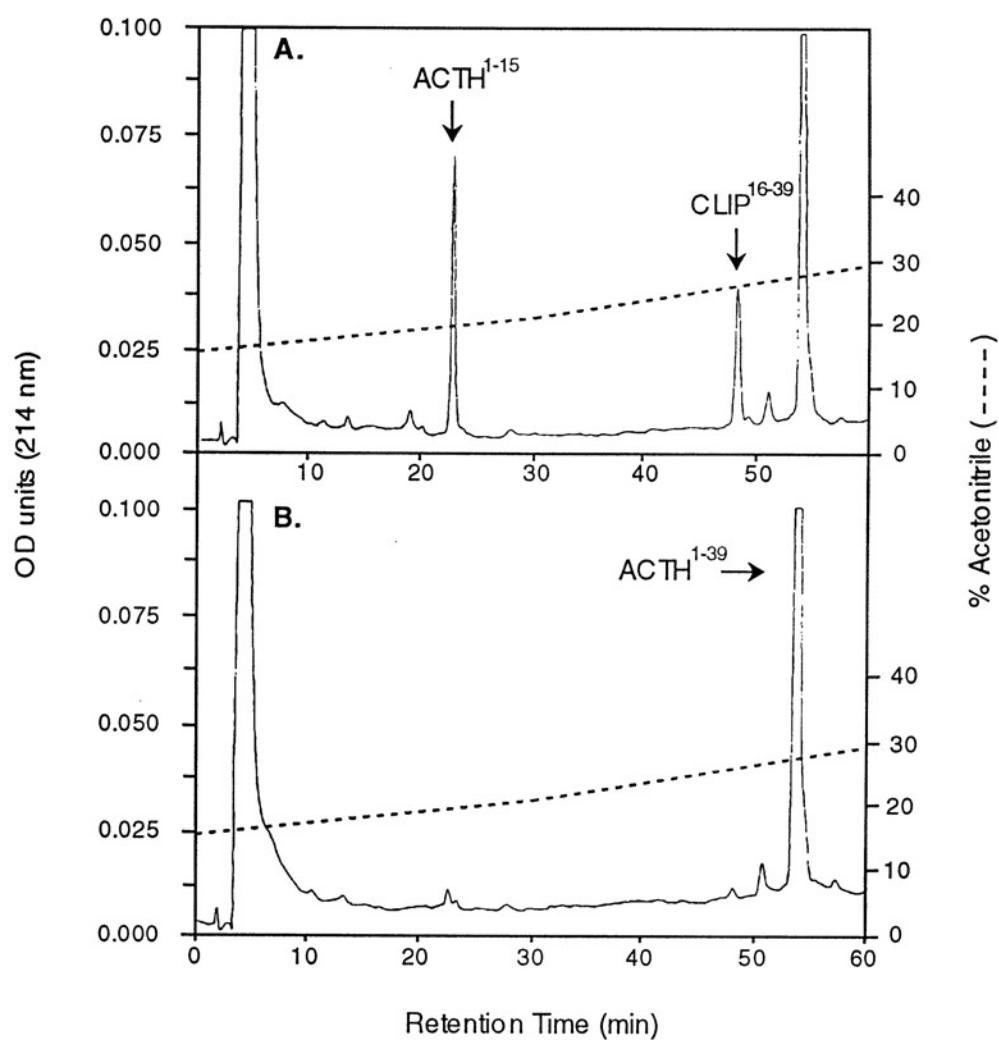


Figure. 12. ACTH¹⁻³⁹ cleaving activity from induced growth media
(A) HPLC profile of the products generated from 10 µg ACTH¹⁻³⁹ by secreted YAP3p. **(B)** Addition of pepstatin A specifically inhibited the generation of these products.

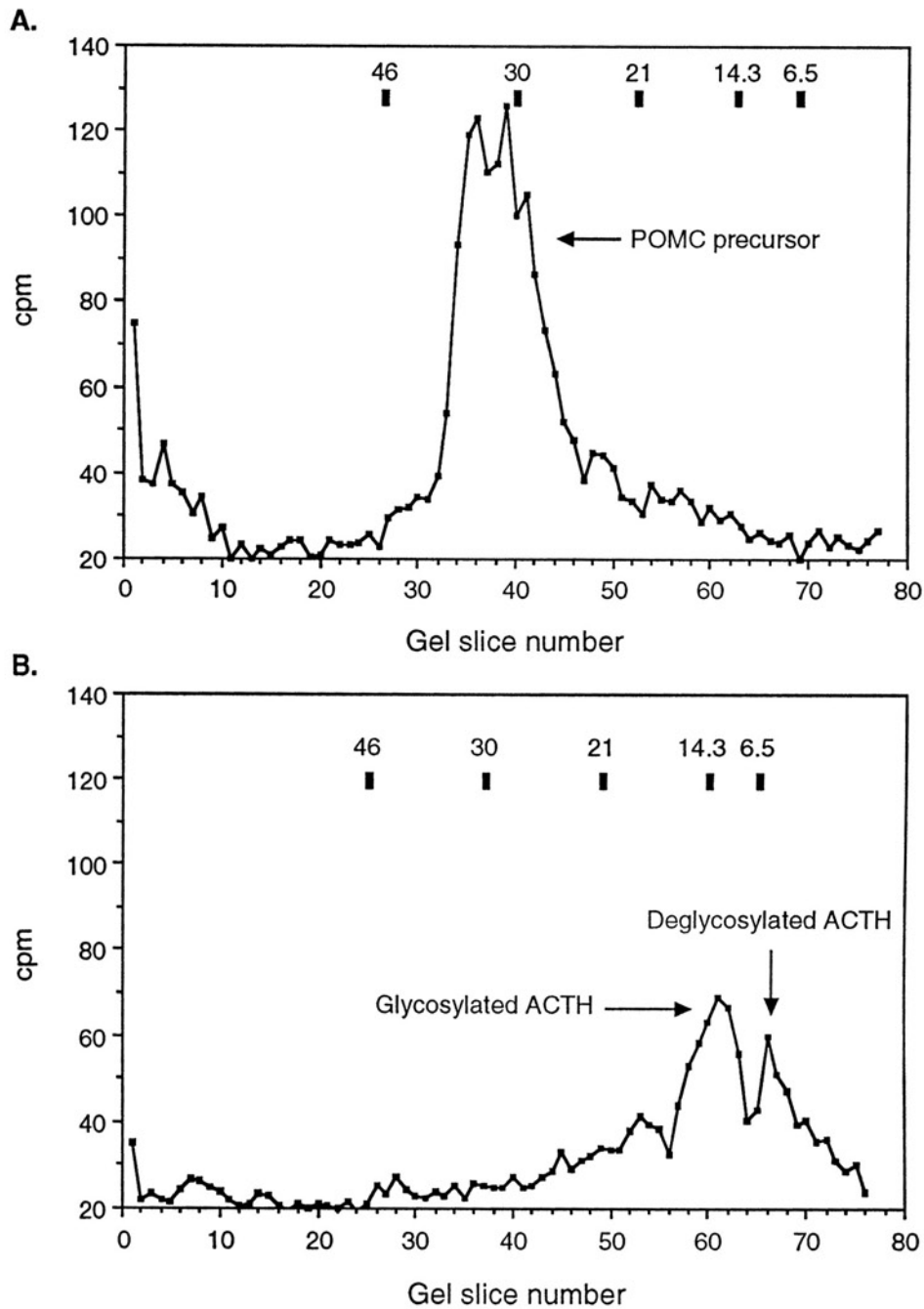


Figure 13. Cleavage of mouse POMC by secreted YAP3p

(A) Incubation of substrate in the absence of enzyme. (B) Incubation of substrate with YAP3p. Following incubation, the reaction mixtures were immunoprecipitated by ACTH-specific antiserum and the products analysed by SDS-PAGE tube gels.

indicating that the reaction had gone to completion. Immunoprecipitation of the control reaction of POMC alone, generated one peak corresponding in size to the uncleaved precursor, Fig.13.A.

pH and temperature studies of secreted YAP3p activity

Secreted YAP3p was characterized with respect to its dependence on pH and temperature for enzymatic activity. Secreted YAP3p activity showed a pH optimum of 4.0-4.5 (Fig.14). Fig.15.A shows that preincubation of YAP3p at 4, 23 and 37°C for 1h had minimal effect on the activity of YAP3p. However, preincubation at 50°C for 1h resulted in an ~80% decrease in activity, while at 60°C and 70°C, no activity remained. Assaying YAP3p activity at various temperatures, 4-70°C, demonstrated a temperature optimum of between 37 and 50°C (Fig.15.B) with a calculated Q_{10} of 1.95 based on the equation, $y=(1.46)e^{0.29x}$, obtained from a plot of ACTH¹⁻¹⁵ produced at 4, 23 and 37°C (Fig.15.C).

Characterization of the physical properties of secreted YAP3p

Secreted YAP3p was found to contain a major and a minor form. Their apparent molecular masses determined by SDS-PAGE followed by Western blot were ~90kDa for the minor one and ~150-180kDa for the major one (Fig.16, lane 1). No immunostaining was present in the preimmune and preabsorption controls (lane 3 and 4, respectively). Upon treatment with endo H, both immunostained bands shifted to one band with an apparent molecular weight of ~65kDa (Fig.16, lane 2). No immunostaining of YAP3p was

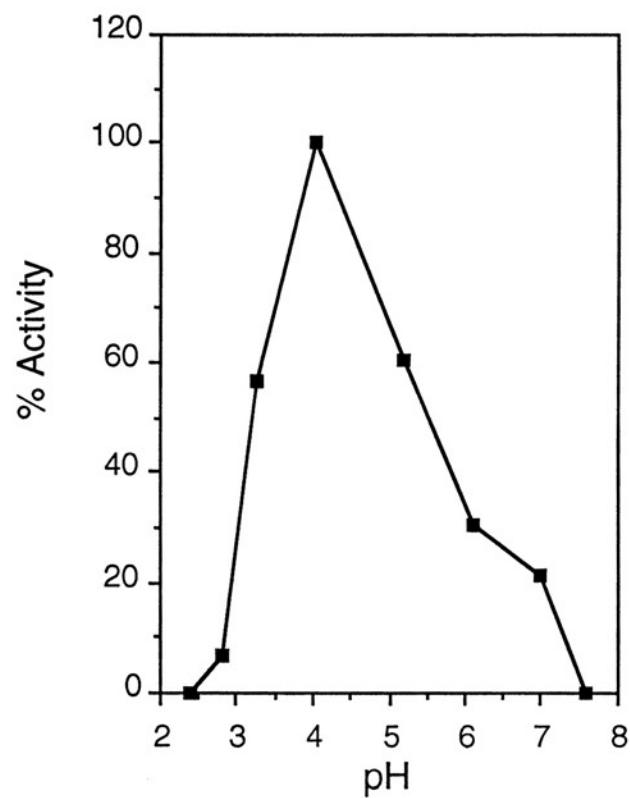
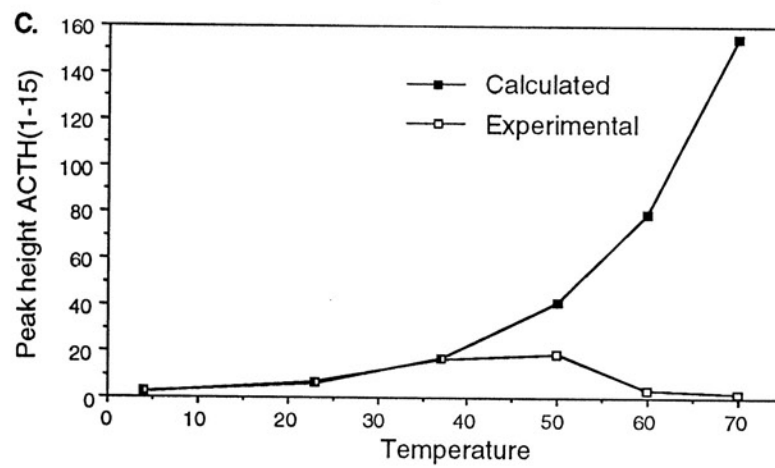
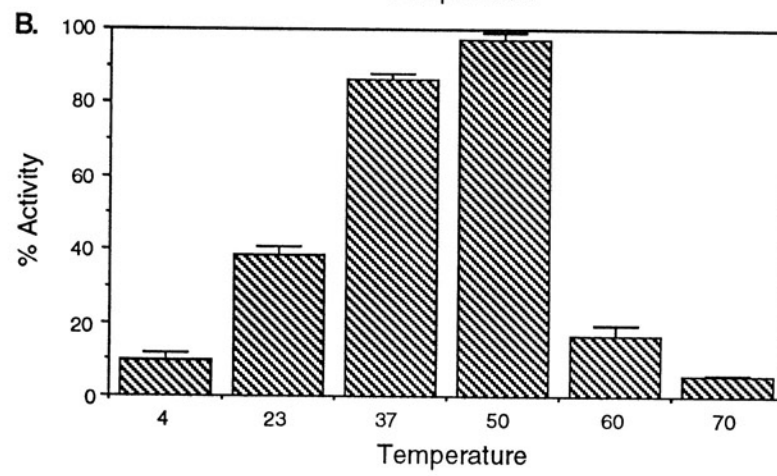
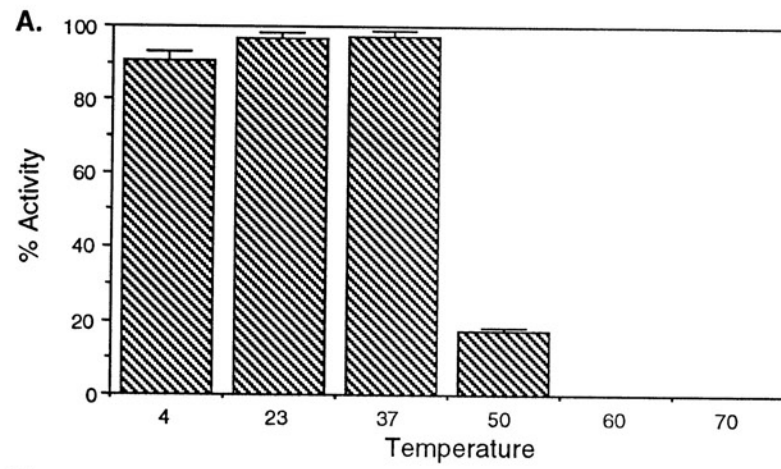


Figure 14. pH profile of secreted YAP3p activity

Equal aliquots of partially purified secreted YAP3p were assayed for enzymatic activity at different pH's. The buffer system used was citric acid/sodium phosphate giving a pH range of 2.3-7.6.

Figure 15. Analysis of stability and dependence of secreted YAP3p activity on temperature

(A) YAP3p was preincubated for 1h at 4-70°C and then assayed for residual activity by the ACTH¹⁻³⁹ assay. **(B)** YAP3p was assayed directly at varying temperatures, 4-70°C. The results shown in A and B are the mean of three experiments, the error bars show the standard error of the mean. Activity is expressed as $\mu\text{g ACTH}^{1-15}$ generated/h. **(C)** A comparison of the calculated and experimental activity dependence of YAP3p on temperature. The ordinate shows the peak height of ACTH¹⁻¹⁵ product generated/30min in arbitrary units. The abscissa shows the temperature.



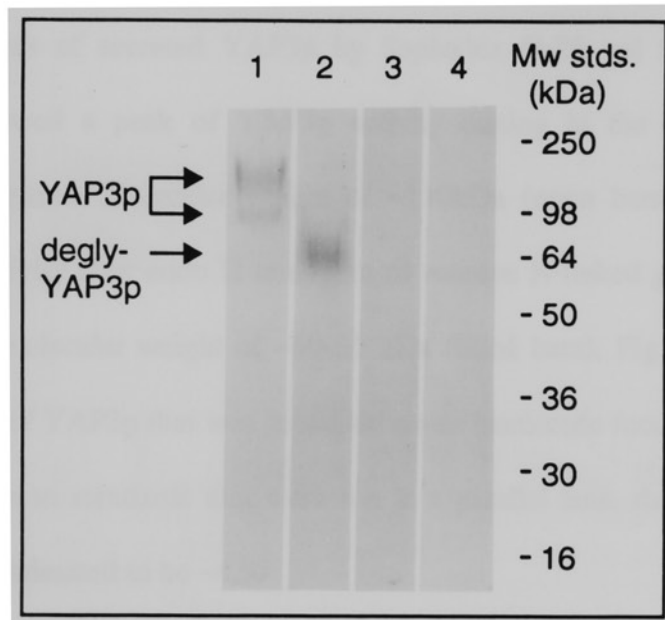


Figure 16. Western blot analysis of secreted YAP3p using antiserum MW283

Identical aliquots of partially purified YAP3p were loaded in each lane, except that the sample in lane 2 was treated with endoglycosidase H prior to the SDS-PAGE. Lane 1 and 2, probed with MW283 antiserum, lane 3, probed with MW283 preimmune serum, and lane 4, probed with MW283 antiserum that had been preabsorbed with MBP-YAP3p fusion protein. Protein standards used were Novex SeeBlue prestained standards, molecular mass range 250kDa-6kDa. All proteins were run in reducing conditions.

apparent in the media from untransformed or transformed/uninduced cells (data not shown).

Analysis of secreted YAP3p by Sephadex G-75 gel filtration chromatography (Fig.17), showed a peak of YAP3p activity eluting in the included volume with a calculated apparent molecular weight of ~110kDa (open bars). YAP3p maintained its enzymatic activity after endo H treatment to remove N-linked glycosylation, eluting with an apparent molecular weight of ~60-65 kDa (filled bars). Fig.18 shows the result of a Western blot of YAP3p that was separated on an isoelectric focussing polyacrylamide gel. In comparison to standards that were run in a parallel lane, the isoelectric point (pI) of YAP3p was estimated to be ~4.5.

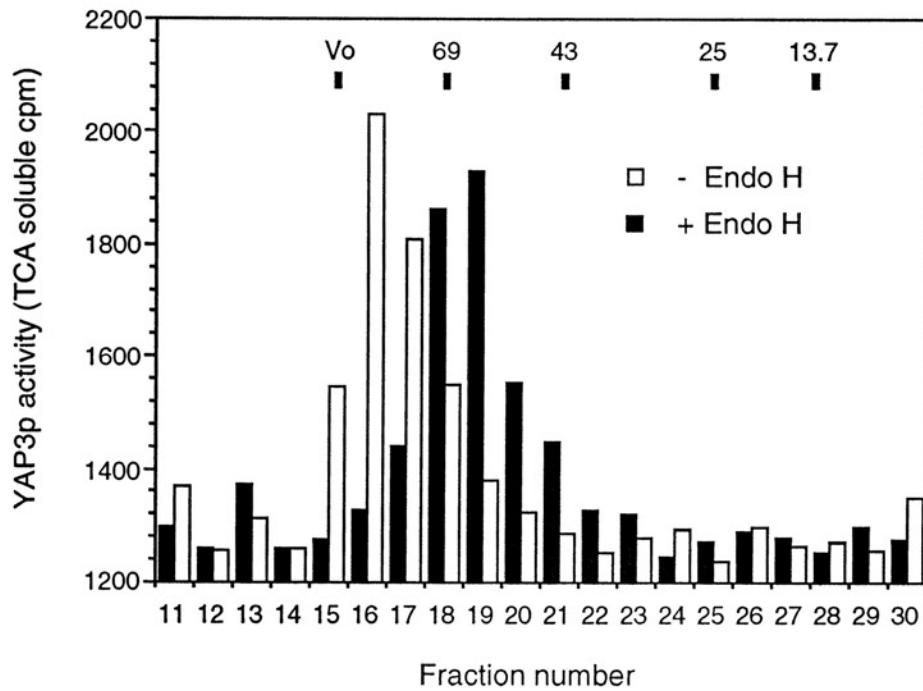


Figure 17. Sephadex G-75 gel filtration of secreted YAP3p

Endoglycosidase H treated (■) and non-endoglycosidase H treated (□) secreted YAP3p activity. Gel filtration standards were Vo = Dextran blue (2000 kDa), BSA (69 kDa), Ovalbumin (43 kDa), Chymotrypsin (25 kDa) and RNase (13.7 kDa).

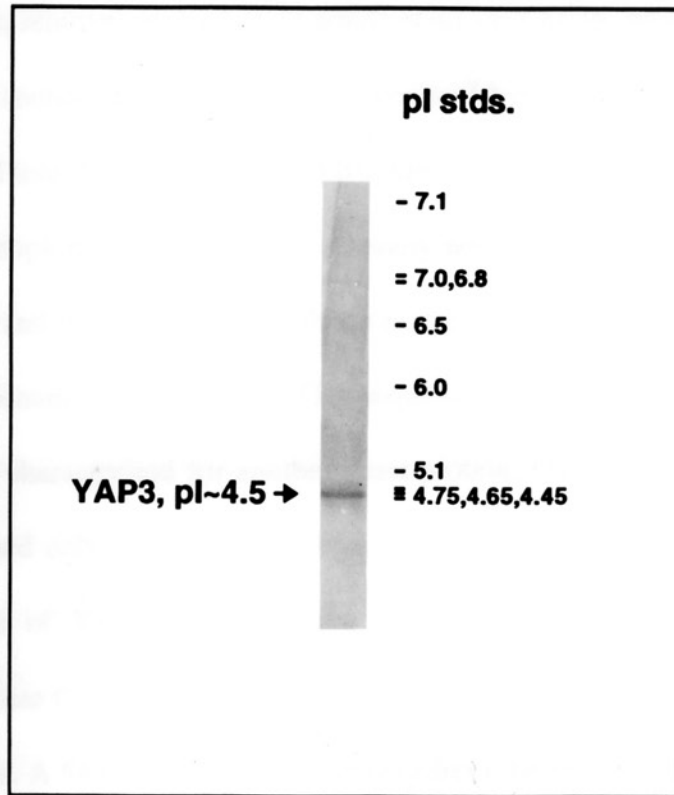


Figure 18. Isoelectric point (pI) determination of YAP3p

An aliquot of secreted YAP3p was separated by isoelectric focussing polyacrylamide gel electrophoresis and then transferred to nitrocellulose for western blot analysis by MW283. Isoelectric focussing protein standards that were run in parallel and stained by aurodye are indicated and YAP3p is shown by the *arrow*.

DISCUSSION

While full length YAP3p was shown to be primarily associated with yeast cell membranes, removal of the last 37 amino acids of YAP3p, which included a putative GPI consensus anchoring sequence and a domain of hydrophobic residues, caused YAP3p to be secreted into the medium (Fig.10.B). Although the last 17 amino acids of YAP3p have a very hydrophobic character, it is generally not considered to be long enough to span a membrane and thus association with the membrane is unlikely to be through an interaction with this domain. The consensus GPI sequence of YAP3p (aa541-548) is similar to that previously characterized for another yeast protein, Gas1p (71). However, until now this has remained only a putative membrane anchoring site of YAP3p. Our results, showing the release of YAP3p activity from the membranes by phosphatidylinositol specific phospholipase C, provide evidence for the membrane association of YAP3p via this GPI binding site. A 54% release of total activity from the membranes was observed but this in fact may be an underestimation due to the possibility that some YAP3p may not have been accessible to the PLC. A low amount of YAP3p activity was detected in the supernatant of the negative control (i.e. incubation of membranes with boiled PLC) even in the presence of PMSF and EDTA, suggesting that this basal release of YAP3p from the membranes is not due to the action of serine, thiol or metallo-proteases on amino acid residues near the GPI anchoring site. It is also unlikely to be due to proteolytic cleavage by YAP3p itself or other yeast aspartic proteases since they are not active at pH 7.4. Most likely, other enzymes that can cause dissociation of the membrane structure such as membrane bound lipases or glycosidases may be responsible for the low basal release.

However, the results clearly demonstrate that treatment of the membranes with PLC causes significant release of YAP3p activity above the basal level.

The generation of a GPI binding site occurs in the endoplasmic reticulum (ER) (83). The mechanism involves specific C-terminal cleavage of the protein to be anchored presumably after the Asn of the GPI consensus sequence. Thus, wild type YAP3p is probably naturally C-terminally truncated at Asn⁵⁴⁸ and is associated with the membrane through this C-terminal amino-acid. Additionally, recognition for a protein to be anchored by this mechanism is facilitated by the C-terminal hydrophobic region, since site directed mutagenesis of a hydrophobic residue to an Arg in the C-terminus hydrophobic domain of Gas1p, which is normally GPI anchored, resulted in the loss of membrane anchoring of this protein and subsequent secretion (71). While other processing proteases, such as furin and Kex2p, also appear to be membrane associated via the C-terminus (75,76) the association of these enzymes appear to be via their transmembrane domain rather than by GPI binding since they lack the appropriate consensus sequence.

The cellular localization of the membrane associated YAP3p has not been determined directly, but it has been deduced to be associated on the extracellular side of the plasma membrane based on the following observations. 1. *YAP3* was initially cloned based on the ability of its gene product to process pro- α -mating factor *in vivo* demonstrating that it was localized to a compartment in the yeast secretory pathway (23). 2. Making spheroplasts by treatment with zymolase, or glass-bead lysis of yeast cells followed by alkali extraction of cell wall mannoproteins, demonstrated that YAP3p sedimented with the spheroplasts upon centrifugation and was not released under the

alkali extraction conditions, indicating that the YAP3p was not associated with the yeast cell wall (72). 3. Since the pH optimum of YAP3p was determined to be at pH 4.0-4.5 it is highly unlikely that YAP3p is functionally active in and therefore localized to the endoplasmic reticulum (ER) or cis- or medial-Golgi compartments. 4. In an elegant experiment by Olsen, (1994), a fusion protein containing the first 150 amino acids of carboxypeptidase Y (CPY) and invertase was constructed. The CPY sequence caused the fusion protein to be sorted to the yeast vacuole resulting in the absence of extracellular invertase activity. When a pro- α -mating factor cleavage site was engineered at the junction between the two proteins, invertase activity was detected extracellularly as a result of its processing by Kex2p in the Golgi. This demonstrated that sorting to the vacuole takes place in a compartment distal to the Kex2p action, most probably in the trans golgi network (TGN). However, in a Kex2 deficient mutant, expressing high levels of YAP3p which is capable of cleaving the pro- α -mating factor cleavage site, the fusion protein was sorted to the vacuole. This indicated that YAP3p was most probably localized to a compartment distal to the TGN, i.e. either in the secretory vesicles or plasma membrane. Any YAP3p that is associated within these secretory vesicles will ultimately be localized to the extracellular side of the plasma membrane after exocytosis. Immunoelectron microscopy would be necessary to directly confirm this localization of YAP3p.

The secreted form of truncated YAP3p was overexpressed and characterized with respect to its physical properties. The predicted molecular mass of the truncated YAP3p is ~49kDa, based on the removal of the signal peptide, putative pro-region and the last 37 amino-acids of the protein. Previously, recombinant truncated YAP3p, purified from the

cellular extract of yeast cells, was determined to be a ~70kDa glycoprotein (80). In this study, the secreted truncated forms of YAP3p were characterized by Western blot as hyperglycosylated enzymes of ~90kDa and ~150-180kDa. Since the ~150-180kDa band was rather broad, it may contain a heterogenous population of differentially hyperglycosylated forms of YAP3p. The possibility exists that the ~150-180kDa form of YAP3p is a dimer of the 90kDa form. However, since the protein sample had been boiled in buffer containing 2% SDS and 5% β -mercaptoethanol prior to SDS-PAGE, this seems highly unlikely. Upon treatment with endoglycosidase H, both bands shifted to one band of ~65kDa. The residual size difference between the ~65kDa form and the predicted molecular mass is probably due to O-linked glycosylation. There was no evidence for the ~70kDa cellular form of YAP3p being secreted. These results suggest that the biosynthetic pathway of YAP3p involves glycosylation to a ~70kDa form followed by hyperglycosylation to ~90kDa and ~150-180kDa forms prior to secretion. The phenomenon of hyperglycosylation is not unusual in yeast. For example, another aspartic protease from yeast, Bar1, is ~300% larger than the expected size due to hyperglycosylation (55). Surprisingly, the secreted forms of YAP3p determined by SDS-PAGE as ~150-180kDa and ~90kDa proteins were found in the included volume (apparent molecular mass ~110kDa) and not the void volume of the Sephadex G-75 gel filtration column. This experiment has been repeated several times using different enzyme preparations with the same result, suggesting that the molecular shape may have a significant influence on the retention of the hyperglycosylated YAP3p on this column independent of molecular mass. In addition, while the conditions of the run were such that

ionic interactions were minimized (see methods) the inclusion of YAP3p may also be the result of non-specific binding of the sugars on the protein with the Sephadex beads.

A comparison of the secreted YAP3p and that of the cellular component, previously described, shows that there is no evident difference in specificity as observed by the ACTH¹⁻³⁹ assay and the profile of products generated from radiolabelled mouse POMC (80). Similarly, the dependence of this activity on pH showed only a slightly broader pH profile than that obtained for the cellular form. Both had a pH optimum between 4.0 and 4.5. The stability of secreted YAP3p at different temperatures show that this enzyme follows a typical heat inactivation profile, going from 100% to 0% activity when preincubated for 1h between 37°C and 60°C (Fig.15.A). However, the ability of YAP3p to generate more product at 50°C than at 37°C in a 30min incubation (Fig.15.B) is an indication that the increase in the rate of enzymatic activity, due to the increased temperature, $Q_{10}=1.95$, (Fig.15.C) is faster than the rate of heat inactivation. This may be important when considering a function for YAP3p *in vivo*. Although the function of YAP3p *in vivo* is still unknown, it is conceivable that it is related to stress reponse, in that it may get induced in a heat shock manner. Upon closer scrutiny of the promoter region of the *YAP3* gene, putative heat shock elements are evident that maybe involved in this reponse in yeast (72). Since yeast normally grow at an optimum temperature of ~30°C, the ability of a heat induced enzyme to function satisfactorily at the higher temperature may have a profound effect on the viability of the cell. Although *YAP3* was previously shown to be a non-essential gene under normal conditions (69), it would be interesting to determine the capacity of its function in yeast at elevated temperatures. In addition to heat

stability, partially purified YAP3p from the growth media was found to withstand two consecutive lyophilizations which did not result in any detectable loss of enzymatic activity (unpublished data). The lyophilized powder was stable indefinitely. Furthermore, YAP3p enzyme that has been stored for over 8 months at -20°C appears to be stable.

In summary, a carboxy-terminally truncated form of YAP3p has been engineered that is secreted from yeast cells and easily harvested. This truncated YAP3p enzyme appears to be identical in specificity to full length YAP3p (Fig.10.A and B, ACTH¹⁻³⁹ assay). The temperature dependence and stability of secreted YAP3p and the ability to store the enzyme for an indefinite period in a lyophilized form without losing enzymatic activity renders this enzyme highly useful commercially for the *in vitro* production of hormones and neuropeptides from recombinant precursors, such as proinsulin. The functionality of YAP3p at higher temperatures found in this study suggests that this enzyme may play an important role in yeast cells *in vivo* under heat induced stress.

CHAPTER 5

CHARACTERIZATION OF THE ENZYMATIC ACTIVITY OF SECRETED YEAST ASPARTIC PROTEASE 3

PART 1. PROCESSING OF ANGLERFISH PROSOMATOSTATIN I AND II BY YAP3p

Based on the published work entitled “Purified yeast aspartic protease 3 cleaves anglerfish pro-somatostatin I and II at di- and monobasic sites to generate somatostatin-14 and -28”. Niamh X. Cawley, Bryan D. Noe and Y. Peng Loh. (1993) *FEBS* **3** 273-276

SUMMARY

YAP3p cleaved aPSS II at a mono-basic residue which has an upstream Arg in the P6 position, to yield somatostatin-28 (aSS-28), but not at the analogous mono-basic residue cleavage site in aPSS I which has the upstream Arg substituted by a histidine. This latter finding indicated that in addition to recognising the paired-basic residue motif, YAP3p also shows specificity for a mono-basic residue motif with an upstream Arg. Furthermore, YAP3p cleaved the mono-basic residue site of aPSS II more rapidly than the paired-basic residue site of aPSS I.

INTRODUCTION

Somatostatin-14 and somatostatin-28 are derived from a common precursor in mammals, but in anglerfish, they are cleaved from two different precursors, pro-somatostatin I (aPSS-I) and pro-somatostatin II (aPSS-II) which are synthesized in different cells, Fig.19. From gene deletion experiments, YAP3p has been implicated to cleave at a mono-basic site of anglerfish pro-somatostatin II to yield the mature hormone, somatostatin-28, when this prohormone gene was transfected into yeast cells (69,73). However, confirmation that this cleavage activity is mediated by YAP3p awaits *in vitro* studies with the purified enzyme.

PROCEDURES

Preparation of [³⁵S]Cys labeled anglerfish pro-somatostatin I and II

Anglerfish islet prohormones, aPSS-I and aPSS-II were radiolabelled by incubating islet tissue with [³⁵S]Cys. Tissue homogenates were subjected to gel filtration and the prohormones were isolated by high-performance liquid chromatography (HPLC) as previously described (84,85). Samples containing aPSS-I and aPSS-II were partially dried down using a speed vac concentrator, and used for incubation with YAP3p enzyme. The specific activities of aPSS-I and aPSS-II were 7.61×10^5 cpm/ μ g protein and 2.9×10^5 cpm/ μ g protein, respectively, based on HPLC absorbance profiles at 210nm.

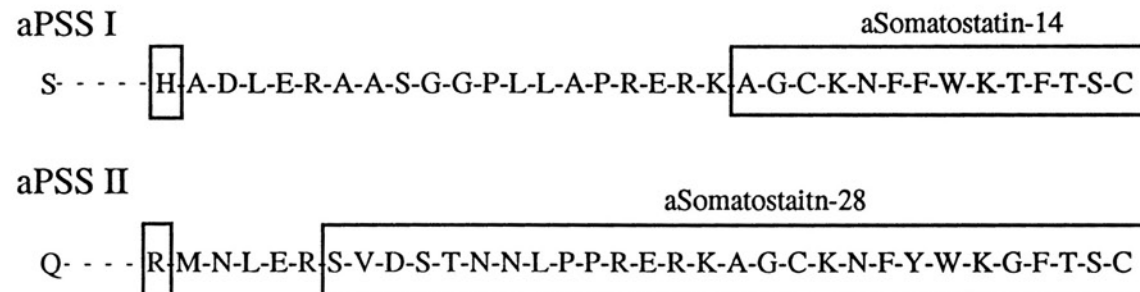


Figure 19. Schematic diagram of anglerfish prosomatostatin I and II

aPSS I and II, anglerfish prosomatostatin I and II, respectively. Amino acids are represented by their single letter codes.

Preparation of Yeast Aspartic Protease 3

Transformed yeast, strain BJ3501 containing the *YAP3* gene were induced to express YAP3p activity as previously described (Chap.4). The YAP3p enzymatic activity that was secreted into the growth media was partially purified by concanavalin A (ConA) affinity chromatography. The ConA eluted protein was desalted, lyophilized, reconstituted with water and stored at -20°C until used. The concentration of YAP3p in this preparation was determined to be ~1.9 pmoles/μl by quantitative Western/dot blot using enhanced chemiluminescence and comparison to a standard curve of a known concentration of YAP3p. The stored activity was stable for over 10 months. This recombinant YAP3p preparation was determined to contain no other proteolytic activity by the following criteria: 1. Growth media or ConA purified growth media from both untransformed and transformed/uninduced yeast cells were found to have no proteolytic activity when assayed by the sensitive ^{125}I - β -LPH assay. 2. Pepstatin A, which is a specific inhibitor of aspartic proteases, completely inhibited the secreted proteolytic activity from the galactose induced transformed yeast. 3. Using ACTH¹⁻³⁹ as substrate, the two products generated by YAP3p which have been identified previously by HPLC and amino acid sequencing, as ACTH¹⁻¹⁵ and CLIP¹⁶⁻³⁹, were stable over time. There were no anomalous cleavages in the presence of pepstatin A, indicating the absence of any other proteolytic activity including carboxypeptidase or aminopeptidase activity in the enzyme preparation.

Incubation of aPSS-I and aPSS-II with YAP3p and analysis of products

ConA purified YAP3p (15.2 pmoles) was incubated with ~5200 cpm [^{35}S]Cys labeled aPSS-I (6.8 ng) or ~4500 cpm aPSS-II (15.4 ng) for 1, 2 and 6 hr at 37°C in 0.1

M sodium citrate buffer, pH 4.0 with and without 10^{-4} *M* pepstatin A (Sigma, St. Louis, MO). The reaction was terminated by the addition of glacial acetic acid to a final concentration of 3 *M*. The products formed were analyzed by reverse phase HPLC as previously described (86). A 0.1% trifluoroacetic acid/acetonitrile gradient system was used for HPLC and 0.8 ml fractions were collected for scintillation counting.

RESULTS

Fig.20.A shows the cleavage of aPSS-I by YAP3p at the pair of basic residues, Arg⁸¹-Lys⁸², to yield SS-14 and [Lys⁻¹]SS-14. The formation of these two products indicates that YAP3p cleaved on the carboxyl side and in between the Arg⁸¹-Lys⁸² pair of aPSS-I. Interestingly, YAP3p did not cleave at the mono-basic Arg of aPSS-I to generate aSS-28. Pepstatin A completely inhibited the formation of SS-14 confirming that the cleavage at the paired basic residues of aPSS-I was due to the aspartic protease YAP3p (Fig.20.A).

Incubation of aPSS-II with YAP3p enzyme resulted in the cleavage of this substrate to yield somatostatin-28 (aSS-28), but not [Tyr⁷,Gly¹⁰] SS-14 (Fig.20.B). The lack of formation of [Tyr⁷,Gly¹⁰] SS-14 was further confirmed using a shallower HPLC gradient (identical to Fig.20.A) which better separated [Tyr⁷,Gly¹⁰] SS-14 from aSS-28 (data not shown). Pepstatin A completely inhibited the generation of aSS-28 from aPSS-II, indicating that the enzymatic activity was due to the aspartic protease, YAP3p (Fig.20.B). No aSS-28 was formed when aPSS-II was incubated without YAP3p. These results indicate that YAP3p cleaved aPSS-II at the monobasic site, Arg⁷³, to yield aSS-28,

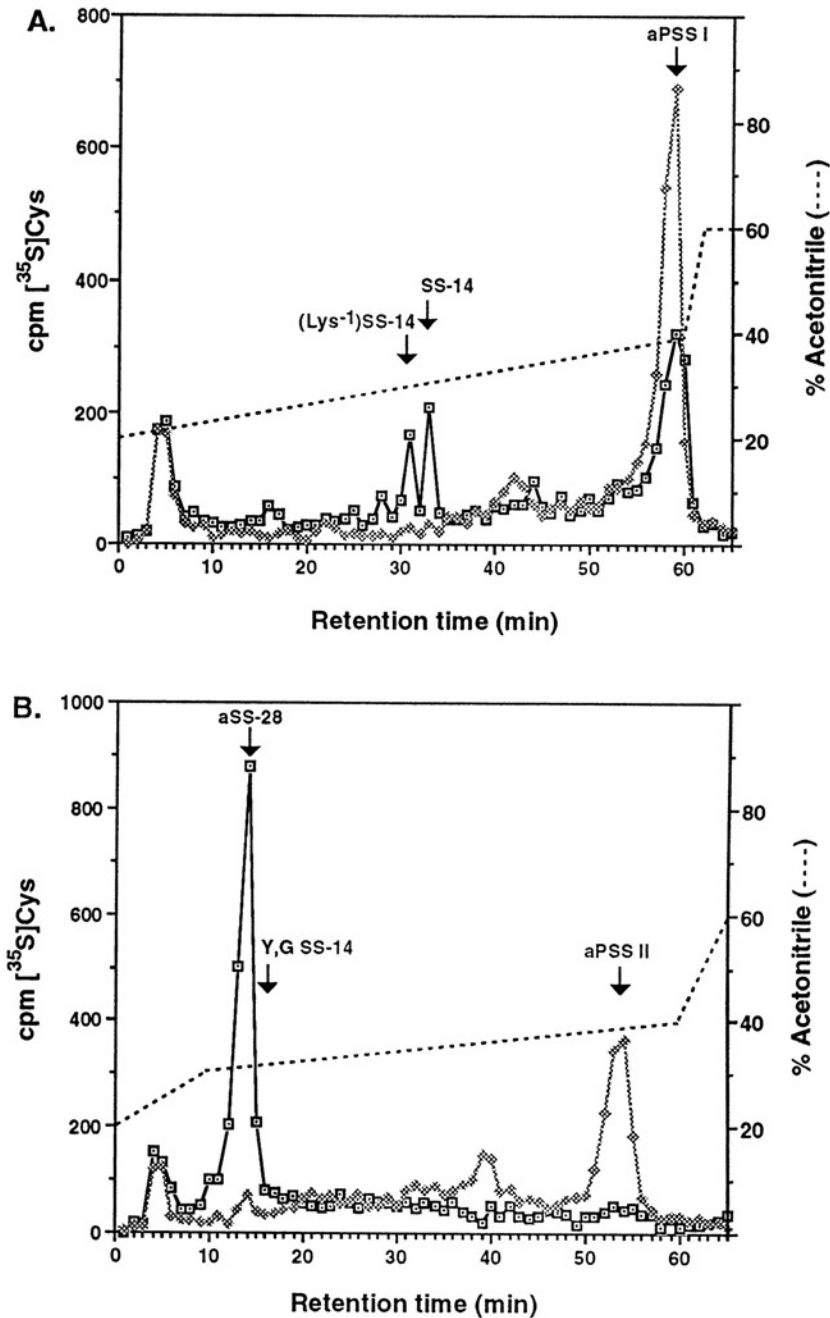


Figure 20. Cleavage of anglerfish prosomatostatin I and II by YAP3p

(A) HPLC profiles of products generated by incubating aPSS I with YAP3p for 6h at 37°C in pH 4.0 buffer without (□) and with (◆) pepstatin A. **(B)** HPLC profiles of products generated by incubating aPSS II with YAP3p for 6h at 37°C in pH 4.0 buffer without (□) and with (◆) pepstatin A. The arrows show where standards elute and the dotted lines show the acetonitrile gradients which ran from 20-39% in 60min in **A** and 20-29% in 10min, 29-33% in 20min, and 33-39% in 30min in **B**. Y = Tyr, G = Gly.

but not at the dibasic, Arg⁸⁶-Lys⁸⁷ site to yield [Tyr⁷,Gly¹⁰] SS-14. See Fig.19 for the primary sequence of aPSS I and aPSS II.

The time course of generation of SS-14 and aSS-28 from aPSS-I and aPSS-II respectively, by YAP3p, was analyzed (Fig.21). Production of SS-14 and aSS-28 was linear between 1 to 6 hr under the incubation conditions used ($r^2 = 0.98$, slope = 54.1 for SS-14 and $r^2 = 0.99$, slope = 271.6 for aSS-28). These results demonstrate that the rate of generation of aSS-28 from aPSS-II by YAP3p was five-fold greater than the rate of SS-14 formation from aPSS-I, however, since there was about twice as much aPSS-II than aPSS-I in the reactions, a more accurate assessment of the relative rates would be a greater than two fold preference for the generation of aSS-28 than SS-14 from aPSS-II and aPSS-I, respectively.

DISCUSSION

Previous studies have identified a subtilisin-related PC2-like serine protease, purified from anglerfish islet secretory granules, as the endogenous enzyme that cleaves aPSS-I to yield SS-14 (87). This enzyme also cleaved aPSS-II to yield [Tyr⁷,Gly¹⁰]SS-14, a tetradecapeptide analogue of SS-14 (87). A different enzyme was purified from anglerfish islet secretory granules that processes aPSS-I to SS-28 at the mono-basic residue. This enzyme was characterized as a 39kDa aspartic protease with a pH optimum of 4.2 (67). More recently, by the use of deletion mutants of the *YAP3* gene in yeast, it was suggested that an aspartic protease encoded by this gene was involved in the processing of aPSS-II to aSS-28 when the prohormone gene was transfected into yeast

cells (69). Results from the present *in vitro* study (Chap.5, part 1) unequivocally demonstrate that YAP3p can specifically cleave the mono-basic Arg⁷³ residue of aPSS-II to generate aSS-28. However, YAP3p did not cleave the mono-basic site of aPSS-I to yield the aPSS-I form of SS-28. Conversely, YAP3p cleaved the Arg⁸¹-Lys⁸² of aPSS-I, but not the equivalent paired-basic pair of aPSS-II to generate [Tyr⁷,Gly¹⁰]SS-14. These data clearly indicate that the structure and conformation of the substrates play a very important role in dictating specificity of cleavage of prohormones. The presence of a single basic residue in the P6 position in aPSS-II is consistent with the rules governing mono-basic cleavage sites (88) and accounts for the processing at Arg⁷³. The lack of cleavage at the mono-basic site of aPSS-I may be due to the presence of His at position P6 instead of a basic residue. Site-directed mutagenesis studies involving substitution of amino acids adjacent to the cleavage sites of human prosomatostatin have identified a region located between Asn⁻¹² and Gly⁺¹² that is important for processing the prohormone to SS-14 and SS-28. Specifically, mutation of the nucleotides encoding Pro⁻⁵ and Pro⁻⁹ for Ala, a β -turn blocker, within the PSS gene, resulted in a dramatic decrease in processing when the mutated gene was transfected into Neuro 2A cells, supporting a role for secondary and tertiary structure in directing cleavage of the prohormone (89).

The ability of YAP3p to cleave aPSS-II at the mono-basic site more rapidly than at the paired-basic site of aPSS-I raises the possibility that the anglerfish SS-28 generating aspartic protease purified from islets may be a fish homologue of YAP3p. While YAP3p may cleave the mono-basic residue of aPSS-II more rapidly than the paired-basic residues of aPSS-I, raising the possibility that YAP3p may have a greater preference for mono-basic residue sites, this relative difference may be only for these two substrates.

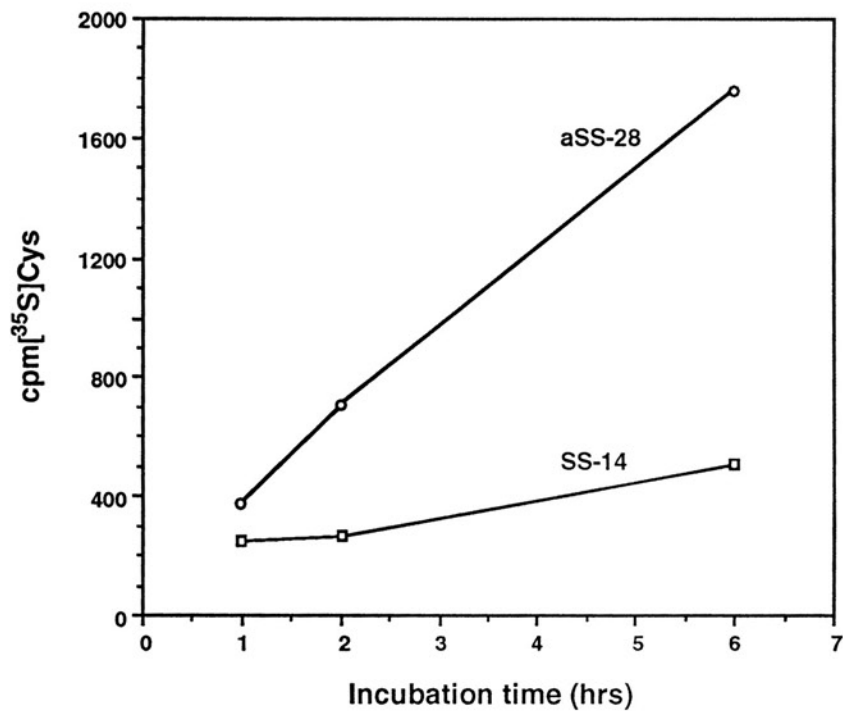


Figure 21. Time course for the cleavage of aPSS I and aPSS II by YAP3p

The products, aSS-14 and aSS-28, generated by YAP3p from aPSS I and aPSS II, respectively, were quantitated from a 1, 2, and 6h incubation. The graph shows that the generation of aSS-28 from aPSS II was at a higher rate than the generation of aSS-14 from aPSS I.

Further work is necessary to determine if YAP3p is generally more efficient in cleaving at mono-basic than paired-basic residues of various prohormones. Also, since the paired-basic and mono-basic sites are present in both precursors, the results indicate that the structure and conformation of these substrates dictate where cleavage occurs.

PART 2. PROCESSING OF PROHORMONE SUBSTRATES CONTAINING MONO- AND/OR PAIRED-BASIC RESIDUE CLEAVAGE SITES BY SECRETED YAP3P

SUMMARY

The specificity and relative efficiency of cleavage of mono- and paired-basic residue processing sites by YAP3p was determined *in vitro* for a number of prohormone substrates: human ACTH¹⁻³⁹, bovine proinsulin, porcine cholecystokinin 33, cholecystokinin 13-33, dynorphin A(1-11), dynorphin B(1-13), and amidorphin. YAP3p generated ACTH¹⁻¹⁵ from ACTH¹⁻³⁹. It cleaved proinsulin at the paired-basic residue sites of the B-C junction as well as the C-A junction. Leu-enkephalin-Arg and Leu-enkephalin-Arg-Arg were generated from dynorphin A and dynorphin B, respectively. YAP3p generated Met-enkephalin-Lys-Lys from amidorphin showing that cleavage by YAP3p can occur at a lone pair of Lys residues. CCK33 was cleaved at Lys²³ and Arg⁹, each containing an upstream Arg residue at the P6 and P5 position, respectively.

The K_m and k_{cat} values were determined for each of these cleavages. K_m values were between 10^{-4} - 10^{-5} M for the various substrates, with the highest affinity exhibited for the tetra-basic site of ACTH¹⁻³⁹, (1.8×10^{-5} M). The relative catalytic efficiency of YAP3p indicates that the tetra-basic residue site of ACTH¹⁻³⁹ was cleaved with the highest relative efficiency ($k_{cat}/K_m = 3.1 \times 10^6 \text{ M}^{-1} \text{ s}^{-1}$), while that of the mono-basic site of CCK13-33 and the paired-basic site of proinsulin B-C junction, were cleaved less efficiently at $4.2 \times 10^4 \text{ M}^{-1} \text{ s}^{-1}$ and $1.6 \times 10^4 \text{ M}^{-1} \text{ s}^{-1}$, respectively.

INTRODUCTION

It is clear that *in vitro* analysis of the specificity of YAP3p on POMC (Chap. 2 and 4) and aPSS I and aPSS II (this Chap., part 1) alone is insufficient to completely define the specificity of YAP3p, or to conclude that YAP3p would in general cleave the mono-basic residue motif of prohormones more efficiently than the paired-basic residue motif. In this study the specificity and kinetic parameters governing the processing of six different substrates of physiological importance; proinsulin, cholecystokinin 33, dynorphin A, dynorphin B, amidorphin and adrenocorticotropin hormone, containing mono- paired- and tetra-basic residue sites, by YAP3p was extensively investigated. This study also provides the first kinetic information on the efficiency of cleavage of paired versus mono-basic residue sites by an aspartic protease processing enzyme.

METHODS

Prohormone substrates

Porcine cholecystokinin 33 (CCK33) was provided by Victor Mutt, (Stockholm, Sweden). Cholecystokinin 13-33 and ACTH¹⁻³⁹ were purchased from Bachem California, (Torrence, CA). Porcine dynorphin A(1-11), dynorphin B/rimorphin(1-13) and amidorphin were purchased from Peninsula Laboratories Inc., (Belmont, CA). Bovine proinsulin was a generous gift from Drs. Jan Markussen and Knud Vad, Novo Nordisk, (Bagsvaerd, Denmark).

Preparation of Yeast Aspartic Protease 3

The procedure described in Part 1 of this Chapter for the partial preparation of YAP3p was used. The enzyme was further purified by anion exchange chromatography through a DEAE-Sephadex column. The YAP3p preparation was desalted, lyophilized, reconstituted with water and aliquoted for storage at -20°C until analysis. A unit of YAP3p activity is expressed as the amount of enzyme that generates 0.18µg ACTH¹⁻¹⁵/h from 10µg ACTH¹⁻³⁹ in 100µl 0.1 M sodium citrate at pH 4.0 and 37°C.

Assay and analysis of products generated by YAP3p

Cholecystokinin 33

One hundred ng of CCK33 was incubated with 0.14 units of YAP3p in 100µl, 0.1 M Na citrate, pH 4.0, for 1, 2, 5 and 8 h at 37°C in the presence and absence of 3.7×10^{-5} M pepstatin A, (ICN Biomedicals Inc., Aurora, OH.). Substrate alone and enzyme alone were incubated in parallel, as controls. The reaction was stopped by addition of 50µl 0.1 M HCl and immediately frozen on dry ice until analysis. Products were separated from the substrate by DEAE-Sephadex A-25 ion exchange resin and then quantitated by radioimmunoassay (RIA) with an antibody that recognizes CCK8, CCK12, and CCK33 (90). The products were then further analysed by Sephadex G-50 gel filtration chromatography and each fraction analysed by RIA. The CCK8-sized peak of immunoreactivity from the Sephadex G-50 column was further analysed by HPLC separation followed by RIA as described previously (90).

Proinsulin, cholecystokinin 13-33, dynorphin A, dynorphin B, amidorphin and ACTH¹⁻³⁹

Ten μg of each peptide were incubated with enzyme (0.028-1.41 units) in 100 μl , 0.1 M Na citrate, pH 4.0, at 37°C. The reactions were stopped by the addition of 10 μl glacial acetic acid. The products were separated on an LKB 2150 HPLC system using a Bio-Rad HiPore RP-318 column (5 x 250mm). Buffer A was 0.1% trifluoroacetic acid and buffer B was 80% acetonitrile in 0.1% trifluoroacetic acid. Products were monitored by OD 214nm and individual peaks were collected for amino-acid sequence identification. The peptide products from several HPLC runs were pooled and prepared for N-terminal amino acid sequence analysis by microcentrifugation in a Pro-Spin cartridge (Applied Biosystems, Foster City, CA.). Amino acid sequence analysis was carried out by Edman degradation using an Applied Biosystems Model 470A Protein Sequencer with an on-line phenylthiohydantoin analyzer. Control experiments for each substrate included incubations with pepstatin A, enzyme alone and substrate alone.

Determination of K_m and V_{max}

The method of Lineweaver-Burk (91) was used to calculate K_m and V_{max} values for the processing of various substrates by YAP3p. Reaction conditions (i.e. incubation time and enzyme amount) were determined such that the formation of product was linear with time within the substrate concentrations used and that 90% of the substrate remained after the reaction thus minimizing product inhibition. Four substrate concentrations, over the range above and below the K_m values obtained from preliminary experiments, were then used for each analysis which was done in triplicate. The initial rates and Lineweaver-

Burk plots obtained for the six substrates can be seen in the Materials and Methods section, Figs. 44-49.

Determination of k_{cat}

The absolute concentration of the active enzyme could not be determined since at present there are no irreversible active site titrants for YAP3p. Also, due to the relatively low affinity of YAP3p for pepstatin A ($K_i=3.7 \times 10^{-7} M$, see Chap.7), it was not possible to approximate the concentration of YAP3p by titration of the activity with this inhibitor. Enzyme concentration was therefore estimated based on protein concentration by comparison of the intensity of a Coomassie blue stained band of the YAP3p used in the reactions to a standard curve generated using purified YAP3p. Serial dilutions of purified YAP3p, quantitated by amino-acid analysis, were run on SDS-PAGE in parallel with an aliquot of the YAP3p solution used in the kinetic studies. The gel was stained by Coomassie blue, dried and scanned with a Digital CCD camera. The scanned image was processed using *NIH Image*, v1.57, and the areas of the stained proteins were quantitated. A plot of arbitrary units of area against the known YAP3p amounts loaded, generated a standard curve with the equation, $y=2.55+0.51x$, $r^2=0.987$. YAP3p in the unknown sample, that fell within the line, was calculated from this standard curve. Using this data, k_{cat} values, obtained from $V_{max}/[E]_T = k_{cat}$, where $[E]_T$ = total enzyme, were calculated. Since the YAP3p protein concentration and not the active enzyme concentration was used to calculate k_{cat} , the values obtained may be an underestimation. However, this will not affect the comparison of the relative cleavage efficiency (k_{cat}/K_m) of YAP3p for different substrates which have been assayed using the same enzyme preparation.

RESULTS

Proteolytic Processing of Proinsulin by YAP3p

Bovine proinsulin was cleaved by YAP3p to generate an intermediate product designated peak A in Fig. 22.B, upper panel. This peak contained three N-terminal amino-acid sequences and their PTH amino acid yields are reported in parenthesis. 1. F-V-N-Q-H-L-(X)-G-S-H (7.8 pmoles) corresponds to the N-terminal sequence of the insulin B chain, and 2. E-(V)-E-G-P-Q-V-G-A-L (5.7 pmoles) corresponds to the N-terminal sequence of the C peptide. The third sequence was the N-terminal Arg extended form of the C peptide (2.4 pmoles). This result demonstrated that YAP3p cleaved primarily on the carboxyl side of the paired-basic site, Arg³¹-Arg³², of the junction between B chain and C peptide of proinsulin. With prolonged incubation (36 hrs, data not shown), the two peaks designated peak B and peak C in Fig.22.B, upper panel, increased. These peaks, pooled from multiple reactions that had been scaled up, were subjected to complete N-terminal amino-acid sequence analysis. Peak B contained two N-terminal amino-acid sequences; insulin B chain, with Arg³¹-Arg³² extensions at the C-terminal; and insulin A chain with and without N-terminal extended Arg. The yields of Arg and Gly were 61.5 and 13.5 pmoles, respectively. The sequences of the A chain revealed that YAP3p cleaved the C-A junction in the middle and on the carboxyl side of the paired-basic site, Lys⁵⁹-Arg⁶⁰. Based on the average yields of PTH amino acids, a 4:1 ratio is calculated between the two cleavages at the bond Lys⁵⁹-Arg⁶⁰ and Arg⁶⁰-Gly⁶¹, respectively. Peak C was identified as C peptide. Pepstatin A inhibited the generation of these products (Fig.22.B, lower panel).

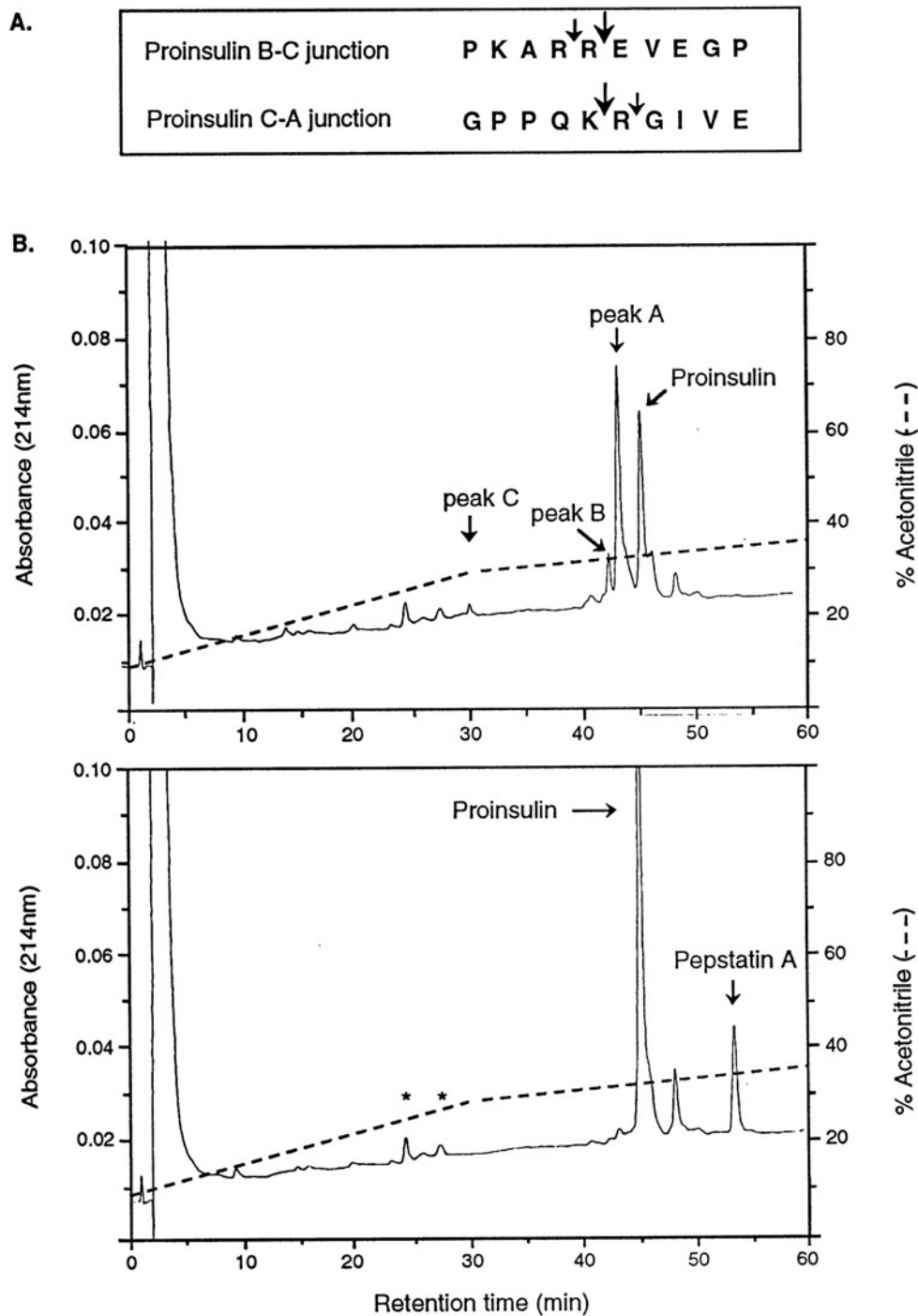


Figure 22. Proteolytic processing of proinsulin

(A) Primary amino acid sequences of proinsulin cleavage sites. Big and small arrows indicate major and minor sites cleaved by YAP3p. **(B) HPLC profile of products generated from bovine proinsulin incubated with YAP3p in the absence (upper panel) and presence (lower panel) of pepstatin A.** * = peaks that were present in the enzyme alone control.

The V_{max} for the processing of the B-C junction was determined to be 7.9 ± 0.4 pmoles/min and the K_m , k_{cat} and k_{cat}/K_m values are shown in Table 2.

Proteolytic Processing of CCK33 by YAP3p

YAP3p generated CCK8-immunoreactive products from CCK33 (Fig.23 for sequence) in a time-dependent manner while the presence of pepstatin A completely inhibited the generation of these products (Fig.24).

When products from the 5h time point were separated on a Sephadex G-50 gel filtration column and assayed by RIA, two peaks of CCK8-immunoreactivity which co-eluted with CCK22 and CCK8 standards were observed (Fig.25.A). Further analysis of the CCK8-sized peak by HPLC showed an elution profile that was identical to oxidized CCK8 standards (92) (Fig.25.B), indicating that YAP3p cleaved on the carboxyl side of the mono-basic Arg⁹ of CCK33 to generate CCK8. To verify the cleavage of YAP3p at Lys²³ of CCK33 that would generate CCK22 (see Fig.23 for sequence), CCK13-33 was incubated with YAP3p and the products were analysed by HPLC. Two homogenous products were generated (Fig.26, upper panel) and identified as CCK23-33 and CCK13-22, respectively, by amino-acid sequence analysis, indicating cleavage by YAP3p on the carboxyl side of Lys²³. The presence of pepstatin A completely inhibited the formation of these products (Fig.26, lower panel). No products were detected when substrate alone or enzyme alone were incubated (data not shown). The V_{max} for the cleavage of CCK13-33 was determined to be 29.2 ± 1.4 pmoles/min and the K_m , k_{cat} and k_{cat}/K_m values are shown in Table 2.

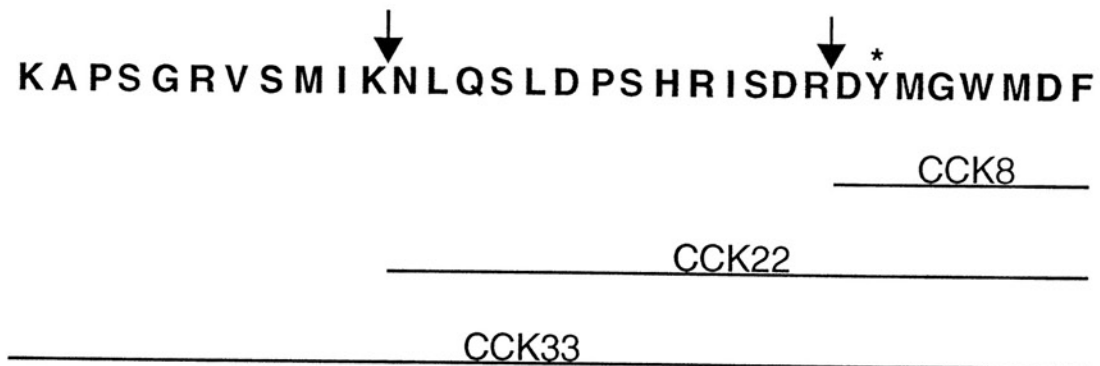


Figure 23. Primary amino acid sequence of CCK33

Arrows indicate the sites cleaved by YAP3p. R=Arginine, K=Lysine, Y=sulfated Tyrosine.*

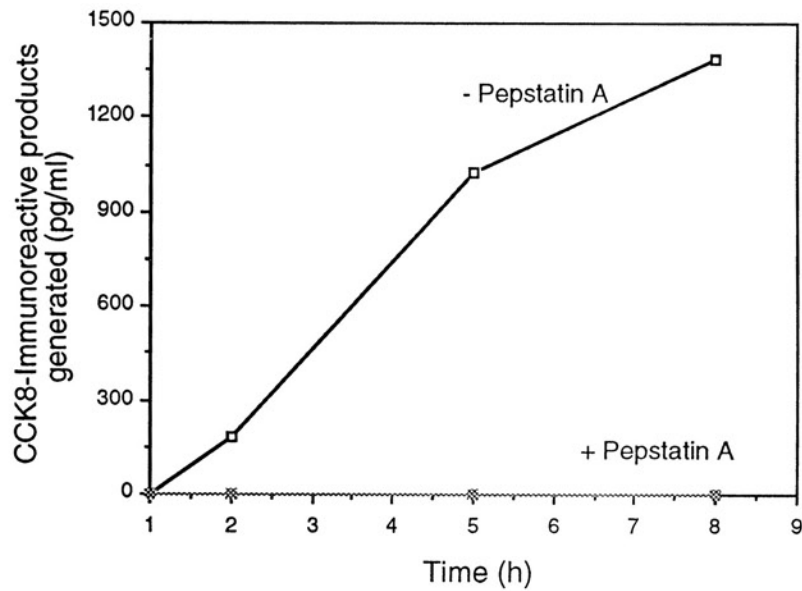


Figure 24. Time course of generation of CCK-immunoreactive products from CCK33 by YAP3p

Products from each time point were first purified with DEAE-Sephadex ion-exchange resin and an aliquot assayed by RIA. Open squares (□) indicate reactions in the absence of pepstatin A. Filled squares (■) indicate reactions in the presence of pepstatin A.

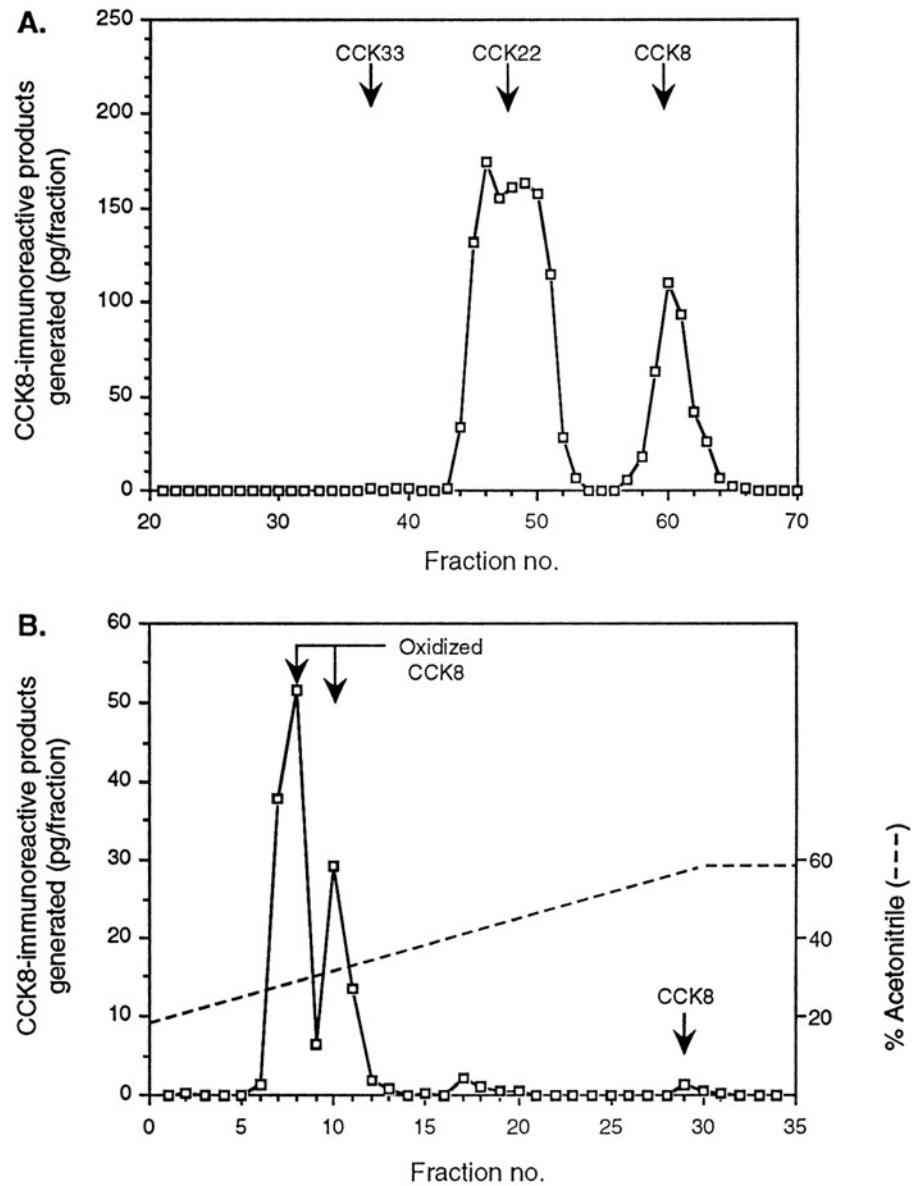


Figure 25. Proteolytic processing of cholecystokinin 33

(A) Sephadex G-50 gel filtration profile of CCK8-immunoreactive products generated by YAP3p. **(B)** Radioimmunoassay of fractions from reverse-phase HPLC separation of the CCK8-sized product generated from incubation of CCK33 with YAP3p. Products were purified by Sephadex G-50 filtration and the CCK8-sized product was further analyzed by HPLC. Arrows indicate positions of standards. Numbering of CCK peptides start from the C-terminus.

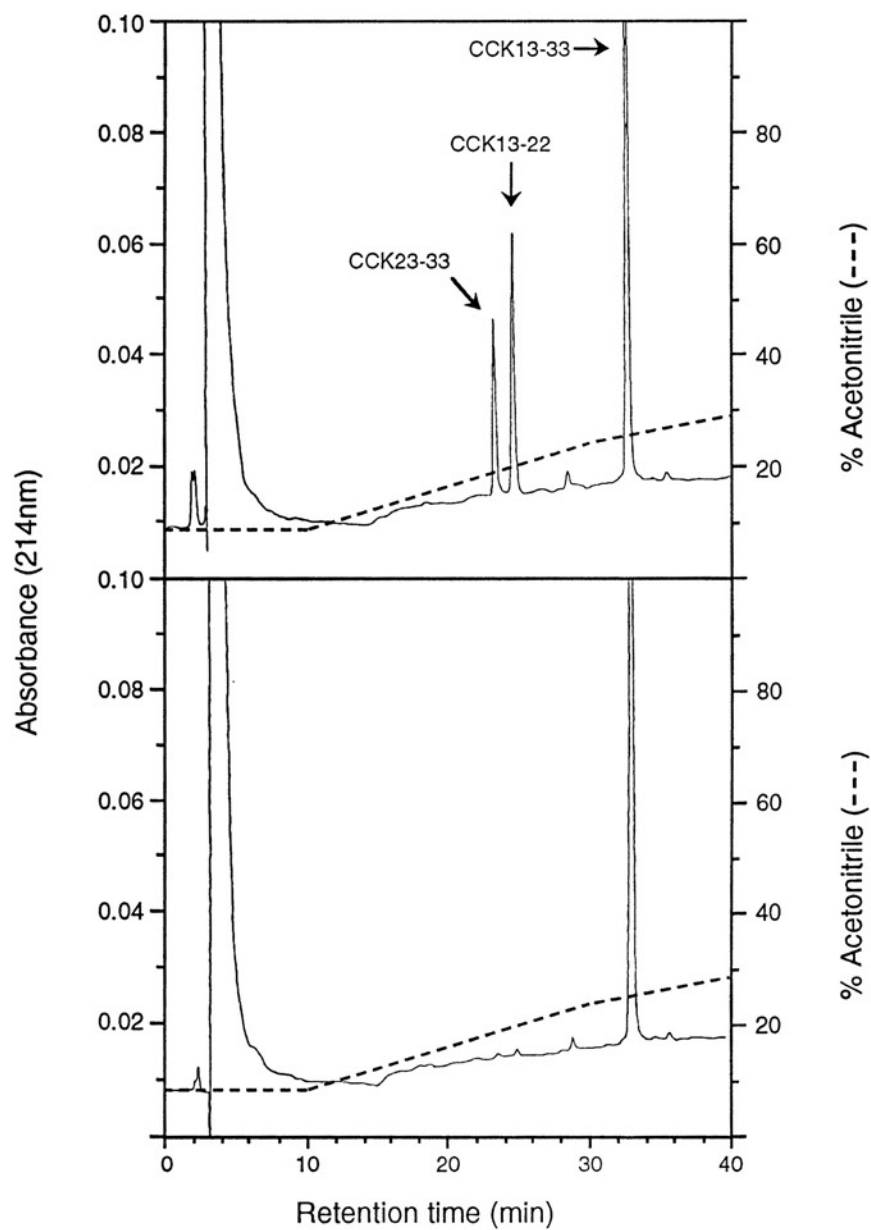


Figure 26. Proteolytic processing of cholecystokinin 13-33

HPLC profile of products generated from CCK13-33 incubated with YAP3p in the absence (upper panel) and presence (lower panel) of pepstatin A.

Proteolytic Processing of Dynorphin A, Dynorphin B and Amidorphin by YAP3p

YAP3p generated Leu-enkephalin-Arg and Leu-enkephalin-Arg-Arg from dynorphin A and dynorphin B, respectively (Fig.27 and Fig.28). Products generated from dynorphin A (Fig.27.B, upper panel) were identified as (R)-I-R-P-K, Leu-enkephalin-Arg-Arg (minor) and Leu-enkephalin-Arg (major), by amino acid analysis and comparison to standards that were run on the same HPLC system. In the peak identified as (R)-I-R-P-K, the ratio of this pentapeptide to its Arg truncated tetrapeptide (I-R-P-K) was approximately 35:1 based on the yields of PTH-Arg and PTH-Ile at cycle 2 of the amino acid sequence analysis and comparison of peak heights between the peaks of Leu-enk-Arg and Leu-enk-Arg-Arg. This demonstrated that YAP3p preferentially cleaved between the Arg⁶-Arg⁷ pair of dynorphin A to yield mainly Leu-enkephalin-Arg. Products generated from dynorphin B (Fig.28.B, upper panel) were identified as Q-F-K-V-V-T and Leu-enkephalin-Arg-Arg which demonstrated a different processing pattern to that of dynorphin A because the preferred site of cleavage was on the carboxyl side of the Arg⁶-Arg⁷ pair of dynorphin B to yield Leu-enkephalin-Arg-Arg. Amidorphin was cleaved by YAP3p to generate primarily Met-enkephalin-Lys-Lys and to a lesser extent Met-enkephalin-Lys (Fig.29.B). The generation of all products by YAP3p was inhibited by pepstatin A (Figs.27.B, 28.B and 29.B, lower panels) and no products were detected when substrate alone or enzyme alone were incubated (data not shown). The V_{max} for the generation of Leu-enkephalin-Arg from dynorphin A was 118.5±4.4 pmoles/min, Leu-enkephalin-Arg-Arg from dynorphin B was 45.9±6.2 pmoles/min and Met-enkephalin-

Lys-Lys from amidorphin was 30.1 ± 3 pmoles/min. The K_m , k_{cat} and k_{cat}/K_m values for the generation of these products are reported in Table 2.

Proteolytic Processing of ACTH¹⁻³⁹ by YAP3p

Secreted YAP3p cleaved ACTH¹⁻³⁹ to yield ACTH¹⁻¹⁵ and CLIP¹⁶⁻³⁹ (Chap.4), products identical to that previously reported for the cleavage of ACTH¹⁻³⁹ by YAP3p purified from yeast cell extracts (80). The V_{max} for the generation of ACTH¹⁻¹⁵ by YAP3p was determined to be 33.2 ± 4.8 pmoles/min and the K_m , k_{cat} and k_{cat}/K_m values are shown in Table 2.

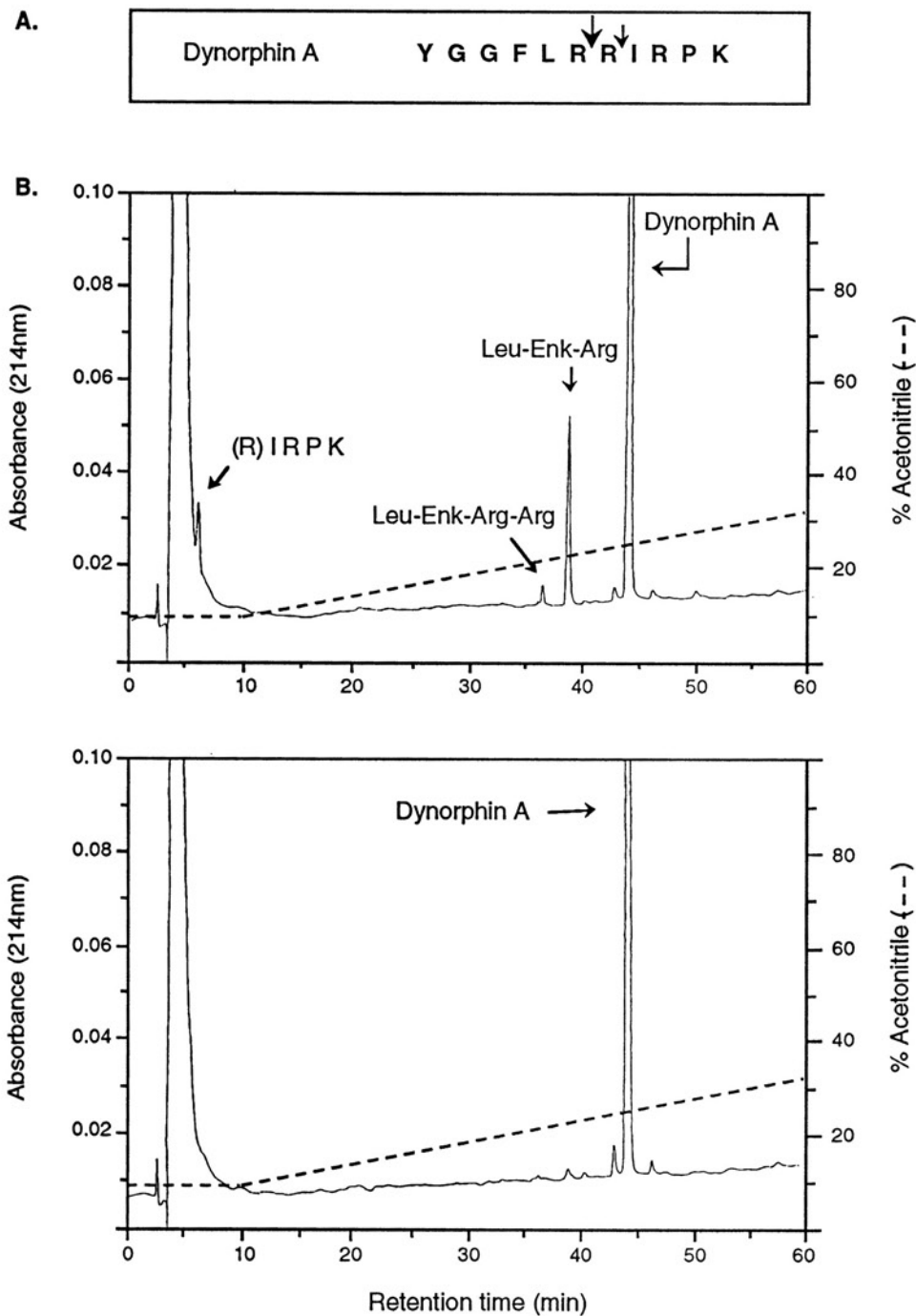


Figure 27. Proteolytic processing of Dynorphin A (1-11)

(A) Primary amino acid sequence of dynorphin A (1-11). Big and small *arrows* indicate major and minor sites cleaved by YAP3p. (B) HPLC profile of products generated from dynorphin A incubated with YAP3p in the absence (upper panel) and presence (lower panel) of pepstatin A.

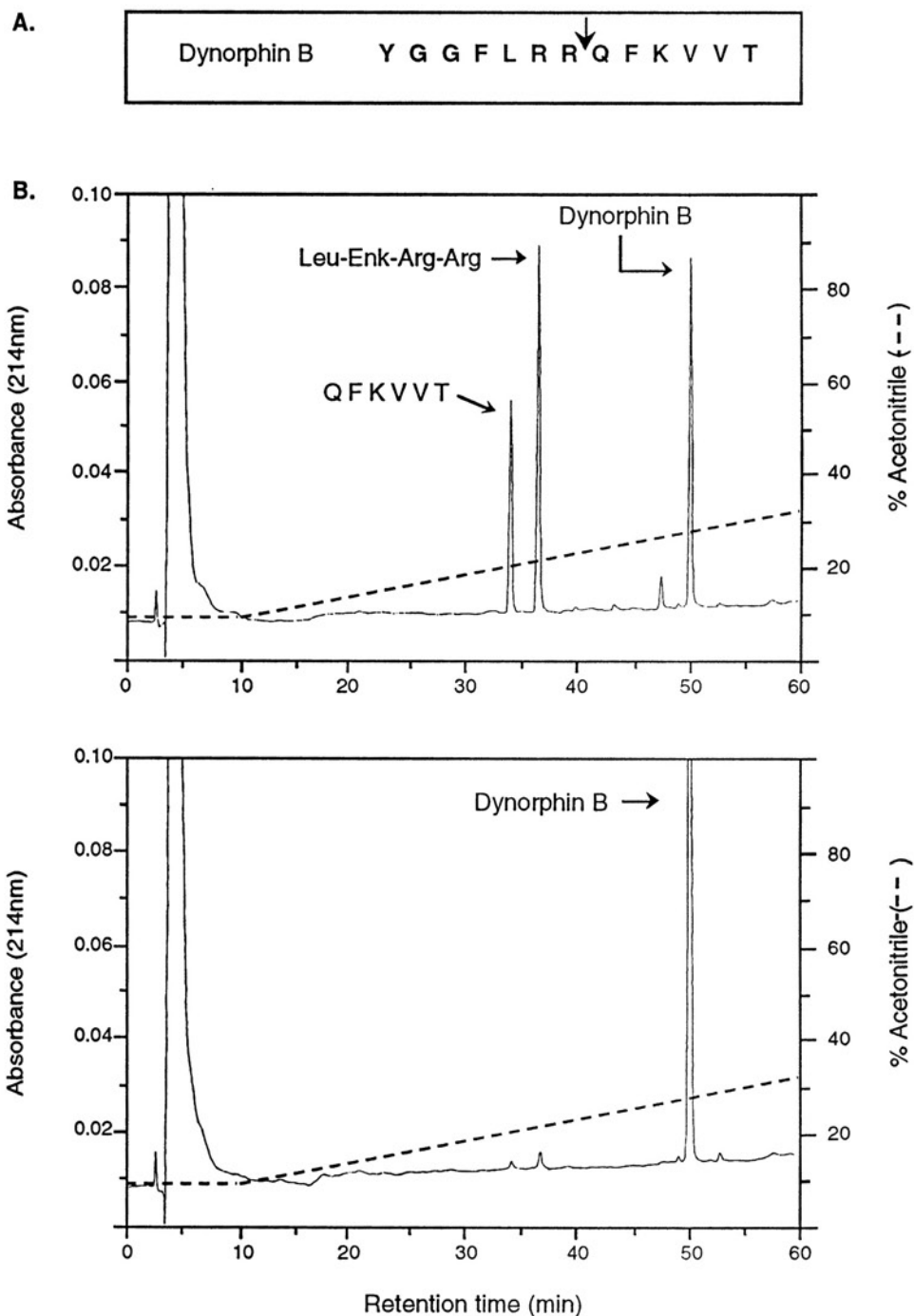


Figure 28. Proteolytic processing of Dynorphin B (1-13)

(A) Primary amino acid sequence of dynorphin B (1-13). *Arrow* indicates site cleaved by YAP3p. **(B)** HPLC profile of products generated from dynorphin B by YAP3p in the absence (upper panel) and presence (lower panel) of pepstatin A.

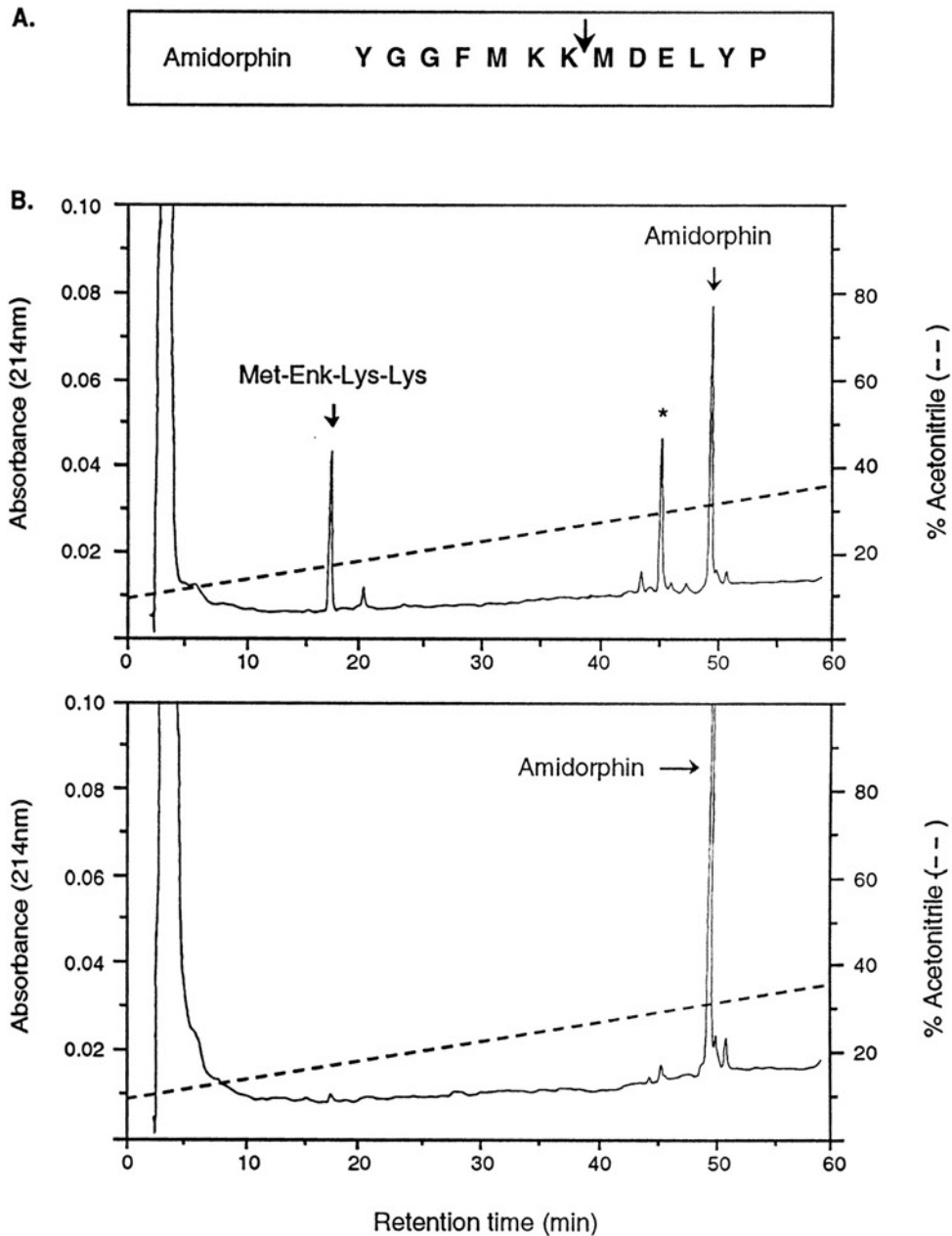


Figure 29. Proteolytic processing of Amidorphin

(A) Partial primary amino acid sequence of amidorphin. *Arrow* indicates the major site cleaved by YAP3p. **(B)** HPLC profile of products generated from amidorphin incubated with YAP3p in the absence (upper panel) and presence (lower panel) of pepstatin A. * This peak was not sequenced for identification, however it is predicted to be the other half of the amidorphin molecule.

TABLE 2

Substrate	-6 -5 -4 -3 -2 -1 1 2 3 4 5 6	Km μM ($\pm\text{SD}$)	kcat s^{-1}	kcat/Km $\text{M}^{-1} \text{s}^{-1}$
ACTH ¹⁻³⁹	G K P V G K K R R P V K	17.7 \pm 2	55.3	3.1 $\times 10^6$
Dynorphin B (1-13)	G G F L R R Q F K V V T	79 \pm 17.8	76.5	9.7 $\times 10^5$
Amidorphin	G G F M K K M D E L Y P	44 \pm 11.3	25.1	5.7 $\times 10^5$
Dynorphin A (1-11)	Y G G F L R R I R P K	136.1 \pm 13.5	49.4	3.6 $\times 10^5$
CCK(13-33)	R V S M I K N L Q S L D	115.3 \pm 8.1	4.9	4.2 $\times 10^4$
Proinsulin (B-C)	T P K A R R E V E G P Q	18.5 \pm 2.1	0.3	1.6 $\times 10^4$

Kinetic parameters for the processing of various substrates by YAP3p. SD Standard deviation

DISCUSSION

YAP3p cleaved bovine proinsulin at the B-C junction which contains the sequence P-K-A-R-R-E (Fig.22.A). Cleavage occurred primarily on the carboxyl side of the Arg-Arg pair, putting the upstream Lys at the P4 position. This cleavage pattern of proinsulin was also exhibited by PC1/3 (93,94). Some cleavage was observed in between the Arg-Arg pair, putting the upstream Lys in the P3 position. An upstream basic residue in the P3 position has not yet been reported as a cleavage site motif for any prohormone substrate. However, the synthetic substrate, Boc-R-V-R-R-MCA was cleaved by YAP3p (80) only in between the Arg-Arg pair, rendering the assignment of the upstream Arg in this substrate in the P3 position (Table 3). The absence of any cleavage on the carboxyl side of the pair of Arg residues is presumably due to the steric hinderance of the AMC moiety in the S1' region of the active site. Anglerfish pro-somatostatin I (aPSS I), containing the sequence P-R-Q-R-K-A, (Table 3) was cleaved by YAP3p primarily on the carboxyl side of the Arg-Lys cleavage site, although some cleavage in between the pair was observed, indicating a degree of tolerance but not preference by YAP3p for a basic residue in the P3 position. The bovine proinsulin C-A junction contains the sequence, P-P-Q-K-R-G, i.e. a pair of basic residues without an upstream basic residue. YAP3p cleaved the C-A junction of proinsulin preferentially in between the Lys-Arg pair. Cleavage at this site was relatively slow compared to the B-C junction, perhaps due to the presence of the two prolines immediately upstream from the cleavage site (P3 and P4). Further support of this hypothesis is borne out by the studies with aPSS I and aPSS II (95). While aPSS I was cleaved by YAP3p at the Arg-Lys pair preferentially after the Lys to yield aSS-14,

TABLE 3

Substrate	Product	-7 -6 -5 -4 -3 -2 -1 1 2 3 4 5 6 7
Proinsulin	cleaved B-C junction	Y T P K A R R E V E G P Q V
Proinsulin	cleaved C-A junction	L E G P P Q K R G I V E Q C
Cholecystokinin 33	CCK8	S H R I S D R D Y M G W M D
	CCK22	G R V S M I K N L Q S L D P
Cholecystokinin 13-33	CCK13-22 and CCK23-33	G R V S M I K N L Q S L D P
Dynorphin A 1-11	Leu-enkephalin-Arg	Y G G F L R R I R P K
Dynorphin B 1-13	Leu-enkephalin-Arg-Arg	Y G G F L R R Q F K V V T
Amidorphin	Met-enkephalin-Lys-Lys	Y G G F M K K M D E L Y P L
N-POMC ¹⁻⁷⁷	Lys- γ_3 -MSH	P L T E N P R K Y V M G H F
mouse POMC	ACTH/LPH junction	F P L E F K R E L E G E R P
α -MF leader seq-proinsulin(1)	extended proinsulin	G V S M A K R E A E A W F V
ACTH ¹⁻³⁹	ACTH ¹⁻¹⁵	W G K P V G K K R R P V K V
aProsomatostatin I	SS-14	L A P R E R K A G C K N F F
*aProsomatostatin II	SS-14	L P P R E R K A G C K N F Y
β -Endorphin ¹⁻³¹	β -Endorphin ¹⁻²⁹	I K N A Y K K G E
Boc-R-V-R-R-MCA	Arg-MCA	R V R R
*aProsomatostatin I	aSS-28	A H A D L E R A A S G G P L
aProsomatostatin II	aSS-28	G R M N L E R S V D S T N N

Prohormone and proneuropeptide basic residue sites cleaved by YAP3p.

* Cleavage by YAP3p not detected. Single letter codes used for amino acids.

(Table 3) the cleavage of aPSS II at the analogous Arg-Lys site was not detected, possibly due to the presence of the two prolines immediately upstream (at P5 and P6) from the expected cleavage site (Table 3). The proline side chain is known to have less conformational freedom resulting in a more rigid structure around the peptide bond. This may prevent the substrate in the cleavage site region from assuming a structure that binds efficiently to the active site pocket of the aspartic protease which generally spans up to 10 amino acids (96,97).

It has already been shown that YAP3p will cleave at a mono-basic Arg residue within a motif containing an upstream Arg at P6 in aPSS II. However, in aPSS I where the upstream basic residue at P6 was substituted by a histidine, cleavage did not occur, indicating a strict requirement for the upstream basic residue for a mono-basic residue site to be cleaved. This is supported by the finding that when the *α -MF-leader-pro-insulin* fusion protein was mutated to delete the Arg at the Lys-Arg junction ((23), and Table 3), YAP3p did not cleave at the mono-basic Lys, presumably since it did not contain an upstream or downstream basic residue within 6 residues of the predicted cleavage site. To determine if YAP3p will cleave a mono-basic Arg, as well as a Lys, within a motif having an upstream basic residue, CCK33 was tested as a substrate. YAP3p cleaved sulfated CCK33 at two mono-basic residue sites, each containing an upstream Arg at either the P6 or P5 position (Fig.23 and Table 2). Cleavage at Arg⁹ generated CCK8 while cleavage at Lys²³ generated CCK22 (Fig.25). YAP3p was also shown to cleave CCK13-33 to CCK13-22 and CCK23-33 at Lys²³ (Fig.26). These results indicate that YAP3p can recognize both a mono-basic Lys or Arg within a motif containing an upstream Arg. This

cleavage specificity exhibited by YAP3p is similar to the CCK8 generating enzyme previously described from rat brain synaptosomes which is capable of both these cleavages (98). Based on the relative concentrations of the products generated at the 5h time point (Fig.25.A), it appears that YAP3p cleaved preferentially at Lys²³ to generate CCK22 rather than at Arg⁹ to generate CCK8. This preference may be an indication that YAP3p prefers mono-Lys sites over mono-Arg sites, or simply that the upstream Arg in the P6 position is more favorable than in the P5 position. The presence of a negatively charged sulfated tyrosine close to Arg⁹ may also render this site difficult to cleave.

The cleavage of dynorphin A(1-11) (dynA) and dynorphin B(1-13) (dynB) was studied because both these substrates contain a potential mono- and paired-basic cleavage site. The results show that YAP3p had a preference for the paired-basic sites over the potential mono-basic sites in both substrates, generating Leu-enkephalin-Arg and Leu-enkephalin-Arg-Arg from dynA and dynB, respectively (Figs.27 and 28). It is interesting to note the presence of a basic residue in the P3' position (Arg in dynA and Lys in dynB) relative to the primary cleavage sites in both substrates. The preference for the paired basic residues exhibited by YAP3p for dynA and dynB suggests that a basic amino-acid present at P3' may also play a role in determining the specificity and efficiency of YAP3p. Since the aspartic proteases exhibit a high degree of symmetry in the active site, it is possible that a given substrate can bind in a manner such that the bond to be cleaved is regulated by a P3' basic residue binding in the S3' pocket.

The cleavage specificity of YAP3p for the substrates tested in this and previous studies (Table 3), indicates that YAP3p recognizes the following motifs: a pair of basic

residues alone, and paired or mono-basic residues with an additional upstream or downstream basic residue within the P2-P6 or P2'-P6' position. Cleavage at paired basic residues can occur either between or on the carboxyl side of the pair of basic residues, the preference being substrate dependent and likely governed by the upstream and downstream basic residues surrounding the cleavage site. Cleavage at a mono-basic site occurs on the carboxyl side of the basic residue. The specificity of YAP3p shows some overlap with that of pro-opiomelanocortin converting enzyme (PCE, EC 3.4.23.17), which has been shown to cleave at paired-basic residue sites of POMC and proinsulin (65,99) but did not cleave ACTH¹⁻³⁹ (65) or β -endorphin¹⁻³¹ (100).

Analysis of kinetic parameters for the cleavage of paired and mono-basic residues shows that YAP3p cleaves prohormone substrates at these sites with k_{cat}/K_m values comparable to chymotrypsin for the substrate N-acetyltyrosine ethyl ester (101). A comparison of the catalytic efficiency (k_{cat}/K_m) of cleavage of the motifs in this study suggests that YAP3p cleaves the motifs containing a paired-basic residue site, with or without a basic residue upstream or downstream, as in ACTH¹⁻³⁹, dynA, dynB and amidorphin more efficiently than the mono-basic residue motif as in CCK13-33. Moreover, having additional basic residues flanking the cleavage site between P2-P6 and P2'-P6' enhances the affinity of binding and catalytic efficiency. This is exemplified by the decrease in K_m and increase in k_{cat}/K_m for ACTH¹⁻³⁹ versus amidorphin, both of which are cleaved at a Lys-Lys pair, but ACTH¹⁻³⁹ has 4 additional basic residues flanking the cleavage site. Tetra-basic residues may well be a highly efficient cleavage site for YAP3p. A comparison of the catalytic efficiency (k_{cat}/K_m) of cleavage of the motifs in this study

suggests that YAP3p cleaves the motifs containing a paired-basic residue site, with or without a basic residue upstream or downstream, as in ACTH¹⁻³⁹, dynA, dynB and amidorphin, 10-100 times more efficiently than the mono-basic residue motif as in CCK13-33. Moreover, having additional basic residues flanking the cleavage site between P2-P6 and P2'-P6' enhances the affinity of binding and catalytic efficiency. This is exemplified by the decrease in K_m and increase in k_{cat}/K_m for ACTH¹⁻³⁹ versus amidorphin, both of which are cleaved at a Lys-Lys pair, but ACTH¹⁻³⁹ has 4 additional basic residues flanking the cleavage site. Tetra-basic residues may well be a highly efficient cleavage site for YAP3p. CCK13-33 and amidorphin were both cleaved on the carboxyl side of a Lys residue, but amidorphin was cleaved with a >10 fold higher efficiency than CCK13-33. This may be an indication of the preference by YAP3p for a basic residue in the P2 position, Lys in amidorphin, rather than P6, Arg in CCK13-33. The pro-insulin B-C junction which has a paired-basic residue motif with an upstream Lys in the P4 position was cleaved less efficiently than the mono-basic site of CCK13-13, although the K_m was comparable to ACTH¹⁻³⁹, the best substrate. This data suggest that the overall conformation of the substrate may also influence the relative rate of cleavage of these different motifs.

From the present studies it would appear that YAP3p can cleave all the motifs recognized by the subtilisin-like serine proteases, PC1/3, PC2 and furin. PC1/3 has been shown to cleave paired-basic residue sites (54,102,103) and at a mono-basic residue site with an upstream Arg in the P4 position (88), while PC2 cleaves only at paired-basic residues (104,105). Furin, on the other hand, prefers a paired-basic residue motif with an additional upstream Arg residue at the P4 position, although the basic residue at P2

appears not to be essential (75,88,106-108). However, since there are no kinetic studies on these enzymes for prohormone substrates thus far, it is not possible to compare the catalytic efficiency of cleavage of these different motifs by the subtilisin-like serine proteases (PC's), versus the aspartic protease processing enzymes. Future kinetic studies on the cleavage of these substrates by PC1 and PC2 will be important in assessing whether these enzymes cleave the same substrates with different efficiencies and the role the structural conformation plays in dictating efficiency of cleavages, independent of the enzyme. Such kinetic information will also be important in determining the relative role the aspartic proteases and the subtilisin-like serine processing enzymes play in cleaving various prohormones, since both families of proteases can be found in the same endocrine cells, e.g. the presence of PCE, PC1 and PC2 in the pituitary intermediate lobe cells (41,65).

CHAPTER 6

PURIFICATION OF SECRETED YEAST ASPARTIC PROTEASE 3

SUMMARY

Glycosylated YAP3p was purified from the growth media of induced yeast by ion exchange followed by gel filtration chromatography. Both steps resulted in a ~60% and ~64% recovery, respectively, however, the overall fold purification was only ~11.6 (Table 4). The purified protein sample contained two forms of YAP3p, the major ~150-180kDa form and the minor ~90kDa form, described in Chap.4, in addition to a contaminating protein at ~32kDa, identified as laminarinase. The estimated yield of YAP3p by this preparation is 0.5 µg YAP3p/g wet yeast. Deglycosylated YAP3p was also purified from the growth media by first purifying glycosylated YAP3p through a MonoQ column (64% recovery and an 11.5 fold increase in specificity activity, Table 5), changing the physical properties of the molecule by removing the N-linked sugars with endoglycosidase H, and then re-running the deglycosylated sample on the MonoQ column. The removal of the N-linked sugars resulted in the elution of the YAP3p in later fractions of the column, allowing separation from the other proteins in the sample. The estimated yield of YAP3p by this preparation was 0.29 µg YAP3p/g wet yeast. The N-terminal amino acid sequences obtained for YAP3p demonstrate that the “pro” region has been removed from the pro-YAP3p. An N-terminal amino acid sequence starting at amino acid #145 indicates that

YAP3p has been cleaved into two subunits (aa68-144 and aa145-532) that may exist as a heterodimer, similar to cathepsin D (63).

INTRODUCTION

Having characterized some of the physical and enzymatic properties of partially purified forms of secreted YAP3p in terms of its size, glycosylation state, stability and specificity and cleavage efficiencies for a number of peptide hormone substrates, it was necessary to develop a purification procedure in order to be able to verify some of these characteristics for the purified enzyme. Since the amino acid sequence of YAP3p reveals that a putative pro-region exists (Fig.1), it would also be interesting to determine if this region is present in the active enzyme, thus supporting the prediction that YAP3p is synthesized as a zymogen that requires activation. To address this question, purified active YAP3p would be necessary. Also, since the purification procedure of Azaryan *et al* (Chap.2) gave a characteristic yield of ~100-150ng of purified YAP3p/g of wet yeast, it was hoped that the growth media of the induced yeast might represent a richer source of starting material which would result in a higher yield of purified enzyme. A procedure for the purification of the glycosylated forms of secreted YAP3p was established first since it appeared that the glycosylated YAP3p is much more stable than the deglycosylated form, hence yielding a purified enzyme preparation that can be stored for extended periods of time without much loss of activity. Secondly, since the long term goal would be to try to resolve the x-ray crystal structure of YAP3p, it would be necessary to have a purified

enzyme that was not hyperglycosylated since these modifications to the protein may interfere with the structure of the protein and the interpretation of the results. With these criteria in mind, a purification procedure was also developed for deglycosylated YAP3p yielding 2-3 fold more purified YAP3p/g wet yeast than that of the previously published procedure.

PROCEDURES

YAP3p and Protein assays

The ACTH¹⁻³⁹ assay was used to quantitate YAP3p activity and SDS-PAGE in reducing conditions followed by colloidal coomassie blue staining was used to analyse the protein profiles from each column and the purity of the final purified protein. Total protein in each step was determined by the Biorad Protein assay procedure using a standard curve generated from BSA (see Materials and Methods).

Yeast enzyme source

Yeast strain BJ3501, transformed with *pYAP3LC* (see Chap.4), was grown to an OD 600nm ~1.0 in glucose selective media. The yeast cells were harvested by low speed centrifugation (2000 g, 5min) and resuspended in galactose selective media. After ~20hr of induction in this media the cells were harvested by centrifugation. One litre of the yeast suspension contained 8.9g of wet yeast. The media obtained in this manner was referred to as the starting material.

Note: Different media preparations were used for the two purification procedures described below.

Procedure for the purification of glycosylated YAP3p

All procedures were carried out at 4°C. The starting material (~7L) was concentrated to ~130ml by a Filtron ultrasette cassette tangential flow concentrator (30kDa molecular mass cutoff omega membrane). The ~130ml was further concentrated and the buffer exchanged with 20 *mM* sodium phosphate, pH 7.0 to a final volume of 20ml by centrifugation in Filtron macroseps (30kDa molecular mass cutoff omega membrane). Ten ml of the concentrated media was subjected to anion exchange chromatography using a prepacked MonoQ column (HR 5X5) coupled to a Fast Protein Liquid Chromatography (FPLC) system from Pharmacia which was equilibrated in buffer A (20 *mM* sodium phosphate, pH 7.0). After a baseline was re-established (20mls) the retained protein was then eluted by increasing the concentration of NaCl obtained from buffer B (buffer A + 1 *M* NaCl). The gradient went from 0%-50% B in 20min. The apex of the activity of YAP3p (#43-46) was saved and the surrounding fractions (#40-42 and #47-49) were re-run under the same conditions. Fractions #43-46 from this run were pooled with the same fractions from the first run and then applied to a third MonoQ column but this time the shallower elution gradient of 0%-25% B in 20 min was used. YAP3p activity eluted in fractions #49-57 (Fig.30.A), and was pooled, lyophilized and reconstituted in 1ml water.

The reconstituted protein was applied to a Sephadex G-200 gel filtration column (Pharmacia) also coupled to the FPLC system. The column was pre-equilibrated in 50% buffer B (see above). The flow rate was 1ml per min and 1ml fractions were collected.

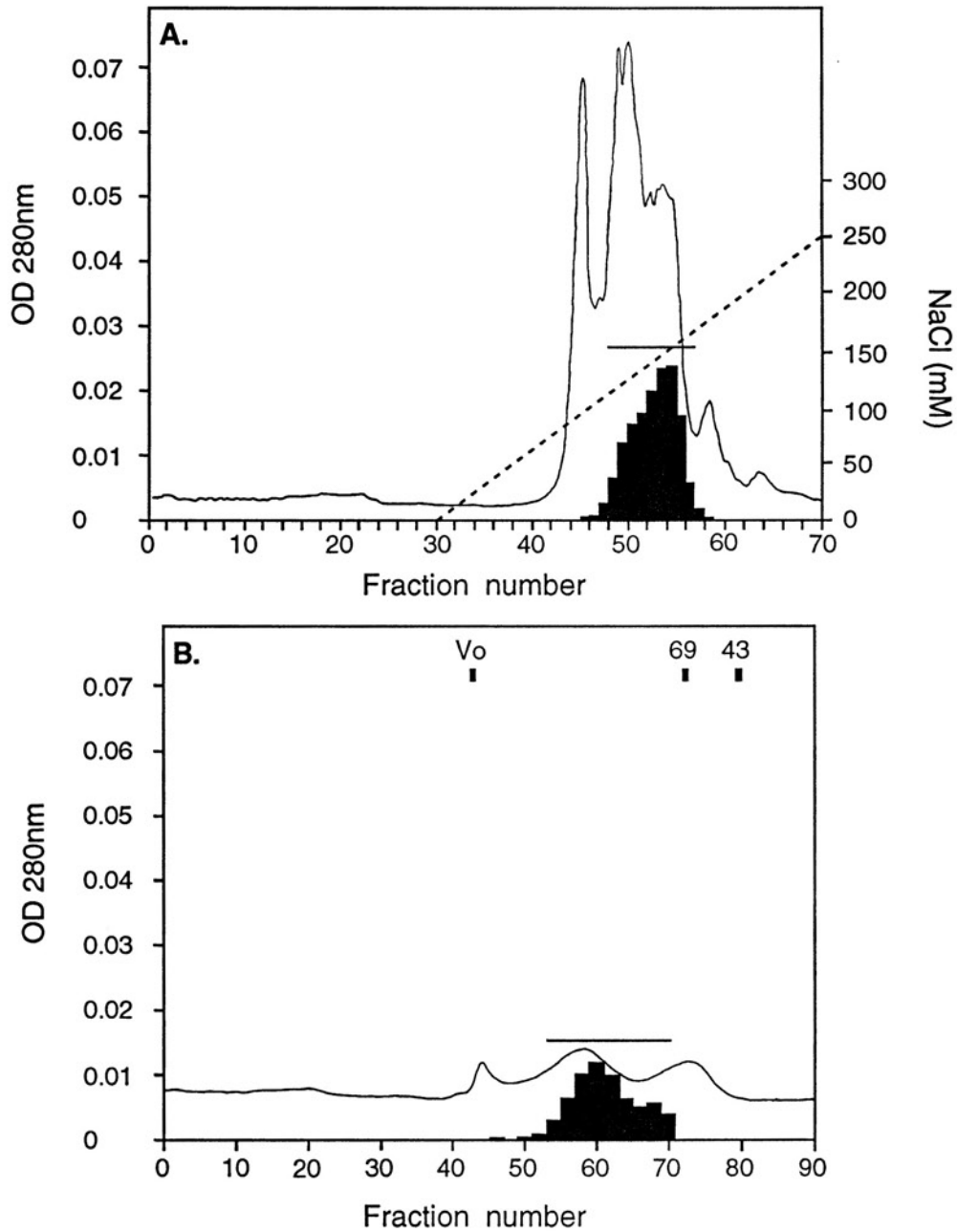


Figure 30. Purification profiles of glycosylated YAP3p

(A) Optical density at 280nm (line) and YAP3p activity (filled bars) profiles for the MonoQ column in the purification of glycosylated YAP3p. **(B)** Optical density at 280nm (line) and YAP3p activity (filled bars) profiles for the Sephadex G-200 gel filtration column in the purification of glycosylated YAP3p. The line over the filled bars indicate the fractions of YAP3p activity that were pooled.

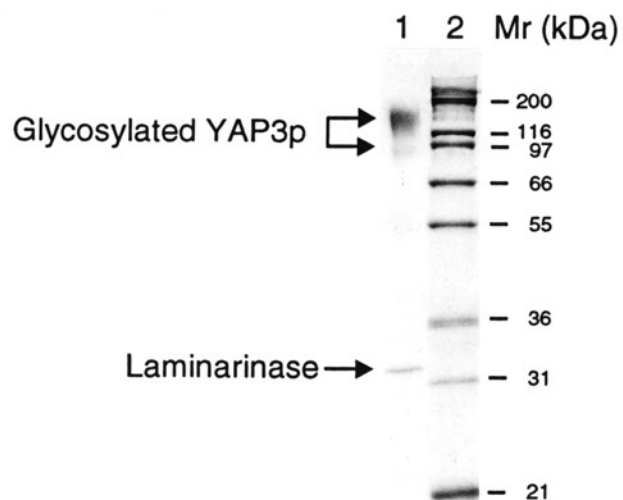


Figure 31. Coomassie blue stained gel of purified glycosylated YAP3p

Purified glycosylated YAP3p (~130ng) was separated by SDS-PAGE electrophoresis under reducing conditions and stained by colloidal coomassie blue (lane 1). Novex Mark12 molecular mass standards were run in lane 2.

YAP3p activity eluted in fractions #54-70 (Fig.30.B) corresponding to a molecular mass range of ~120kDa-150kDa and was pooled. Analysis of this protein by SDS-PAGE demonstrated a predominant high molecular mass protein at ~150-180kDa and a minor ~90kDa corresponding to secreted YAP3p (Fig.31). There was also present a contaminating ~32kDa protein that was identified as glucan 1,3- β -glucosidase (laminarinase, E.C. 3.2.1.58) by N-terminal amino acid sequence analysis carried out by Dr. Chen, ERRL, NICHD, NIH.

Procedure for the purification of deglycosylated YAP3p

The starting material (~1L) was diluted with 1 volume of 20 *mM* sodium phosphate buffer containing 0.42 *mM* AEBSF, pH 7.0 and applied to two 10ml DEAE-Sephadex columns that had been pre-equilibrated in 20 *mM* sodium phosphate, pH 7.0 buffer. The columns were each eluted with 40 mls of equilibration buffer containing 0.33 *M* NaCl. The DEAE-Sephadex eluate was then centrifuged in two Filtron macrosep centrifugal concentrators (50 kDa cutoff omega membrane) resulting in a concentrated sample (9mls) that had undergone a buffer exchange with 20 *mM* sodium phosphate, pH 7.0 to remove the salt. The concentrated sample was applied to the MonoQ column described above and after equilibration, the protein was eluted with the gradient that went from 0% B to 25% B in 20min. The flow rate was 1ml per min and 0.5ml fractions were collected. The protein was continuously monitored by absorbance at 280nm and the presence of YAP3p was determined by the ACTH¹⁻³⁹ assay (Fig.32.A). Thirty μ l from every second fraction, starting at #45 and ending at #61, was analysed by 4-20%

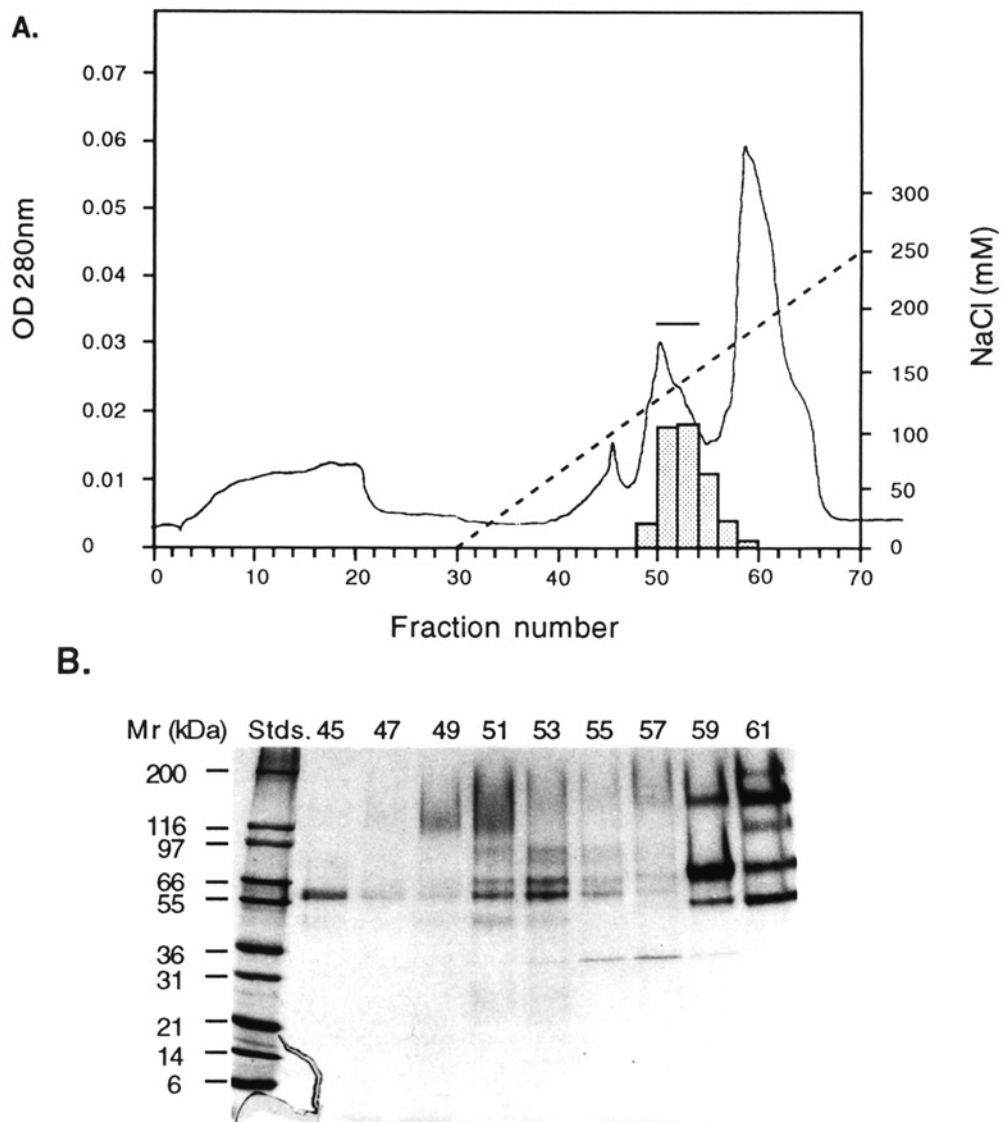


Figure 32. Analysis of glycosylated YAP3p by anion exchange chromatography
(A) Optical density at 280nm (line) and YAP3p activity (filled bars) profiles for the first MonoQ column in the purification of deglycosylated YAP3p. Line over the filled bars indicate fractions of YAP3p activity pooled. **(B)** Coomassie blue stained gel of the fractions from the first MonoQ column.

tris/glycine gradient SDS-polyacrylamide gel electrophoresis (SDS-PAGE) and stained by a colloidal coomassie blue staining kit from Novex, (Fig.32.B). The apex of the peak of YAP3p activity (#51-54) was pooled and saved. The surrounding fractions (#48-50 and #55-57) were also pooled, diluted with buffer A to 10mls and re-run on the MonoQ column under the same conditions. Fractions #51-54 from this run were pooled with the same fractions from the first run.

The pool of YAP3p activity was then treated with endoglycosidase H (0.005 units, 0.1 *M* sodium phosphate, pH 5.5 at 37°C for 12hrs) in the presence of freshly prepared 2 *mM* PMSF. The treated enzyme was then run on the MonoQ column under the same conditions as described above. YAP3p activity was again determined by the ACTH¹⁻³⁹ assay, (Fig.33.A) and 30 µl of the protein in each fraction from #50-63 was analysed by 4-20% tris/glycine gradient SDS-PAGE, (Fig.33.B). YAP3p enzymatic activity eluted in fractions #55-61, however, fractions #56-59 were pooled and referred to as purified YAP3p. An aliquot of the purified YAP3p was analysed by SDS-PAGE and stained as before, showing the apparent homogeneity of the purified YAP3p at 65kDa (Fig.34).

N-terminal amino-acid analysis of purified YAP3p

Both glycosylated and deglycoylated YAP3p were analysed by direct N-terminal amino acid sequencing and found to have two N-terminals. They were 1. Ala-Asp-Gly-Tyr-Glu-Glu-Ile-Ile which corresponds to YAP3p amino acids starting at #68, and 2. Asp-Ile-Asn- Pro-Phe-Gly-Trp-Leu-Thr-Gly which corresponds to YAP3p amino acids starting at #145, Fig.35. The ratio of these two N-termini were 1.3:1, respectively.

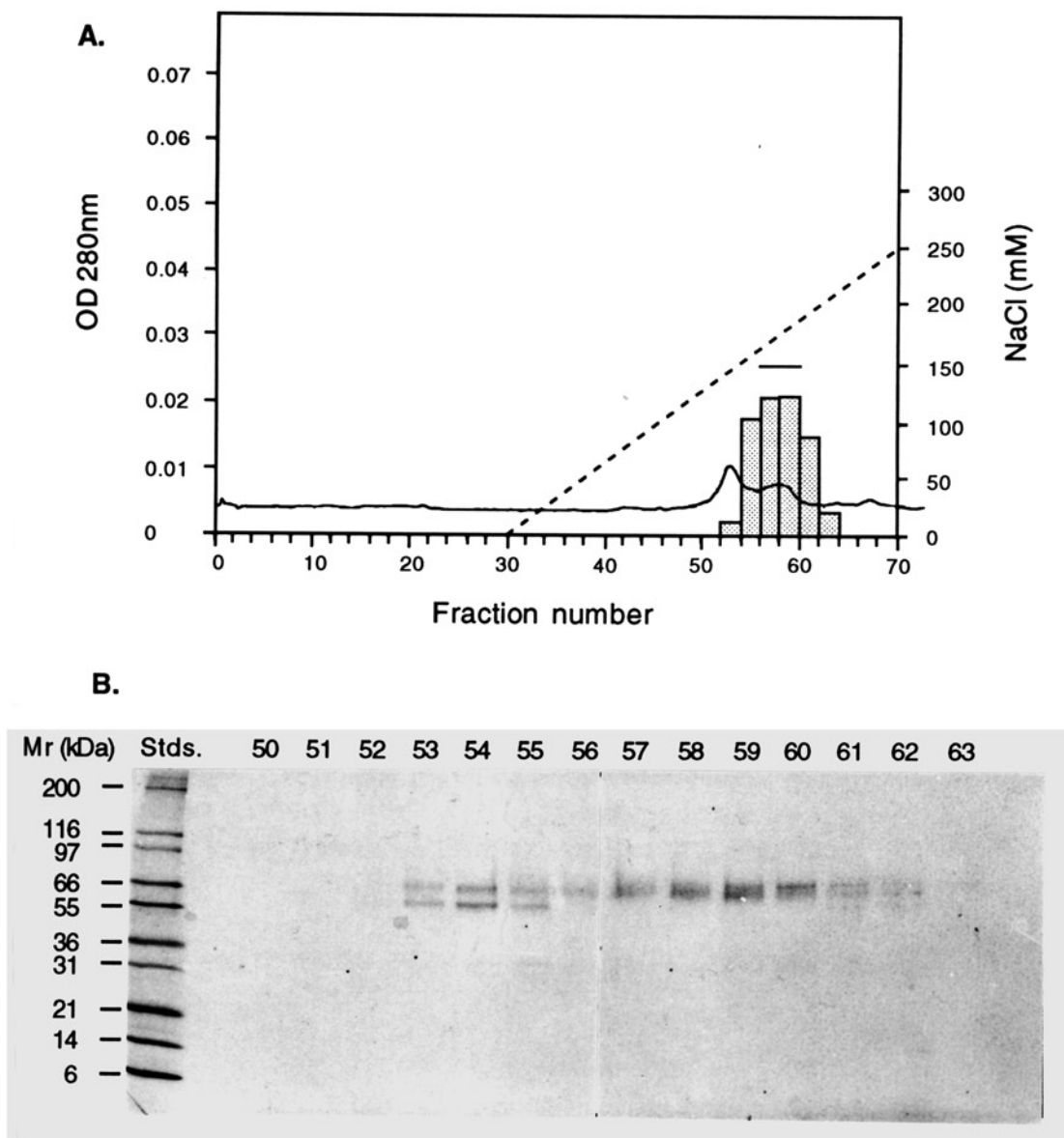


Figure 33. Analysis of deglycosylated YAP3p by anion exchange chromatography

(A) Optical density at 280nm (line) and YAP3p activity (filled bars) profiles for the second MonoQ column in the purification of deglycosylated YAP3p. Line over the filled bars indicate fractions of YAP3p activity pooled. **(B)** Coomassie blue stained gel of the fractions from the second MonoQ column.

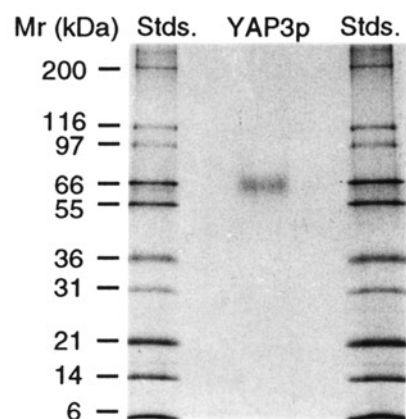


Figure 34. Coomassie blue stained gel of purified deglycosylated YAP3p

Purified deglycosylated YAP3p (~40ng) was separated by SDS-PAGE electrophoresis under reducing conditions and stained by colloidal coomassie blue (center lane). Novex Mark12 molecular mass standards were run on either side of the YAP3p lane.

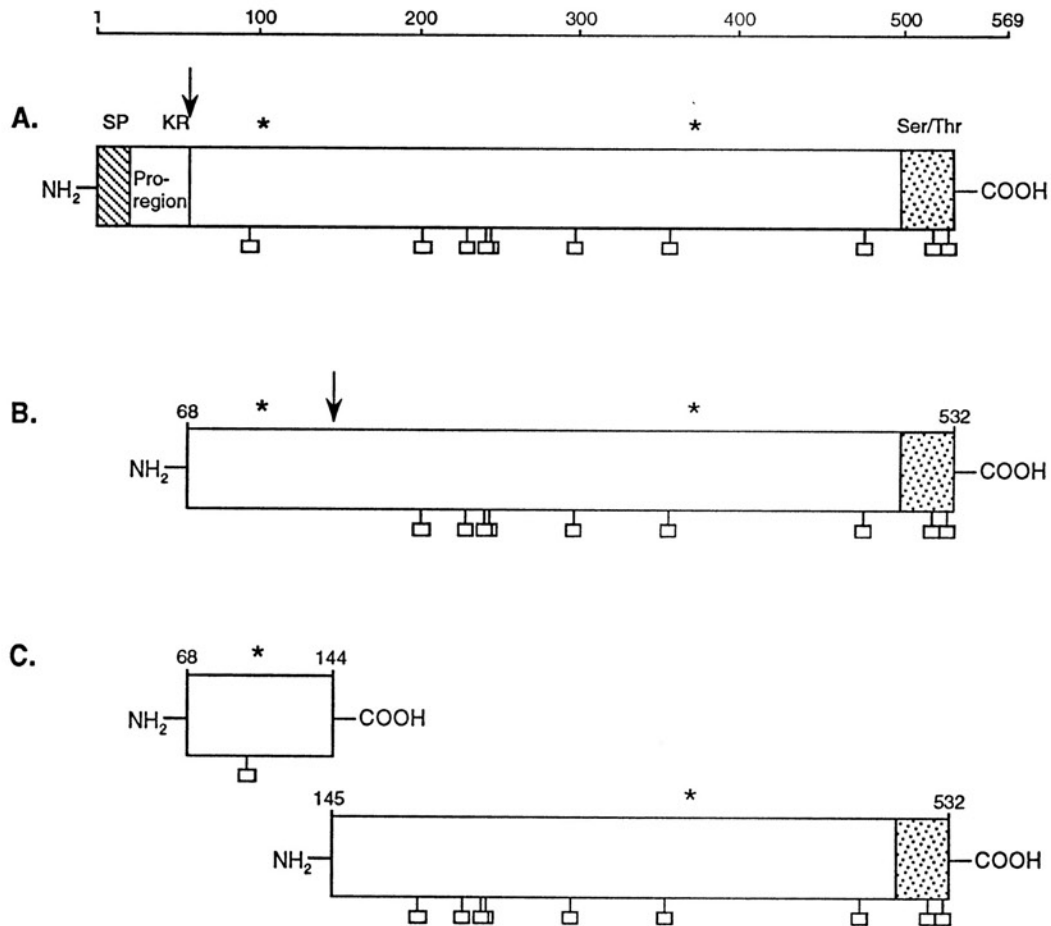


Figure 35. N-terminal amino acid analysis of purified YAP3p

(A) Schematic diagram of full length YAP3p. **(B)** Diagram of activated YAP3p as a result of the removal of its pro region. **(C)** Diagram of a possible heterodimeric association for YAP3p activity. Arrows indicate the amino terminal of YAP3p determined by direct N-terminal amino acid analysis.

DISCUSSION

The purification of YAP3p from the media was first attempted by the procedure described in Chap.2, which involved concanavalin A and pepstatin A affinity chromatography. However, it was determined that the efficiency of the pepstatin A affinity column was inconsistent depending on the batch number of the beads purchased from Pierce. It is also possible that the high degree of glycosylation of the secreted YAP3p prevented efficient binding to this column. An alternate procedure was developed utilizing anion exchange chromatography based on the findings that the isoelectric point (pI) of YAP3p was ~4.5 (Chap.4), thus rendering this enzyme negatively charged at pH 7.0. Hydrophobic interaction chromatography was also attempted unsuccessfully on a phenyl-superose column, since precipitation of some proteins caused by 'salting-out' resulted in clogging of the column and subsequent slower and inconsistent flow rates. In addition, the presence of high concentrations of ammonium sulphate in the buffers appeared to inhibit the activity of the enzyme. Since secreted YAP3p was determined to be hyperglycosylated, primarily giving a molecular mass of ~150-180kDa, this information was utilized in the form of a gel filtration column, Sephadex G-200, where YAP3p could be separated from the vast majority of the other secreted proteins based on apparent molecular size and shape. A combination of both anion exchange and gel filtration chromatography was therefore used to attempt to purify secreted YAP3p to apparent homogeneity. This procedure demonstrated an overall recovery of 25.1%, while the fold purification was only 11.5 (Table 4). While the first step involved concentrating the 7L volume to 130mls in a relatively short time (1.5hr) using the ultrasette cassette from

TABLE 4

Step	Protein conc. ($\mu\text{g/ml}$)	Total protein (μg)	Specific activity ($\mu\text{g ACTH}^{1-15}/\text{h}/\mu\text{g protein}$)	Total activity ($\mu\text{g ACTH}^{1-15}/\text{h}$)	Fold purification	% Recovery
Media	0.9	3177.4	925.3	2939678.1	1	100
Concentrated media	248.9	2489	755.3	1879941.7	0.82 (0.82)	63.9 (63.9)
MonoQ	74.6	273.8	4093.2	1120718.2	4.42 (5.42)	38.1 (59.6)
Sephadex G-200	4.2	67.5	10704.8	722574	11.57 (2.61)	24.6 (64.5)
Cumulative					12	25

Purification table for glycosylated YAP3p. Values in brackets represents fold purification and % recovery for individual steps.

Filtration, it can be seen that there was a slight decrease in specific activity as a result of this procedure. This is assumed to be as a result of the high flow rates of the circulating media (~600-700 ml/min) in the ultrasette concentrator causing denaturation of the enzyme. The relatively low fold purification obtained for overall purification of YAP3p is an indication of the abundance of the induced enzyme in the starting material. Since the expression of the recombinant YAP3p is under the control of the galactose inducible promoter there is a 1000 fold increase in expression (109) when the yeast are switched from glucose to galactose selective media. It is therefore not surprising to have the media enriched in the overexpressed protein. Although apparent homogeneity was not attained in this procedure, since laminarinase was present as a contaminating protein, it can be seen from Fig.30.A and B that if smaller fractions from the columns were collected and pooled then the level of contamination of the final purified YAP3p by the laminarinase can be greatly reduced. Glycosylated YAP3p (the ~150-180kDa form), has been purified to apparent homogeneity by taking these finer cuts, using a combination of gel filtration and anion exchange chromatography, but the overall yield was reduced to ~14% (data not shown). A complete purification table for this experiment was not obtained and is therefore not reported here.

The presence of laminarinase (~32kDa) in the final sample of glycosylated YAP3p indicates that it is behaving as a high molecular mass aggregate since it was pooled with the YAP3p from the Sephadex column. This is surprising in light of the fact that the Sephadex G-200 column was run in 0.5 M NaCl, i.e. a concentration of salt that should minimize ionic interaction and hence aggregation. It is possible that this protein was

stabilized by disulphide bridges. However, analysis by SDS-PAGE in reducing and non-reducing conditions showed the presence of this protein at ~31kDa-36kDa in both cases, indicating that this protein is not aggregating due to disulphide bridges. Conditions of the Sephadex G-200 buffer system that would effectively de-aggregate the laminarinase should result in a YAP3p solution with apparent homogeneity. The activity profile of the glycosylated YAP3p obtained from the Sephadex G-200 column indicates a shoulder of YAP3p activity observed in fractions #66-70 (Fig.30.B). This is presumed to correspond to the ~90kDa form of YAP3p which was described in Chap. 4.

Deglycosylated YAP3p was purified to apparent homogeneity from the induced media using anion exchange chromatography only. The overall yield was 23.3 while the fold purification was 57.3 (Table 5). The use of DEAE-Sephadex as a concentration step was used because of its mild conditions and overall effectiveness. There was only a ~5% loss in total protein in this step while the specific activity increased by 1.36 and the % yield of total activity was 128.7%, (Table 4). Obviously, this step has resulted in an overall increase in total activity from the starting material probably due to the removal of an endogenous inhibitor or regulator that did not bind to the DEAE-Sephadex beads. The existence of endogenous inhibitors to processing enzymes has been shown by the ability of 7B2, a pituitary specific protein with no other known function, to specifically inhibit PC2 and not PC1 (110). Also, the novel prohomone thiol protease (PTP) from bovine adrenal medulla chromaffin granules, capable of cleaving proenkaphalin, has been shown to be inhibited specifically by an α_1 -antichymotrypsin-like protein present in secretory vesicles of bovine adrenal medulla and pituitary (111), and for a short review see (112).

TABLE 5

Step	Protein conc. $\mu\text{g/ml}$	Total protein μg	Specific activity ($\mu\text{g ACTH}^{1-15}/\text{h}/\mu\text{g protein}$)	Total activity ($\mu\text{g ACTH}^{1-15}/\text{h}$)	Fold purification	% Recovery
Media	0.7	683.3	191.4	130785.1	1	100
DEAE-Sephadex	7.6	600.4	260.4	156344.2	1.36 (1.36)	128.7 (128.7)
MonoQ 1	11.1	33.3	3005.6	100086.5	15.7 (11.54)	76.5 (64)
MonoQ 2	1.3	2.6	10958.6	28492.4	57.3 (3.65)	21.8 (28.2)
Cumulative					57	22

Purification table for deglycosylated YAP3p. Values in brackets represents fold purification and % recovery for individual steps

Sequence analysis of the purified proteins demonstrated that YAP3p is synthesized as a zymogen that gets cleaved on the carboxyl side of the Lys⁶⁶-Arg⁶⁷ pair resulting in an activated enzyme. The presence of another internal YAP3p sequence, that which resulted from a cleavage after Asn¹⁴⁴, can be interpreted in two ways. 1. The enzyme has been cleaved non-specifically resulting in the separation of the two active site triads thus giving an inactive enzyme or 2. this cleavage is specific resulting in the generation of two subunits with apparent molecular masses of ~8kDa and ~45kDa for the protein backbone. As mentioned above, this processing is similar to that observed for Cathepsin D, where both active site triads are also separated into two subunits that require association for enzymatic activity. Since this internal sequence of YAP3p, starting at Asp¹⁴⁵, has been obtained on three different occasions each with a different enzyme preparation (data not shown), it is assumed that this cleavage is specific and plays an important role in the biosynthesis of YAP3p *in vivo*. It has been predicted that cleavage after an Asn also had to occur at the putative GPI site for membrane anchoring of full length YAP3p similar to Gasp1 (71). A similar cleavage site for the synthesis of yeast killer toxin has also been shown. Thus, a highly specific enzyme recognizing certain Asn residues exists in yeast.

The yeast strain BJ3501 containing the *pYAP3LC* plasmid (Chap.4), has been licenced to Worthington Biochemicals for the commercial sale of the truncated YAP3p enzyme to the research community. They will be capable of purifying the enzyme in quantities sufficient for X-ray crystal analysis. A collaboration with Dr. Tom Blundell of Birkbeck College, London, who will carry out the analysis, has been initiated.

CHAPTER 7

CHARACTERIZATION OF PURIFIED SECRETED YAP3p

SUMMARY

The K_m of purified YAP3p for the synthetic substrate Boc-Arg-Val-Arg-Arg-MCA was calculated as $102 \mu M$ while the V_{max} was calculated as 138 ± 8.3 pmoles/min. The K_i of YAP3p for the inhibitor, pepstatin A, was calculated as $0.375 \pm 0.13 \mu M$ which represents an average of the two K_i values obtained by the two methods. The specificity of the purified YAP3p for the substrates ACTH¹⁻³⁹, CCK13-33, dynorphin A, dynorphin B and amidorphin was determined to be identical to the partially purified preparation of YAP3p that was used in the specificity study described in Chap.5

PART 1: DETERMINATION OF THE K_i OF YAP3p FOR THE ACTIVE SITE INHIBITOR, PEPSTATIN A.

Assay of the synthetic substrate, Boc-RVRR-MCA

The synthetic peptide Boc-Arg-Val-Arg-Arg-MCA (Peninsula), was incubated ($0.2 mM$), with ten fold serial dilutions of the above purified deglycosylated YAP3p in 0.1

M sodium citrate, pH 4.0, at 37°C for 1hr. The reactions were stopped by addition of 10 μ l glacial acetic acid and applied to an HPLC column for separation of the products by reverse-phase chromatography. The product released from Boc-Arg-Val-Arg-Arg-MCA, which is Arg-MCA (Chap.2), was detected and quantitated by extrapolation of a standard curve that was generated with Arg-MCA standards, also obtained from Peninsula.

Two methods were used to determine the value of K_i .

1. This method involved the incubation of the purified YAP3p with varying concentrations of the substrate with and without a fixed concentration of pepstatin A. The method of Lineweaver-Burk (91) was used to process the data obtained.

2. This method involved the titration of YAP3p with serial dilutions of pepstatin A, using the same substrate. A Dixon plot was used to calculate the K_i .

Introduction-Method 1

From the Michaelis-Menton equation, Fig.36, eqn.1, which describes the mechanism of a simple enzymatic reaction represented by $[E]+[S]\leftrightarrow[ES]\rightarrow[E]+[P]$, a derivation can be obtained such that when $1/V$ versus $1/[S]$ is plotted, a straight line is obtained. This equation is called the Lineweaver-Burk equation and can be seen in Fig.36, eqn.2. The effect of a competitive inhibitor, which pepstatin A represents for aspartic proteases, can be included by adding in an extra term, Fig.36, eqn 3. It can be seen that a plot of $1/V$ versus $1/[S]$ will give an X intercept of $-1/K_m$ for the reaction in the absence of inhibitor and $-1/K_m(1+[I]/K_i)$ in the presence of the inhibitor, while the V_{max} should

remain unchanged. Determining the X-axis intersection in these cases can result in the calculation of both the K_m and K_i of the enzyme for substrate and inhibitor, respectively.

Assay procedures

From the preliminary assay conditions mentioned above it was determined that 4 μ l of the purified YAP3p (i.e. ~ 0.08 pmoles) resulted in the generation of $<5\%$ product from 0.2 mM substrate in one hour. Using this concentration of enzyme (20 nM final concentration), initial rates of cleavage for the concentration of substrate at 0.8 mM , 0.4 mM , 0.2 mM and 0.1 mM were determined in the presence and absence of 3.0×10^{-6} M pepstatin A by taking six time points from each reaction within the 1 hr incubation. The initial rates (V_o) were calculated per minute from the equations of the lines obtained from the curve fits of the plots of products generated versus time, Fig.37.A. A plot of $(1/V_o)$ versus $1/[S]$ resulted in the characteristic straight lines of a Lineweaver-Burk plot, Fig.37.B. K_m , V_{max} , $K_{m_{app}}$ and $V_{max_{app}}$ values were calculated from these plots.

Calculations: Method 1

Equations of the lines generated from the Lineweaver-Burk plots.

Without inhibitor

$$y = 15.39 + 1.57x \quad r^2 = 0.989$$

$$K_m = 102 \mu M$$

$$V_{max} = 77.9 \mu M/h$$

With inhibitor

$$y = 13.62 + 18.68x \quad r^2 = 0.953$$

$$K_{m_{app}} = 1371 \mu M$$

$$V_{max_{app}} = 88.1 \mu M/h$$

From the Lineweaver-Burk equation with inhibitor, Fig.36, eqn.3.

$$K_{m_{app}} = K_m(1 + [I]/K_i)$$

$$1371 \mu M = 102 \mu M (1 + (3 \mu M / K_i))$$

$$K_i = 0.24 \mu M$$

Introduction-Method 2

This method involved keeping the substrate constant while varying the concentration of the inhibitor. It can be seen that if eqn.3 in Fig.36 is rearranged to give eqn.4, a plot $1/V$ versus $[I]_{\text{final}}$ would generate a straight line with a Y intercept of $1/V_{\text{max}_{\text{app}}} (K_m/[S] + 1)$ and an X intercept of $-K_i(1 + [S]/K_m)$. Since the substrate concentration and K_m (see Method 1, above), are known, the K_i can be calculated from the X-axis intersection.

Assay procedures

0.08 pmoles of purified YAP3p were pre-equilibrated with two fold serial dilutions of pepstatin A (2.4×10^{-5} to 1.9×10^{-7} M) in 0.1 M sodium citrate, pH 4.0, for 5 min at 37°C. Boc-Arg-Val-Arg-Arg-MCA (0.2 mM) was then added and the reaction which went for 30 min at 37°C. A plot of % activity versus $[I]_{\text{final}}$ gave a characteristic titration profile, Fig.38.A, and when plotted as $1/V$ versus $[I]_{\text{final}}$, a straight line was obtained, Fig.38.B. The experiment was repeated to obtain a duplicate set of results.

Calculations: Method 2

Equation of the line generated from the plot of $1/V$ versus $[I]_f$

$$y = 4.99 + 3.3e-6x \quad r^2 = 0.995$$

From the Dixon equation, Fig.36, eqn. 4.

$$\text{at } 1/V = 0, [I] = -K_i(1 + [S]/K_m)$$

$$-1.51 \mu M = -K_i(1 + (200 \mu M / 102 \mu M))$$

$$K_i = 0.51 \mu M$$

Equation 1. $V = V_{\max}[S]/K_m + [S]$

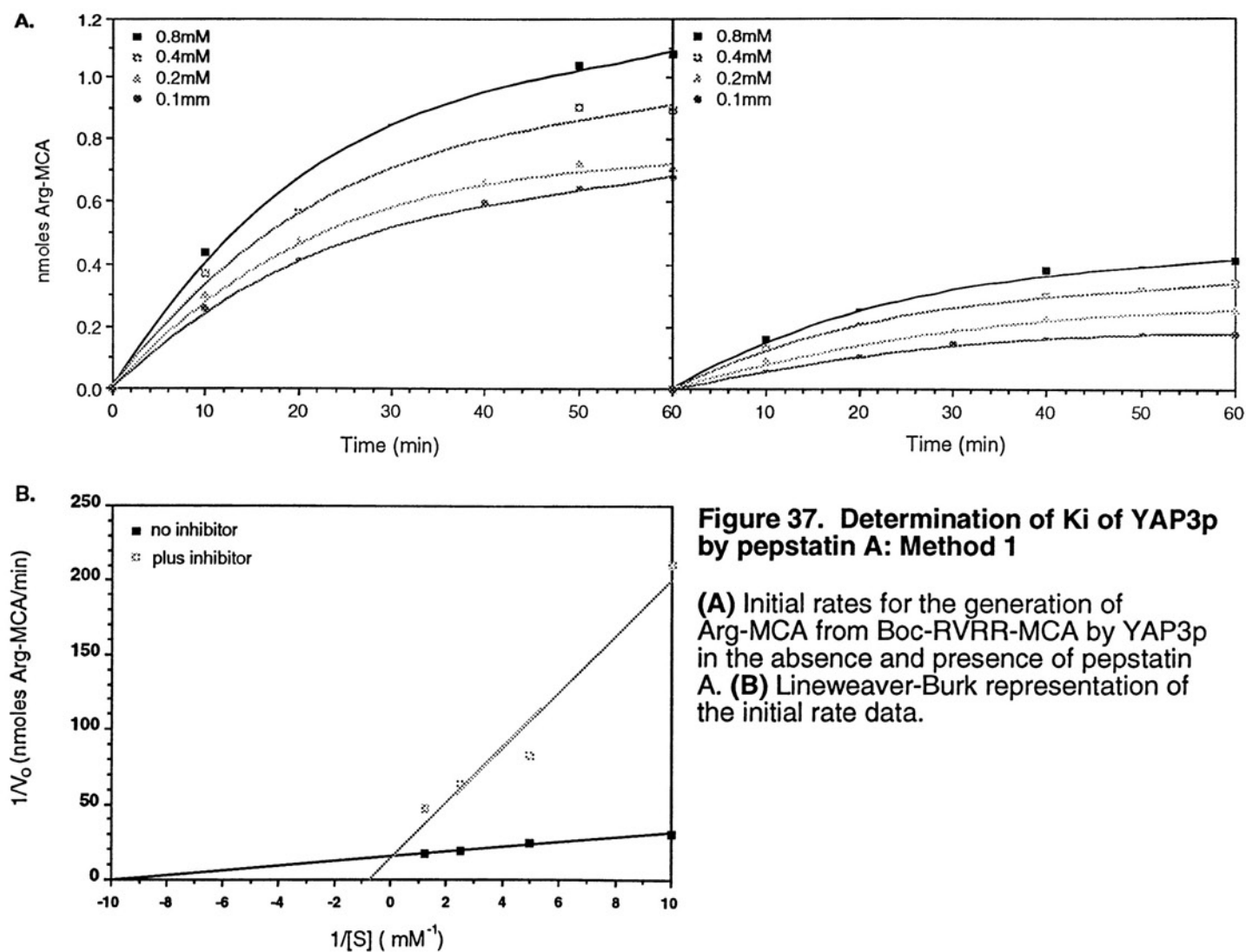
Equation 2. $1/V = K_m/V_{\max}[S] + 1/V_{\max}$

Equation 3. $1/V = K_m(1+[I]/K_i)/V_{\max}[S] + 1/V_{\max}$

Equation 4. $1/V = (1+K_m/[S])/V_{\max} + K_m[I]/K_i.V_{\max}[S]$

Figure 36. Equations governing kinetics of enzyme reactions

Equation 1, Michaelis-Menton eqn., Equation 2, Lineweaver-Burk eqn., Equation 3, Lineweaver-Burk eqn. in the presence of a competitive inhibitor, Equation 4, Dixon eqn. V = rate, V_{\max} = maximum rate, $[S]$ = substrate concentration, K_m = substrate concentration at which the rate of the reaction is half the maximum rate, $[I]$ = inhibitor concentration, K_i = a measurement of the affinity of the enzyme for the inhibitor.



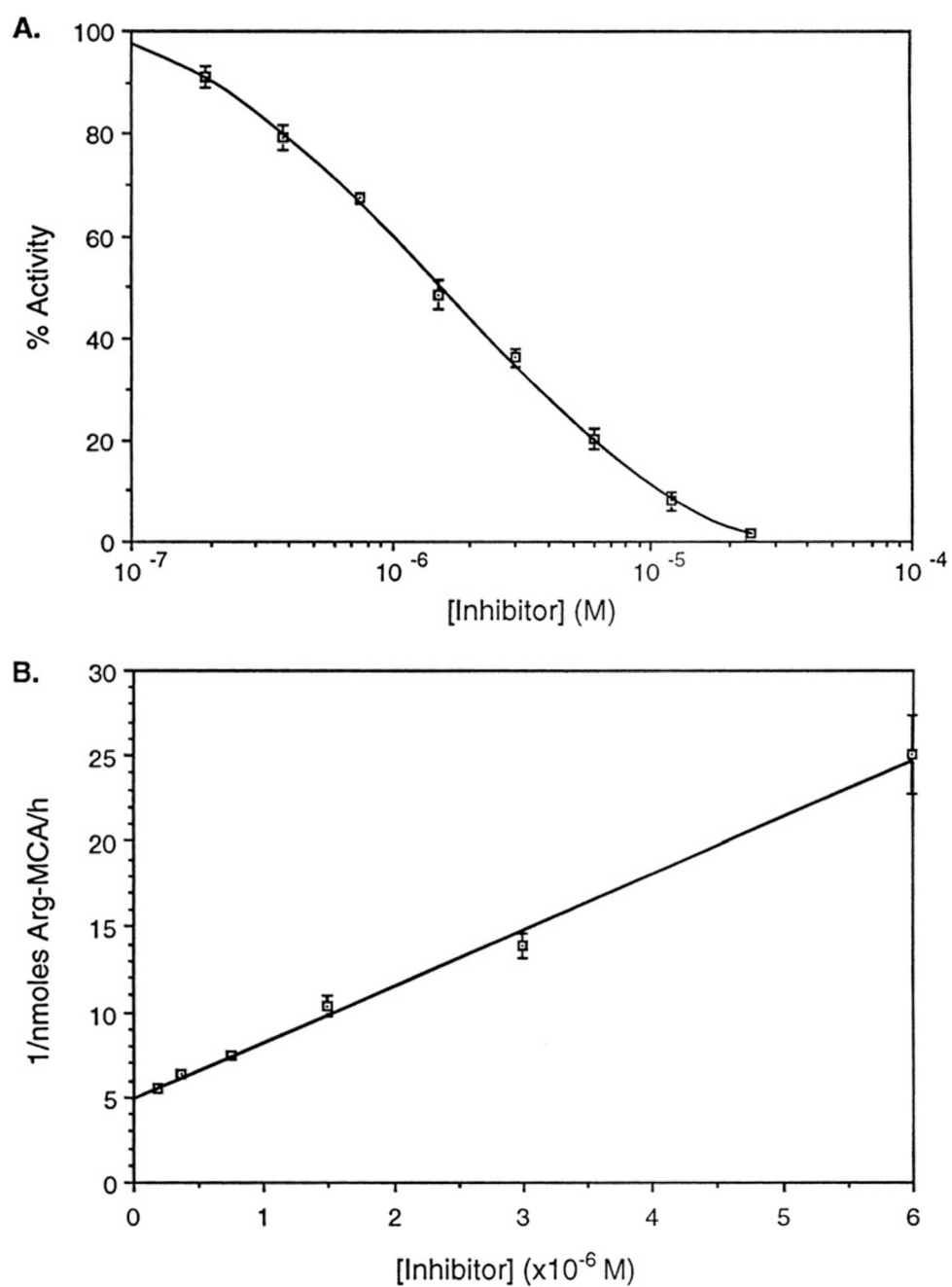


Figure 38. Determination of K_i of YAP3p for pepstatin A: Method 2

(A) Titration profile of YAP3p activity with serial dilutions of pepstatin A.

(B) Dixon plot representation of the titration data.

PART 2: ANALYSIS OF THE SPECIFICITY OF PURIFIED YAP3p

Assay procedures

Ten fmoles of purified YAP3p were incubated with 10 μ g CCK13-33, dynorphin A, dynorphin B or amidorphin for 30 min at 37°C in 0.1 *M* sodium citrate, pH 4.0, in the presence and absence of 3.0x10⁻⁶ *M* pepstatin A. The reactions were stopped by addition of 10 μ l glacial acetic acid and the products analysed by HPLC as described in Chap.5. The results (data not shown) demonstrate that purified YAP3p exhibits the same specificity profile for these substrates as described for the partially purified YAP3p preparation reported in Chap.5.

DISCUSSION

Proteases are divided into four classes; serine and cysteine proteases, which utilize a nucleophilic amino acid in their catalytic site to form covalent enzyme-substrate intermediate complexes, and aspartic and metallo-proteases, that rely on general acid/base catalysis of the attack of a water molecule without the aggressive nucleophilic attack of a functional group of the enzyme. Aspartic and metallo-proteases do not form covalent intermediates with the substrate (113). Most protease inhibitors are considered as 'active-site-directed', where they can combine with the catalytic and substrate-binding sites of the protease to generate a tight and stable complex (114). These inhibitors have allowed

proteases to be characterized as a member of a certain class or family of proteases. Such characterization allows information about the primary amino acid sequence of the protease to be deduced. Likewise, when the amino acid sequence of a protease is known, a prediction about its catalytic mechanism can be made.

YAP3p was initially identified by its pro- α -mating factor cleaving activity (23) and when the sequence was deduced from its nucleotide sequence after being cloned, the characteristic amino acid residues of an aspartic protease active site were identified, rendering the characterization of YAP3p as an aspartic protease (Fig.3). The expressed, purified enzyme was verified as an aspartic protease by showing 85-95% inhibition of its activity in the presence of pepstatin A (Chap.2), a highly specific competitive inhibitor of aspartic proteases (115,116). However, the structure of pepstatin A is hydrophobic in character, i.e. isovaleryl-Val-Val-statine-Ala-statine, where statine is the common name given to 4-amino-3-hydroxy-6-methylheptanoic acid. Since YAP3p exhibits specificity for positively charged residues e.g. Arg and/or Lys, the efficacy of pepstatin A as an inhibitor of YAP3p was necessary to be determined. The results demonstrate that in fact pepstatin A is a relatively poor inhibitor of YAP3p ($K_i \sim 0.4 \mu\text{M}$) when compared to its ability to inhibit other aspartic proteases that show specificity towards hydrophobic residues ($\sim\text{nM}$ range, (117)). The results also show that V_{max} and $V_{\text{max}_{\text{app}}}$ are very similar (see Method 1, above), supporting the role of pepstatin A as a competitive inhibitor of YAP3p.

Based on the substrate specificity determined in Chap.5, it might be possible therefore to engineer or identify a more potent inhibitor which could be used in the discovery and characterization of other basic-residue specific aspartic protease processing enzymes.

CHAPTER 8

ANALYSIS OF IMMUNOLOGICALLY RELATED MAMMALIAN HOMOLOGUES OF YEAST ASPARTIC PROTEASE 3

SUMMARY

A PCE sized protein was stained with MW283 antiserum in the soluble extract of intermediate and neural lobe secretory vesicles of bovine pituitary, where PCE has been purified from and where POMC and provasopressin, respectively, are processed *in vivo*. Immunocytochemistry of mouse brain sections indicated a specific staining pattern corresponding to peptide-rich regions, e.g. in the PVN and arcuate nucleus of the hypothalamus and in the hippocampus. The anterior pituitary of bovine and mouse generated similar immunostaining patterns of YAP3p-like immunoreactivity, supporting the hypothesis that YAP3p-like molecules exist across species. In addition, a punctate staining pattern was observed in the bovine intermediate lobe sections indicative of a secretory vesicle staining pattern. Western blot analysis of mouse anterior pituitary soluble protein demonstrated specific immuno-crossreactivity with a ~90kDa protein and to a lesser extent with a ~70kDa protein, while mouse hypothalamus specifically stained the 90kDa protein.

INTRODUCTION

The phenomenon of prohormone processing is recognized as an evolutionarily conserved event. It is therefore expected that enzymes involved in prohormone processing across species, exhibit some structural homology to each other. Based on this premise, mammalian homologues (PCs) of Kex2p (27,118-120), a prohormone processing enzyme involved in the maturation of α -mating factor, were cloned using a PCR strategy and the prediction that the active site of this serine protease (Kex2p) would be the most likely conserved region across species.

Therefore, with the discovery, cloning and characterization of an aspartic protease (YAP3p) (23), also from yeast, that can evidently carry out the pro- α -mating factor cleaving function of Kex2p, it is predicted that mammalian homologues of YAP3p exist similar to the homology seen between Kex2p and the PC's. It is also predicted, based on the similarities between YAP3p and the mammalian pro-opiomelanocortin converting enzyme (PCE), i.e. size, specificity, inhibitor profile and pH optimum, that these two enzymes are homologues. Figure 39 and Table 6 illustrates the similarities between YAP3p and PCE.

The characterization of the physical properties of YAP3p along with the studies of its specificity and catalytic properties have yielded a vast amount of information that may be useful in the cloning and characterization of mammalian homologues of YAP3p. In addition, the generation of an antiserum to YAP3p may prove useful in the identification of these homologues by immuno-crossreactivity. To determine if the YAP3p antiserum (MW283) could be used in a future possible expression cloning strategy, it was important

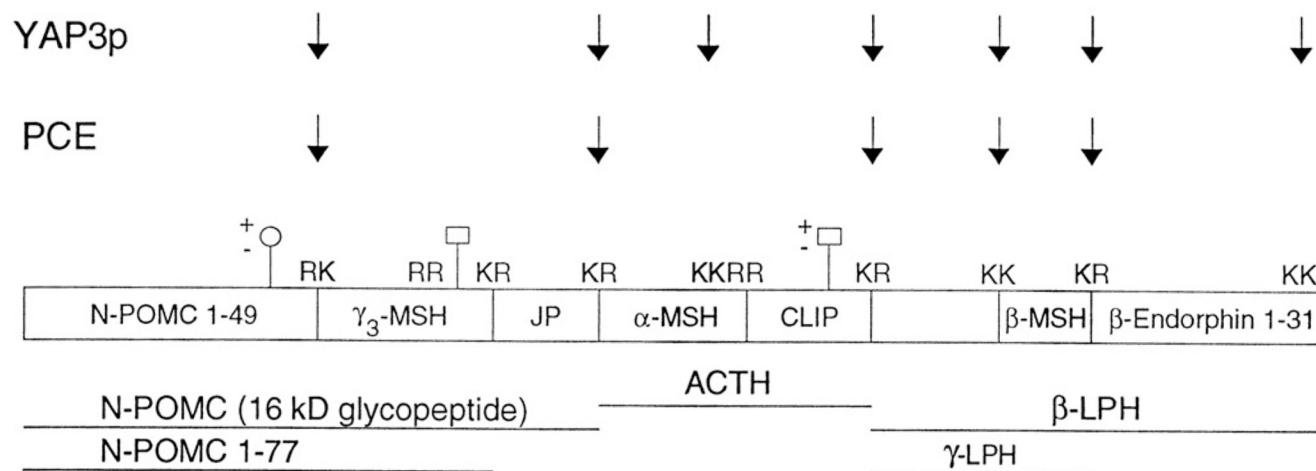


Figure 39. Schematic diagram of bovine pro-opiomelanocortin

POMC = pro-opiomelanocortin; ACTH = adrenocorticotropin hormone; MSH = melanocyte stimulating hormone; CLIP = corticotropin-like intermediate lobe peptide; LPH = lipotropin hormone.

Arrows indicate the sites cleaved by YAP3p and PCE, *in vitro*.

○ = O-linked glycosylation site. □ = N-linked glycosylation sites.

Table 6.

Properties	Yeast Aspartic Protease 3	POMC Converting Enzyme
Size	~70kDa, ~90kDa and ~150-180kDa glycoproteins	~70kDa glycoprotein
pH optimum	4.0-4.5	4.0-5.0
Specificity	Paired- and mono-basic residues of prohormones	Paired-basic residues of prohormones
Localization	Yeast secretory pathway	Secretory vesicles of the bovine pituitary intermediate and neural lobes

Table of comparison between yeast aspartic protease 3 (YAP3p) and the mammalian pro-opiomelanocortin converting enzyme (PCE).

to attempt to identify any crossreactivity of the YAP3p antiserum with specific proteins from mammalian tissue. Immunocytochemistry and western blot analysis were performed to attempt this identification.

PROCEDURES

Immunocytochemistry on mammalian brain and pituitary sections

This procedure was carried out in collaboration with Dr. Le-Ping Pu, LDN, NICHD, NIH. Serial sections of bovine pituitary and mouse whole brain and pituitary (6-12 μ m) were prepared as described in Materials and Methods. Prior to immunocytochemistry, several sets of tissue sections were warmed at room temperature (RT) for 10min, fixed in 4% paraformaldehyde in 1X PBS for 30min and then washed in 1X PBS three times. Sections were then processed for immunocytochemistry using the indirect immunofluorescence method (see Materials and Methods). The controls for the immunocytochemical reaction showed that there was no immunofluorescence when the primary antiserum was replaced by either buffer or pre-immune serum. Moreover, immunoreactivity was completely abolished by omission of the secondary antibody. It is necessary to emphasize that the immunoreactivity obtained from this study is the cross-reaction with structurally related molecules sharing a common antigenic site. Therefore, the immunoreactive materials will be described as YAP3p-like immunoreactivity.

Immunocytochemistry performed on mouse brain sections demonstrated the presence of YAP3p-like immunoreactivity in neurons and endocrine cells, defined by the observation of fluorescence primarily within neuronal perikarya and cytoplasmic regions of

endocrine cells. Specific YAP3p-like immunoreactivity was found in different regions of the mouse central nervous system. The most intense immunostaining was observed in the granular cell layer of the dentate gyrus and in the pyramidal cells of the hippocampus (Fig.40.B) which is a neuropeptide-rich brain structure. YAP3p-like immunoreactivity was also evident in the arcuate nucleus (Fig.40.A) and paraventricular nuclei of the hypothalamus (data not shown), where POMC and provasopressin are synthesized, respectively. In addition, immunostaining was found in the cortex and some thalamic nuclei. There was no detectable immunostaining in the lateral hypothalamic areas.

In the bovine (Fig.41.a and c) and mouse pituitary (Fig.41.e), YAP3p-like immunoreactivity was observed in the pituitary anterior lobe and to a lesser extent in the intermediate lobe as well. In the anterior pituitary, immunoreactivity was localized in a subset of cells, characteristic of the distribution of corticotrophs. In the bovine intermediate lobe, a punctate staining pattern was observed characteristic of the staining of secretory vesicles (Fig.41.a, *arrows*). No specific immunostaining was shown when secondary antibody was omitted, Fig.41.b, or when primary antiserum was omitted, Fig.41.d, or when primary antiserum was substituted by preimmune serum, Fig.41.f.

Western blot analysis of mammalian brain and pituitary proteins

1. Previously, PCE has been purified from the secretory vesicles of the bovine intermediate (65) and neural lobes (66) of the pituitary and characterized. The soluble extract of these secretory vesicles was therefore analysed by western blot using MW283 antiserum to test if PCE showed any immuno-crossreactivity with anti-YAP3p antiserum. The ECL procedure of Amersham was used to detect YAP3p-like immunoreactive bands.

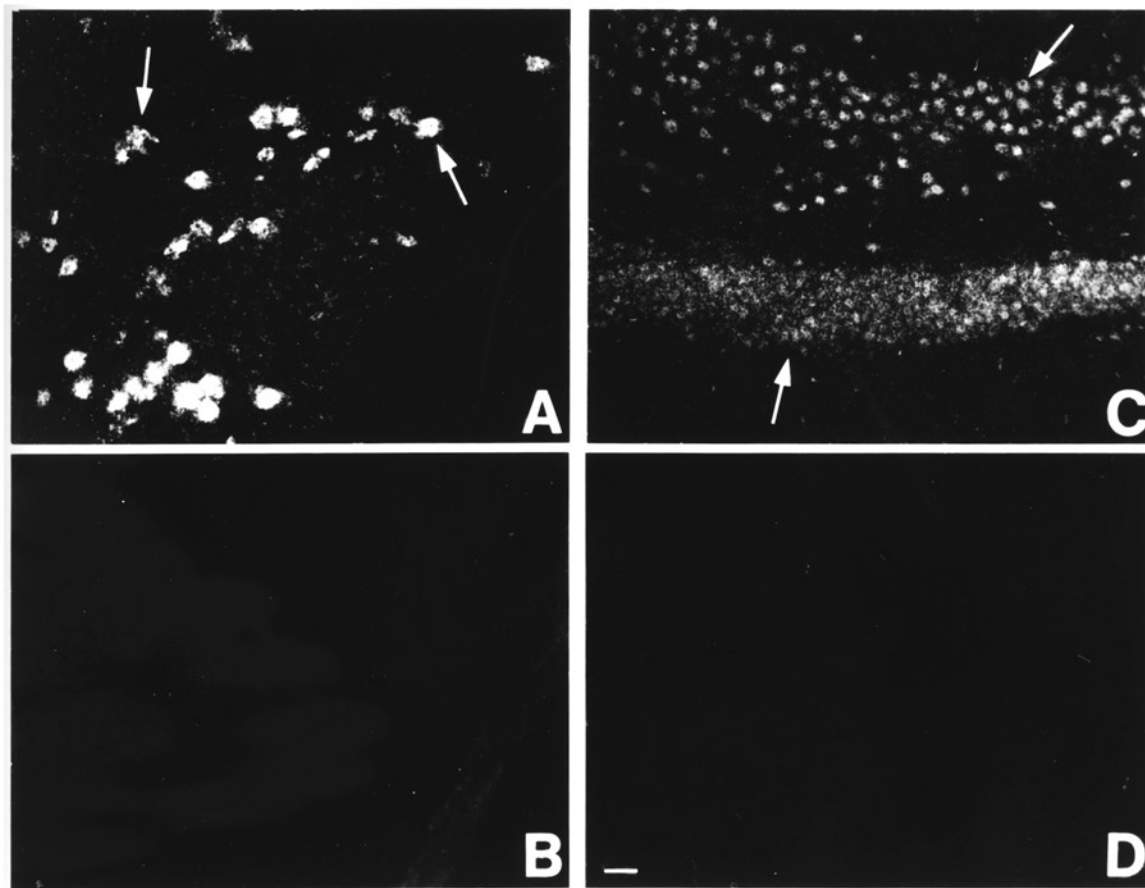


Figure 40. Immunocytochemistry of mouse brain sections with YAP3p antiserum

(A-D) Indirect immunofluorescence of coronal mouse brain sections showing YAP3p-immunoreactive cells (*arrows*) in the arcuate nucleus **(A)** and hippocampus **(C)**. Negative controls include adjacent sections of A and C using pre-immune **(B)**, and omission of primary antibody **(D)**. Bar is 12 μm **(A and B)**, 25 μm **(C and D)**.

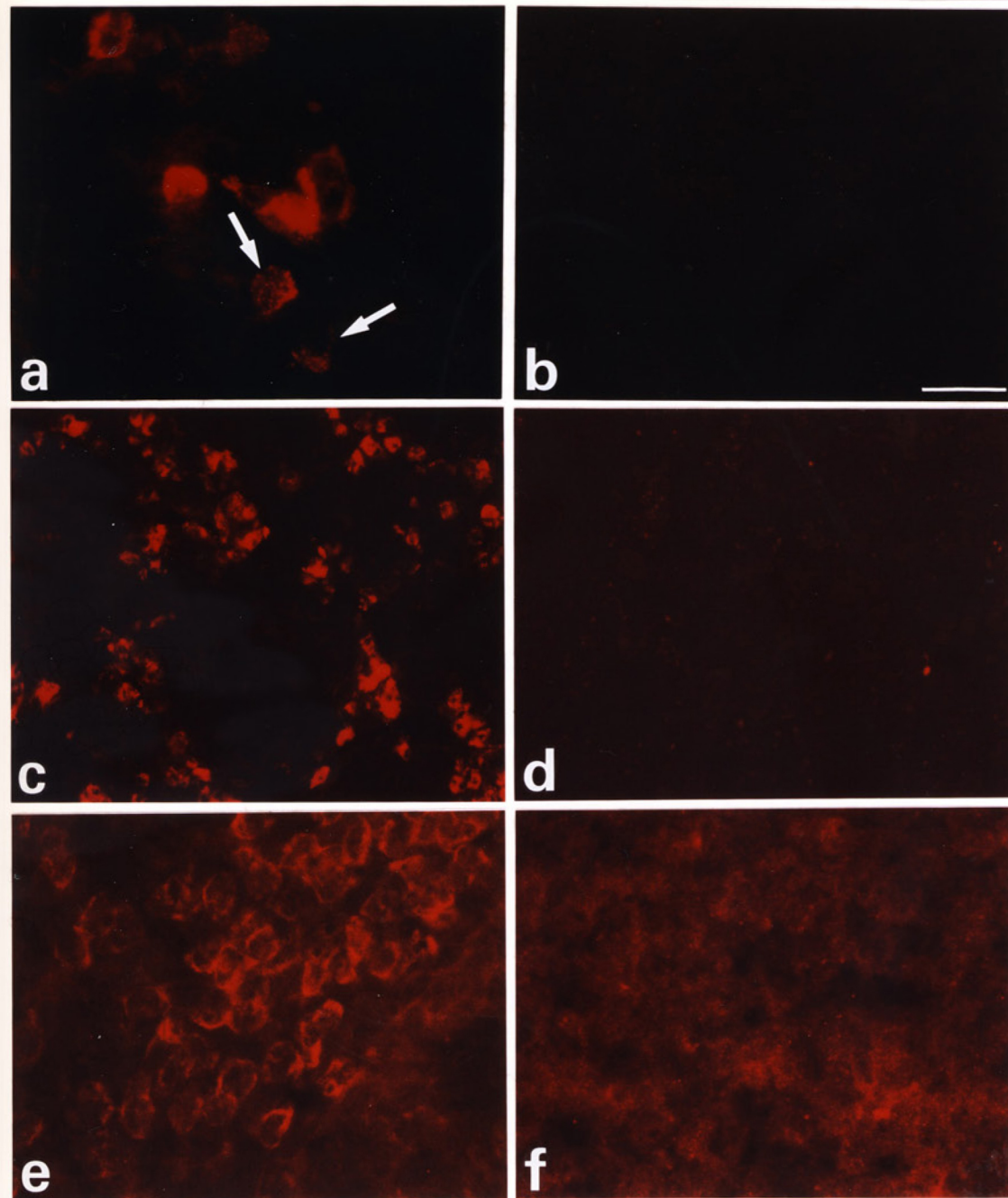


Figure 41. Immunocytochemistry of bovine and mouse pituitary sections with YAP3p antiserum

(a-f) Indirect immunofluorescence of bovine and mouse pituitary sections showing YAP3p-immunoreactive cells in the bovine intermediate lobe **(a)** and anterior lobe **(c)**. Mouse anterior lobe showed immunostaining in a subset of anterior pituitary cells **(e)**. Arrows indicate the characteristic punctate staining pattern of secretory granules **(a)**. Negative controls include omission of secondary antibody **(b)**, omission of primary antibody **(d)**, and substitution of primary antiserum with preimmune serum. Bar is 20 μm **(a and b)**, 30 μm **(c and d)**, 25 μm **(e and f)**.

Intermediate lobe (IL) and neural lobe (NL) secretory vesicles were prepared from bovine pituitaries by the method of Loh et al, (1984). The vesicles were freeze-thawed six times in 5 mM sodium succinate, pH 5.9, to lyse the vesicles and centrifuged at 100,000 g for 30 min to sediment the membranes. The supernatant was fractionated by SDS-PAGE, transferred to nitrocellulose and a western blot was performed with MW283 antiserum. Control lanes of the IL and NL soluble protein were probed with pre-immune antiserum. The results of the western blot demonstrated the immuno-staining of a PCE sized band (~70kDa) in both the IL and NL secretory vesicle soluble protein preparations (Fig.42.A and B, lane 1) that was absent in the pre-immune control lanes (Fig.42.A and B, lane 2).

2. The soluble extract of mouse pituitary anterior lobe (AL) and mouse hypothalamus was also analysed by western blot. Twenty mice were sacrificed by decapitation. The top of the skull was removed and the brain folded back gently and removed to expose the pituitary. The anterior lobe of the pituitaries were collected and homogenized on ice in a 1ml dounce hand homogenizer in Tris/EDTA buffer, pH 8.0. The suspension was centrifuged at 15,000 g for 20min and the supernatant was saved. The cell debris was freeze-thawed three times in 5X PBS and centrifuged as before. The supernatant from this spin was added to the first supernatant and the combined pool was referred to as the soluble extract of mouse anterior pituitary. An identical procedure for the extraction of soluble protein from 10 mouse hypothalamus was used. All steps were carried out on ice. The soluble protein of the anterior pituitary and hypothalamus were

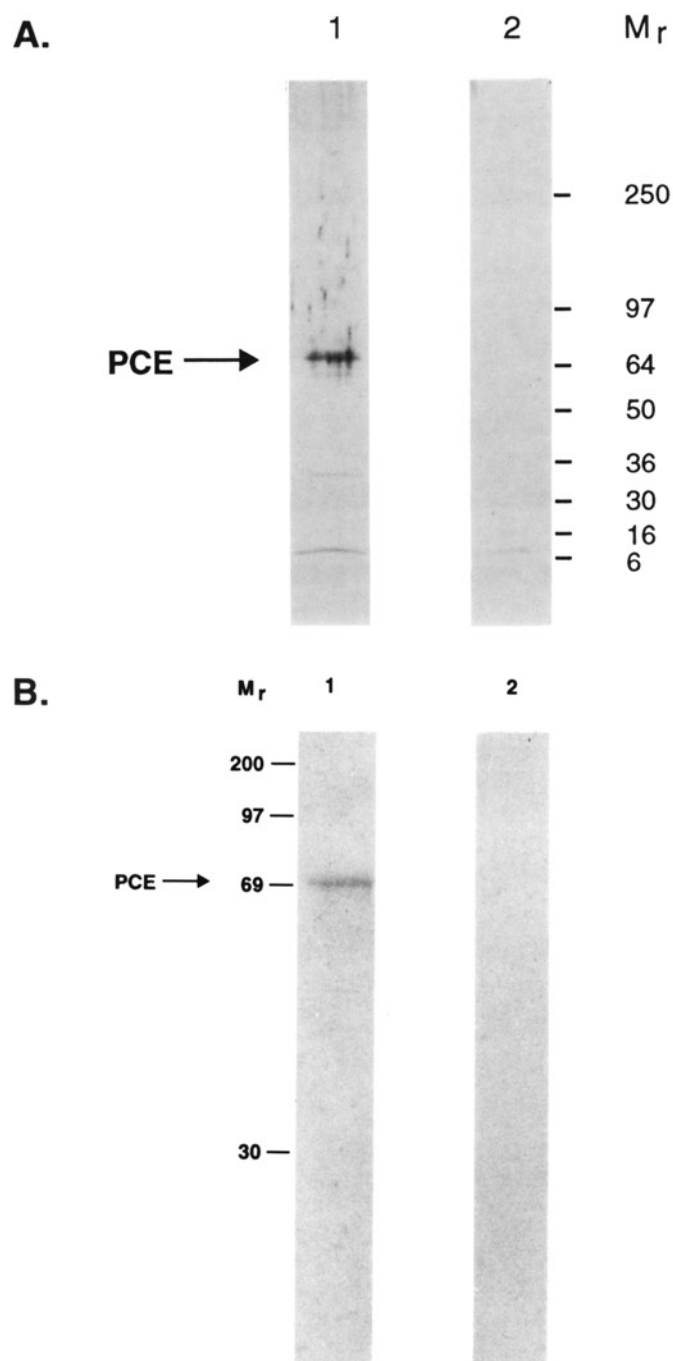


Figure 42. Western blot analysis of bovine intermediate and neural lobe secretory vesicle soluble extract

The soluble extract of either bovine pituitary intermediate lobe (**A**) or neural lobe (**B**) secretory vesicles were analysed by western blot with MW283 (**lane 1**) or MW283 preimmune serum (**lane 2**). Antigen detection was by the enhanced chemiluminescence method of Amersham. *Arrows* indicate the immunopositive staining of a PCE-sized band in both secretory vesicle extracts.

analysed by western blot as follows. Four identical aliquots of both protein samples were fractionated on an 8-16% SDS pre-cast gradient polyacrylamide gel from Novex, Sorento, Ca. After transferring to nitrocellulose, a western blot was performed with MW283 antiserum, antiserum MW283 that had been pre-absorbed with purified YAP3p (see Chap. 6), pre-immune serum and omission of primary antibody. Antiserum MW283 was used at a dilution of 1:20,000 while the pre-immune serum was used at a dilution of 1:5,000. Antigen detection was by the enhanced chemiluminescence method of Amersham. The results showed the immuno-staining of a protein with an apparent molecular mass of ~90kDa in both tissues (Fig.43.A and B, lane 1). Also in both cases, the intensity of the staining of this band was dramatically reduced in the lanes that were probed with MW283 that had been pre-absorbed with purified YAP3p (Fig.43.A and B, lane 2). Additionally, in the AL lanes probed with antiserum MW283 there was evidence of a ~70kDa band that was absent in the two control lanes (Fig.43.B, lanes 3 and 4). A ~70 kDa protein was not seen in the hypothalamic extract. The presence of other staining bands (Fig.43.A and B) indicate the possibility that there are other YAP3p-like proteins representing other members of the sub-class of aspartic protease prohormone processing enzymes in the protein preparations. However, the band at ~40kDa in Fig.43.A, lane 1, which corresponds in size to Cathepsin D, appears not to be specific since it is present in the preimmune control lane (lane 3) and upon longer exposure of the western blot to the photographic film, this band also appeared in lane 4, where no primary antiserum was applied.

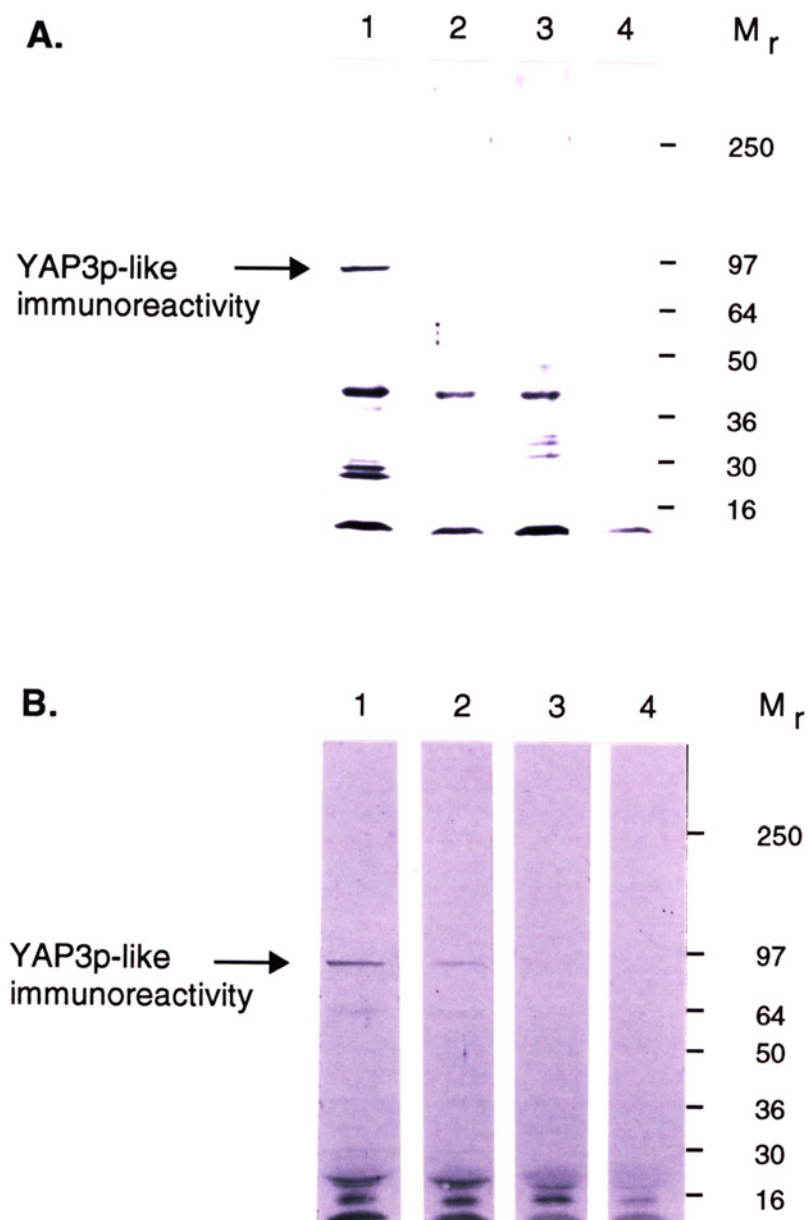


Figure 43. Western blot analysis of the soluble extract of mouse hypothalamus and mouse anterior pituitary

The soluble extracts of either mouse hypothalamus (**A**) or mouse anterior pituitary (**B**) were analysed by western blot with MW283 (**lane 1**), MW283 that was preabsorbed with purified YAP3p (**lane 2**), MW283 preimmune serum (**lane 3**), and omission of primary antibody (**lane 4**). Antigen detection was by the enhanced chemiluminescence method of Amersham. The *arrows* indicate the immunopositive staining of a YAP3p-like immunoreactive band at ~90kDa in both extracts.

DISCUSSION

Immunocytochemistry and western blot analysis using an antiserum to YAP3p were performed to determine if there were mammalian proteins that were immunologically related to YAP3p. The detection of an immunoreactive ~70kDa, PCE sized protein band in the bovine IL and NL secretory vesicle soluble extracts and mouse AL soluble extract, supports the hypothesis that PCE is structurally homologous to YAP3p. In addition, the presence of an anti-YAP3p immunoreactive ~90kDa protein in the mouse AL and mouse hypothalamus indicates that additional homologues of YAP3p exist which may represent a family of mammalian basic-residue specific aspartic proteases. These findings provide a basis for future attempts at cloning these mammalian homologues using strategies that include the use of the YAP3p antibody for screening a mouse brain expression library.

CHAPTER 9

CONCLUSIONS

Yeast aspartic protease 3 represents the only cloned member of the novel sub-class of aspartic protease processing enzymes that has been published. Since Kex2p has been characterized as a processing enzyme in yeast, the ability of *YAP3* to suppress the phenotype of a *Kex2* null mutant, allows this enzyme to be characterized also as processing enzyme of the aspartic protease family.

The cloning of YAP3 has allowed us to overexpress, purify and characterize this unique enzyme with respect to its size, pH optimum, inhibitor profile and specificity. Wild type YAP3p was predicted to be associated on the extracellular side of the yeast periplasm *in vivo* and that its association with the membrane is via a glycosphosphatidylinositol (GPI) anchor at amino acid Asn⁵⁴⁸. The function of YAP3p *in vivo* is still unknown, however, putative heat shock elements in its promoter region and the temperature studies reported here suggest a function for YAP3p in heat stressed yeast cells. A soluble form of YAP3p was engineered by removing 37 amino acid residues from the carboxy-terminus which included the putative GPI anchoring site. The enzyme was subsequently secreted into the growth media where it was purified and characterized. The secreted forms of YAP3p were found to be hyperglycosylated with Asn-linked sugars, representing 200-300% of the apparent molecular mass of the protein backbone. The glycosylated YAP3p was found to

be extremely stable while the deglycosylated form was not, when measured by their ability to withstand a lyophilization procedure. The specificity of YAP3p for the basic residue cleavage sites of prohormone and proneuropeptide substrates was extensively analysed. It demonstrated a preference for paired- versus mono-basic cleavage sites in general with the highest catalytic efficiency for a substrate with six basic residues in the cleavage site area.

The literature describes a number of mammalian aspartic proteases that exhibit specificity for the basic residues of prohormones, however, whether or not they are homologues of YAP3p still remain to be determined. Based on the fact that somatostatin-28 generating enzyme from anglerfish islet cells can perform the exact same cleavage as YAP3p, it was predicted that this enzyme might be the anglerfish homologue of YAP3p (69). However, the size and N-terminal amino acid sequence of this enzyme does not support this prediction. The fact that it is an aspartic protease that cleaved after an arginine residue cleavage site of prosomatostatin II to generate somatostatin-28 does predict that it may indeed belong to a broader superfamily of prohormone processing aspartic proteases.

The major protease activity observed from the soluble extract of ultrapurified secretory vesicles of the bovine pituitary intermediate lobe was determined to be from the aspartic protease family. This activity was subsequently characterized as PCE and determined to be able to cleave POMC *in vitro* at basic residue cleavage sites. Additionally, pulse-chase experiments, in the presence of pepstatin A, of primary cultures of mouse pituitary intermediate lobe demonstrated a significant inhibition of POMC processing over the negative control indicating that an aspartic protease played an

important role in the processing of POMC *in vivo*. These results provide evidence that PCE is a physiologically relevant prohormone processing enzyme.

Although in the absence of direct sequence data of PCE, the circumstantial evidence alone concerning the characteristics of size and specificity of PCE, in addition to pH optimum and inhibitor profile, allow us to provisionally label PCE as a mammalian homologue of YAP3p. Further support of this hypothesis is obtained from our studies with the YAP3p antiserum. Western blot analysis of the soluble extract of bovine pituitary intermediate and neural lobe secretory vesicles, where PCE has been purified from, demonstrate the immuno cross-reactivity of the YAP3p antiserum with a PCE sized protein. Similar results were seen with a partially purified preparation of PCE (Concanavalin A purified), however, due to variabilities in the pepstatin A-agarose affinity column i.e. the second step in the purification of PCE, a purified preparation of PCE has not been tested. The specificity differences observed between PCE and YAP3p, i.e. the ability of YAP3p to cleave the tetra-basic residue site of ACTH and Lys²⁸-Lys²⁹ site of β -endorphin¹⁻³¹, while PCE did not make these cleavages, is a distinction that has a precedent that is seen between that of Kex2p and PC1 and PC2.

The study of the physical and catalytic properties of YAP3p will lead us to a better understanding of the physiological role YAP3p may play in yeast, and as a model of this sub-class of aspartic proteases, will provide important and useful information for the future identification and characterization of putative mammalian homologues of YAP3p. In addition, the specificity of YAP3p renders it a potentially commercially useful enzyme for processing recombinant prohormones *in vitro*.

CHAPTER 10

MATERIALS AND METHODS

Concanavalin A chromatography

The soluble extract of the yeast cells or growth media were diluted with four volumes of Con A equilibration buffer, (10 *mM* Tris/HCl, 0.7 *mM* MgCl₂, 1 *M* NaCl, 0.1% Triton X-100, pH 7.4). This enzyme solution was batch processed by addition to 1-5ml of pre-equilibrated Con A-sepharose beads (Pharmacia LKB Biotechnology Inc.) followed by gentle mixing for 2h. The Con A-Sepharose beads were then used to pour a column and the flow-through was collected. The column was washed with equilibration buffer until there was no detectable protein in the washes. For maximum recovery of YAP3p enzymatic activity, the column was allowed to sit in 2-3 volumes of elution buffer (Con A equilibration buffer with 0.5 *M* methyl- α -D-mannopyranoside) overnight. The eluent was then collected and assayed. This procedure was carried out at 4°C.

Protein desalting and lyophilization

2.5mls of a protein solution was applied onto a pre-equilibrated disposable 5ml PD 10 desalting column (Sephadex G-25 M, Pharmacia LKB) following the procedures of the manufacturer. The column was pre-equilibrated with the desalting buffer, e.g 50 *mM* ammonium bicarbonate/0.02% Tween 20. The sample was loaded and the salt allowed to

elute by gravity. 3.2ml of the desalting buffer was then used to elute the retained protein. Use of this buffer allowed complete lyophilization without salts remaining. The 3.2ml desalted protein sample was frozen in a 50ml Falcon tube. Parafilm, with a number of pinholes for ventilation, was used to cover the top of the tube. The tube was placed on the lyophilizer and carefully monitored initially to be sure that the sample remained frozen. The desalting procedure can be carried out at room temperature or at 4°C, however, equilibration at that temperature is required prior to the procedure.

YAP3p assay procedures

A rapid and sensitive assay has been developed for the purification of YAP3p based on the principle that this enzyme cleaves human β -lipotropin (β_{h} -LPH) at paired-basic residue sites to generate β -endorphin and β -melanocyte stimulating hormone (β -MSH) and the finding that the products are soluble in 10% trichloroacetic acid (TCA), while the substrate is not. This allows YAP3p enzymatic activity to be assayed as TCA soluble counts generated from custom iodinated human β -lipotropin ($^{125}\text{[I]}$ β_{h} -LPH). β -LPH is obtainable from the National Pituitary Agency (Baltimore, MD, USA). Samples to be assayed were incubated in a final volume of 160 μl of 0.1 *M* sodium citrate, pH 4.0 with $^{125}\text{[I]}$ β_{h} -LPH (~10,000-20,000cpm) for 30min at 37°C. The reaction was stopped by the sequential addition of 20 μl of ice cold bovine serum albumin (BSA), (0.1% w/v final) and 20 μl of TCA (10.0% v/v final) and allowed to precipitate on ice for 30min. After centrifugation at 10,000 g for 10min, two aliquots of 75 μl of the supernatant were counted in a gamma counter to determine TCA soluble products generated.

For a more sensitive and quantitative assay for YAP3p, adrenocorticotropin hormone (ACTH¹⁻³⁹) can be used as a substrate. YAP3p has been shown to cleave ACTH¹⁻³⁹ at the tetra-basic residue site, Lys₁₅-Lys₁₆-Arg₁₇-Arg₁₈, to release ACTH¹⁻¹⁵ and the N-terminally extended corticotropin-like intermediate lobe peptide (CLIP¹⁶⁻³⁹). These products can be detected and quantitated by HPLC analysis (C18 column, buffer A was 0.1% trifluoroacetic acid (TFA), buffer B was 80% acetonitrile/0.1% TFA, a linear gradient from 20% B to 27% B in 30 min followed by 27% B to 37% B in 30 min was used to separate the products). 10µg of ACTH¹⁻³⁹ was incubated with the enzyme in a volume of 100µl, 0.1M sodium citrate, pH 4.0, for 30min. The reaction was stopped with 10µl glacial acetic acid (~10.0% v/v final) and 50µl was analysed by HPLC. The products, ACTH¹⁻¹⁵ and CLIP¹⁶⁻³⁹, eluted from the column at ~21 and ~46 minutes, respectively, while the substrate eluted at ~52 minutes. The products were detected and quantitated by absorbance at 214nm allowing the specific activity of YAP3p to be calculated.

Polyacrylamide gel electrophoresis

Sample preparation

Protein samples were prepared for SDS-PAGE under reducing conditions by the addition of 0.33 volumes of a 4X SDS sample buffer. This buffer was composed of 0.25 M Tris/Cl, pH 6.8, 8% SDS, 40% glycerol and 20% β-mercaptoethanol. Bromophenol blue was also present at a concentration of 0.05%. The sample was boiled for 5min in a screw top eppendorf tube and after boiling, was allowed to cool. After flash centrifugation to collect the condensation, the sample was loaded onto the gel. For lyophilized protein

samples, the same procedure was used except that a 1X dilution of the sample buffer was used to reconstitute the protein.

Preparation of polyacrylamide gels

The procedure described in detail in the catalogue of Hoefer Scientific Instruments, San Francisco, CA, was used in the preparation of polyacrylamide gels. The running gels, which varied in acrylamide concentration, were allowed to polymerize at room temperature under either a layer of water or isopropanol. The stacking gels were consistently prepared at an acrylamide concentration of 2.5%. Prior to loading the protein samples, the wells were rinsed gently three times with running buffer to remove unpolymerized acrylamide solution. The running buffer consisted of 0.025 *M* Tris (0.05%), 0.192 *M* glycine (1.44%), 0.1% SDS, pH 8.3, and used at both the cathode and anode reservoirs.

Precast polyacrylamide electrophoresis gels

Since the generation of gradient polyacrylamide gels is a specialized and time consuming technique, a number of commercially available precast polyacrylamide gels were used. Also, the use of gradient gels allowed the consistent transfer to nitrocellulose of high and low molecular weight proteins in the western blotting procedure (see below). The pre-cast gels were purchased from Novex, Sorrento, CA. These gels generated consistent and accurate results. Sample loads were limited to 40 μ l and gel runs took as little as 1hr.

Protein staining procedures

Coomassie blue

The protein binding property of the dye, coomassie brilliant blue, was used to stain the gel. A 0.25% solution of the dye was made up in 30% methanol and 10% glacial acetic acid. This solution fixes and stains the protein in the gel at the same time. The time required for complete staining to occur depended on the thickness of the gel, usually 1-2hrs. Destaining of the gel was accomplished by incubation of the stained gel in 30% methanol/10% glacial acetic acid.

A novel colloidal coomassie blue staining procedure has been developed by Novex, which involves the specific staining of the proteins in the gel and not the gel itself. This releases the necessity to destain the gel. Also, the limit of detection of this procedure is ~5 fold better than that of the regular coomassie blue staining.

Silver stain

The gel was fixed in 30% methanol/10% glacial acetic acid for 1hr after which it was washed extensively with distilled water. The gel was then processed according the procedure of the manufacturer, Novex, Sorenta, CA. The procedure was completed in 2hr.

Western blotting procedures

Transfer of the proteins

Once the proteins have been separated by SDS-PAGE electrophoresis, the gel was washed for 15min in transfer buffer (i.e. same as SDS-PAGE running buffer but with 20% methanol and no SDS). The gel was then placed on a wet piece of 3M filter paper, followed by a piece of nitrocellulose paper, that had been pre-equilibrated in transfer buffer, and then a final piece of wet 3M filter paper was placed on the nitrocellulose to complete the sandwich. The filter paper and nitrocellulose was pre-cut to fit the size of the gel. The nitrocellulose was placed on the gel avoiding the trapping of air bubbles. This sandwich was set up in the transfer module and allowed to transfer at 300mA for 3hr. Addition of dye-labelled molecular weight standards allowed the efficiency of transfer to be monitored. To check how the transfer was proceeding, the power supply was stopped, the sandwich removed and one corner of the nitrocellulose that corresponded to the position of a high molecular weight pre-stained marker was very carefully peeled back. The gel was visually inspected for the presence of the marker.

When the proteins have been transferred, the nitrocellulose (blot) was removed and placed in blocking solution (3% BSA, 0.1% tween 20, 0.02% sodium azide) for 1-2hr at room temperature. For probing of the blot, the antiserum (i.e. primary antibody) was diluted with 1X PBS/0.1% tween 20 and 1.5% normal goat serum, and incubate at 4°C, overnight.

Antigen detection by Vectastain ABC kit

The blot was washed with wash buffer (1X PBS/0.1% tween 20) for 30min, changing the wash several times, and then incubated for 30min with the biotinylated goat anti rabbit IgGs (i.e. secondary antibody) diluted with wash buffer to the dilution recommended by the manufacturer. The blot was then washed as before and incubated for 30min with the complex of biotin and avidin conjugated alkaline phosphatase. This complex was made by pre-incubating the free biotin and the avidin conjugated alkaline phosphatase for 30min prior to addition to the blot. After the last wash, the blot was developed with a colorimetric assay for alkaline phosphatase.

Antigen detection by Amersham enhanced chemiluminescence kit

After overnight incubation of primary antibody, the blot was washed as described above. The secondary antibody (donkey anti rabbit conjugated horse raddish peroxidase) diluted with wash buffer to a dilution of 1:20,000 was then added for 1hr. The blot was washed thoroughly and then incubated for 1-2min at room temperature with the kit reagents that resulted in the liberation of light from the chemical, luminol. The blot was drained of the reagents for 20sec, wrapped in saran wrap and exposed to photographic film for 1-20min.

Immunodepletion/immunoprecipitation

An aliquot of the enzyme/protein sample was diluted with 10 μ l of 10X PBS, 1 μ l of freshly prepared PMSF (30mg/ml), 5 μ l of aprotinin (10mg/ml), 0.5-5 μ l of antiserum and water to a volume of 100 μ l. The sample was then mixed by rotation at 4°C, for 16hrs. 50 μ l of protein A-Sepharose beads (1.5g/10ml 1X PBS) was then added and mixed by

rotation for 45min at room temperature. The beads were sedimented by centrifugation (10,000 g, 5min) and the supernatant assayed for enzymatic activity. For analysis of the immunoprecipitated antigens, the beads were washed twice with 1X PBS/0.1% tween 20 and then either boiled in 1X SDS sample buffer for analysis by SDS-PAGE or vortexed in 0.01 M HCl for analysis by HPLC. By lowering the pH and increasing the salt concentration enzymatic activity can be released and assayed.

Indirect Immunofluoresence of Yeast

Yeast cells, transformed with the pEMBLyex4-YAP3 construct were induced as described in Chap. 3. The cells were harvested by centrifugation at 2000 g for 5min and rapidly resuspended in buffer A (40 mM potassium phosphate with 0.5 mM MgCl₂) containing 4% paraformaldehyde. After a 2hr fixation at room temperature, the cells were centrifuged and washed three times with buffer B (buffer A with sorbitol at 1.2 M). To remove the cell wall, the yeast cells were resuspended in 1ml buffer B containing 55µl glucuslase (Du Pont NEN, Boston, MA) and 10µl β-mercaptoethanol and digested for 1hr at 37°C. Digested yeast were washed twice with buffer B and once with a 1:1 mixture of buffer B and 1X PBS and then resuspended in 1X PBS. Multiwell slides were treated by adding approximately 50 µl of 0.1% poly-L-lysine (Sigma, St. Louis, MO) to each well for 10min and then air dried. The treated slides were hydrated by incubation in water for 10min and then air-dried completely. Fifty µl of yeast cell suspension was added to each well and allowed to stand for about 10min. After aspirating the excess fluid, 50µl of primary antibody (MW283, diluted with 1X PBS to 1:500-1:10,000) was applied to each well. Cells were incubated in a moist chamber for 24hr at 4°C. After 6 washes with 1X

PBS, cells were incubated with fluorescein (FITC)-conjugated goat anti-rabbit immunoglobulin (Vector Labs, Burlingame, CA), diluted with 1X PBS to 1:100 in a dark, moist chamber for 1hr at room temperature. The slides were washed with 1X PBS for 15min and coverslipped in gel mount. The slides were observed under a Nikon microscope using a 40 Plan-APO objective either in 490-495 nm excitation wavelength for FITC or in bright field.

Determination of K_m and V_{max}

The method of Lineweaver-Burk (91) was used to calculate K_m and V_{max} values for the generation of each major product (see Chap.5, Part 2 for products). Reaction conditions (i.e. enzyme amount and incubation time) were determined such that >90% of the substrate remained after the reaction and that the formation of product was linear with time within the substrate concentrations used. Once the correct amount of enzyme was determined, a time course for the generation of each product was done by incubating YAP3p with the highest and lowest concentrations of each substrate that would be used in the kinetic assays. This was done to determine the time frame for a linear response in the generation of the products. It was assumed that a linear response (i.e. initial rate) obtained at both these substrate concentrations, would also generate linear responses at any concentration within these two limits (Figs.44-49.A). Products were measured in centimeters of peak height when analysed by reverse phase HPLC and detected by absorbance at 214nm. After determining the incubation times that were most linear for the lowest and highest concentrations of that substrate, four substrate concentrations, spanning approximate K_m values obtained from preliminary experiments, were incubated

with the enzyme. The products were analysed as described in Chap.5, part 2, and each substrate concentration was incubated in triplicate. The product of the ACTH¹⁻³⁹ reaction, ACTH¹⁻¹⁵, was quantitated by comparison to a standard curve generated from ACTH¹⁻¹⁴, while the products of dynorphin A, dynorphin B and amidorphin were quantitated by standard curves of Leu-enkephalin-Arg, Leu-enkephalin-Arg-Arg and Met-enkephalin-Lys-Lys, respectively. The product of proinsulin, a proinsulin intermediate, was quantitated by a standard curve of proinsulin itself. Since there were no commercially available standards for CCK23-33, one of the cleavage products of CCK13-33, it was quantitated based on the molar decrease of the substrate. The Lineweaver-Burk plots were generated by plotting 1/average peak height (as a measure of rate) versus 1/[substrate] (Fig.44-49.B). The corresponding kinetic parameter, K_m was determined directly from the plots, however the V_{max} values ($\text{cm}^{-1}/\text{time}$) obtained from the plots were converted to the correct units (pmoles/min) using the standard curves mentioned above.

Calculations of K_m , V_{max} , k_{cat} and k_{cat}/K_m

1. Amidorphin

Incubation time: 10min

[YAP3p] = 0.2 nM

Lineweaver-Burk equation: $y = 0.1937 + 27.152x$, $r^2 = 0.999$

$K_m = 140.2 \mu\text{M}$,

$V_{max} = 5.16\text{cm}/10\text{min}$

$= 3.85 \mu\text{g Met-Enk-Lys-Lys}/\text{hr}$

$= 4.64 \times 10^{-5} \text{ M}/\text{hr}$

$$V_{\max}/[\text{YAP3p}] = k_{\text{cat}} = 64.4 \text{ s}^{-1}$$

$$k_{\text{cat}}/K_{\text{m}} = 4.6 \times 10^5 \text{ M}^{-1} \text{ s}^{-1}$$

2. ACTH¹⁻³⁹

Incubation time: 15min

[YAP3p] = 0.1 nM

Lineweaver-Burk equation: $y = 0.09468 + 1.7236x$, $r^2 = 0.973$

$K_{\text{m}} = 18.2 \text{ } \mu\text{M}$, $V_{\max} = 10.56 \text{ cm}/15 \text{ min}$

$$= 3.65 \text{ } \mu\text{g ACTH}^{1-15}/\text{hr}$$

$$= 1.99 \times 10^{-5} \text{ M/hr}$$

$$V_{\max}/[\text{YAP3p}] = k_{\text{cat}} = 55.3 \text{ s}^{-1}$$

$$k_{\text{cat}}/K_{\text{m}} = 3.04 \times 10^6 \text{ M}^{-1} \text{ s}^{-1}$$

3. Dynorphin A

Incubation time: 5min

[YAP3p] = 0.4 nM

Lineweaver-Burk equation: $y = 0.18226 + 23.383x$, $r^2 = 0.995$

$K_{\text{m}} = 128.3 \text{ } \mu\text{M}$, $V_{\max} = 5.49 \text{ cm}/5 \text{ min}$

$$= 4.99 \text{ } \mu\text{g Leu-Enk-Arg/hr}$$

$$= 7.01 \times 10^{-5} \text{ M/hr}$$

$$V_{\max}/[\text{YAP3p}] = k_{\text{cat}} = 48.7 \text{ s}^{-1}$$

$$k_{\text{cat}}/K_{\text{m}} = 3.7 \times 10^5 \text{ M}^{-1} \text{ s}^{-1}$$

4. Dynorphin B

Incubation time: 10min

[YAP3p] = 0.1 nM

Lineweaver-Burk equation: $y = 0.21988 + 19.315x$, $r^2 = 0.996$

$K_m = 87.84 \mu\text{M}$,

$V_{\max} = 4.55\text{cm}/10\text{min}$

$= 2.72 \mu\text{g Leu-Enk-Arg-Arg/hr}$

$= 3.13 \times 10^{-5} \text{ M/hr}$

$V_{\max}/[\text{YAP3p}] = k_{\text{cat}} = 86.9 \text{ s}^{-1}$

$k_{\text{cat}}/K_m = 9.7 \times 10^5 \text{ M}^{-1}\text{s}^{-1}$

5. Proinsulin

Incubation time: 20min

[YAP3p] = 4 nM

Lineweaver-Burk equation: $y = 0.25294 + 7.0016x$, $r^2 = 0.999$

$K_m = 27.68 \mu\text{M}$,

$V_{\max} = 3.95\text{cm}/20\text{min}$

$= 4.39 \mu\text{g Proinsulin intermediate/hr}$

$= 5.05 \times 10^{-6} \text{ M/hr}$

$V_{\max}/[\text{YAP3p}] = k_{\text{cat}} = 0.35 \text{ s}^{-1}$

$k_{\text{cat}}/K_m = 1.2 \times 10^4 \text{ M}^{-1}\text{s}^{-1}$

6. CCK13-33

Incubation time: 15min

[YAP3p] = 1 nM

Lineweaver-Burk equation: $y = 0.2386 + 27.6298x$, $r^2 = 0.994$

$$\begin{aligned}K_m &= 115.8 \mu\text{M}, & V_{\max} &= 4.19 \text{ cm}^3 / 15 \text{ min} \\& & &= 1.97 \mu\text{g CCK23-33/hr} \\& & &= 1.72 \times 10^{-5} \text{ M/hr} \\V_{\max} / [\text{YAP3p}] &= k_{\text{cat}} = 4.8 \text{ s}^{-1} \\k_{\text{cat}} / K_m &= 3.9 \times 10^4 \text{ M}^{-1} \text{ s}^{-1}\end{aligned}$$

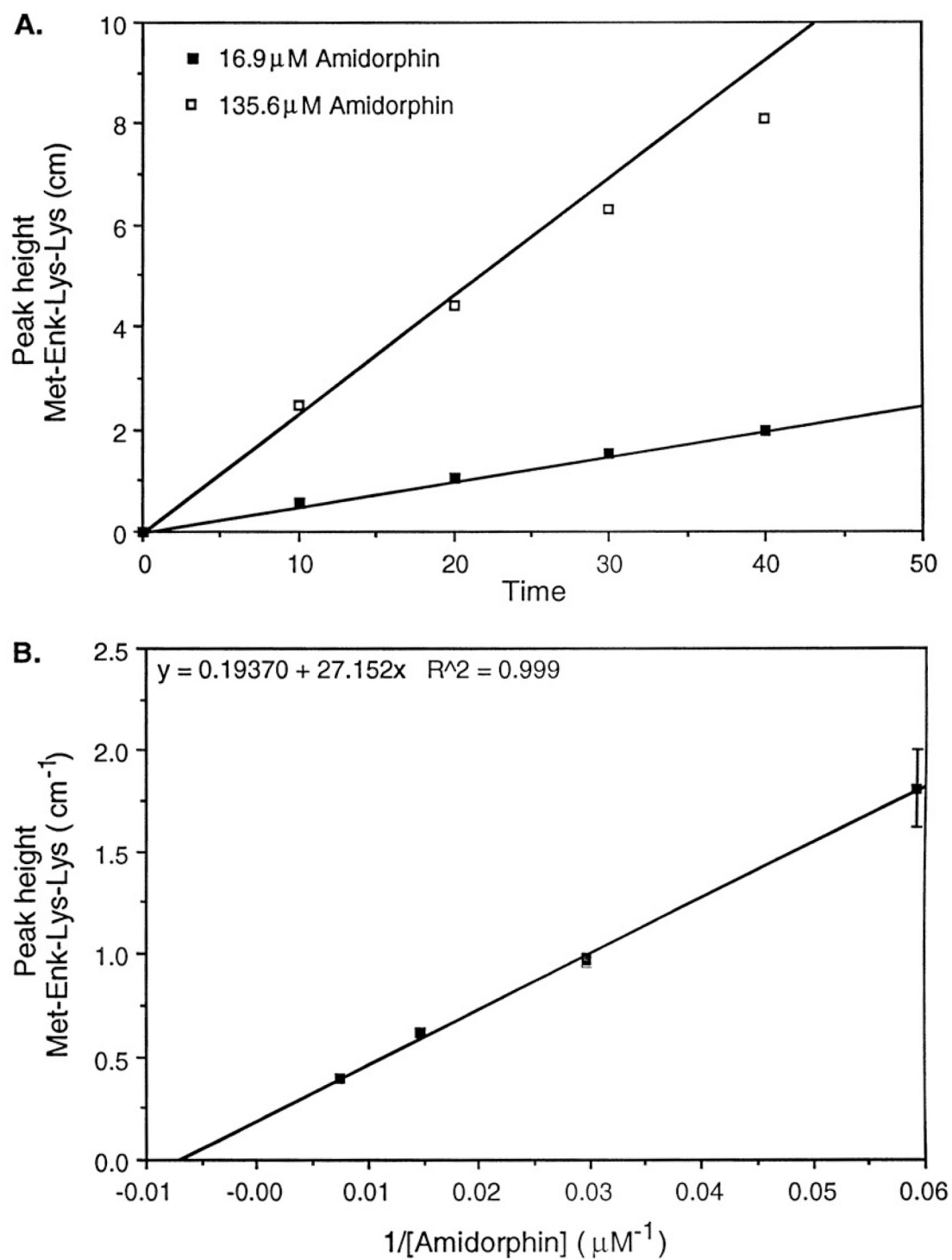


Figure 44. Initial rate (A) and Lineweaver-Burk (B) plots for the cleavage of amidorphin by YAP3p

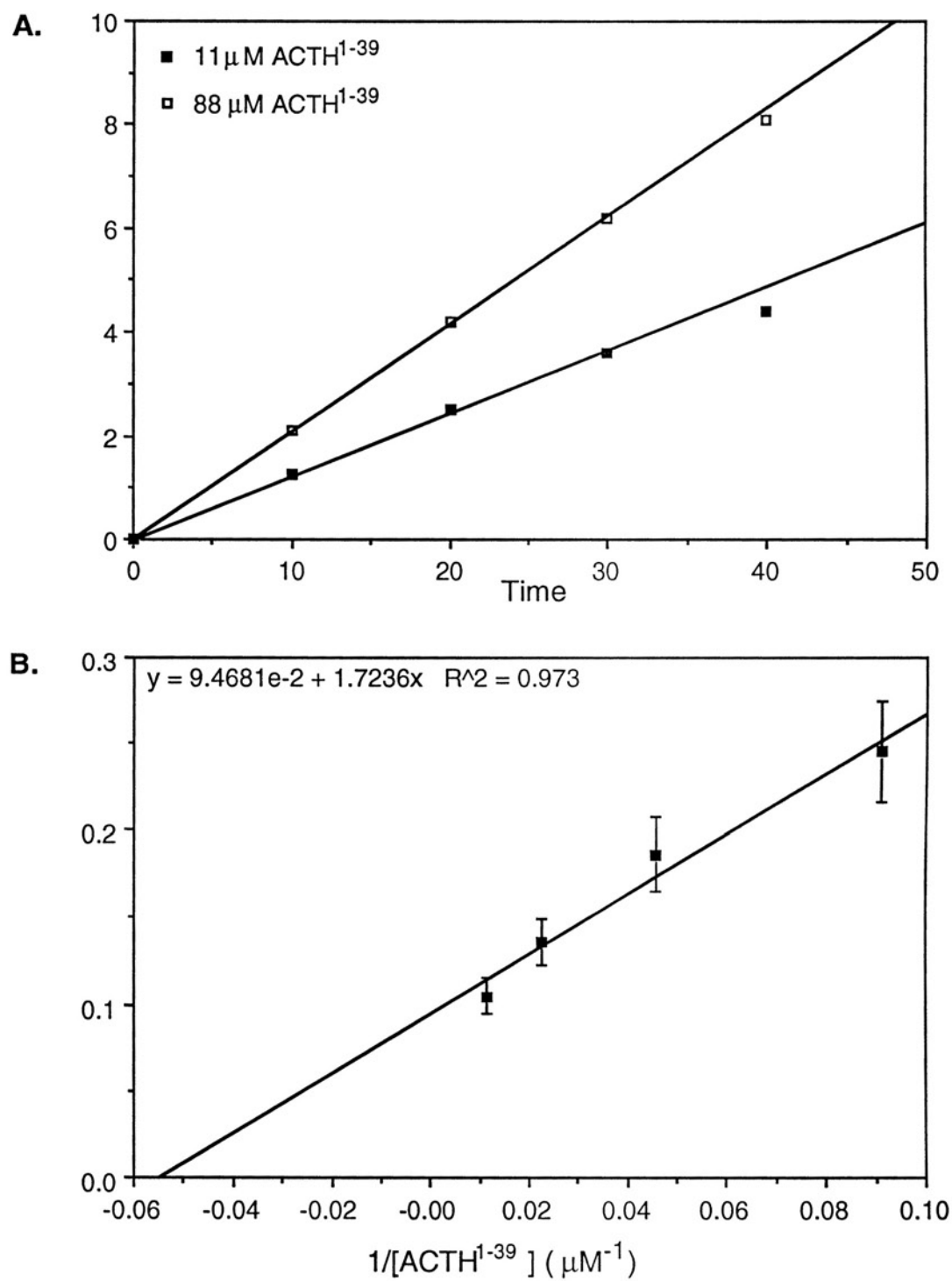


Figure 45. Initial rate (A) and Lineweaver-Burk (B) plots for the cleavage of ACTH¹⁻³⁹ by YAP3p

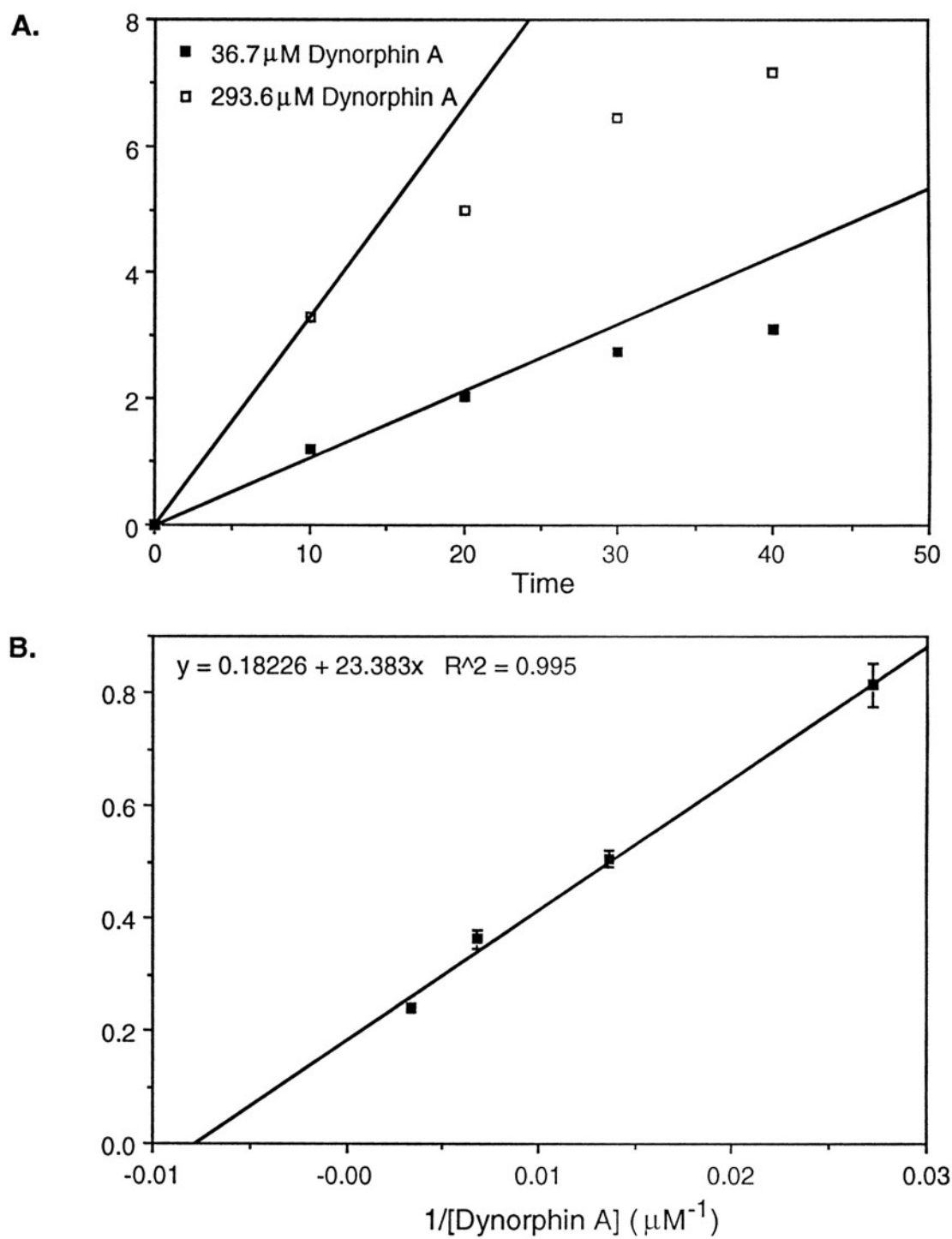


Figure 46. Initial rate (A) and Lineweaver-Burk (B) plots for the cleavage of dynorphin A by YAP3p

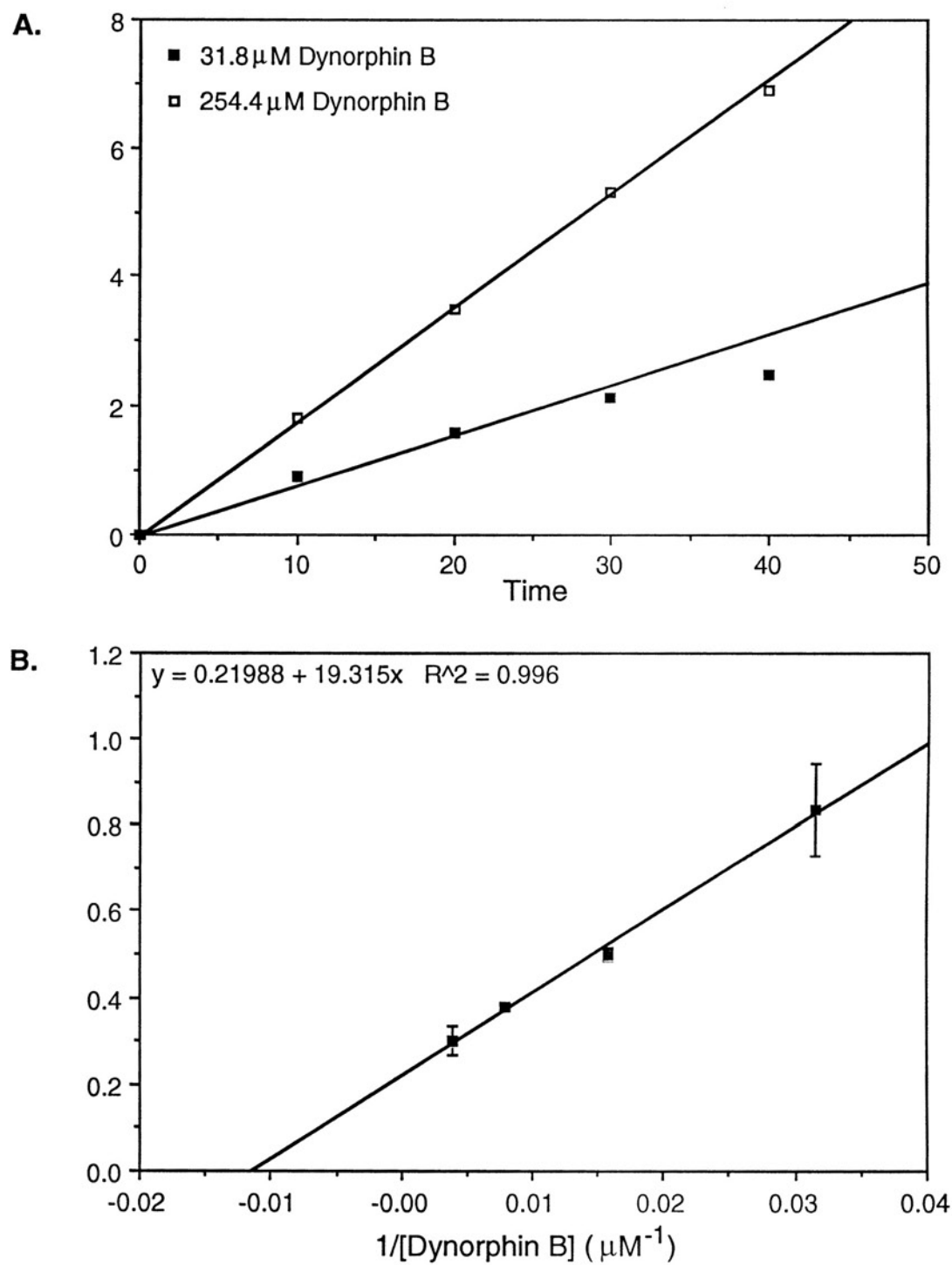


Figure 47. Initial rate (A) and Lineweaver-Burk (B) plots for the cleavage of dynorphin B by YAP3p

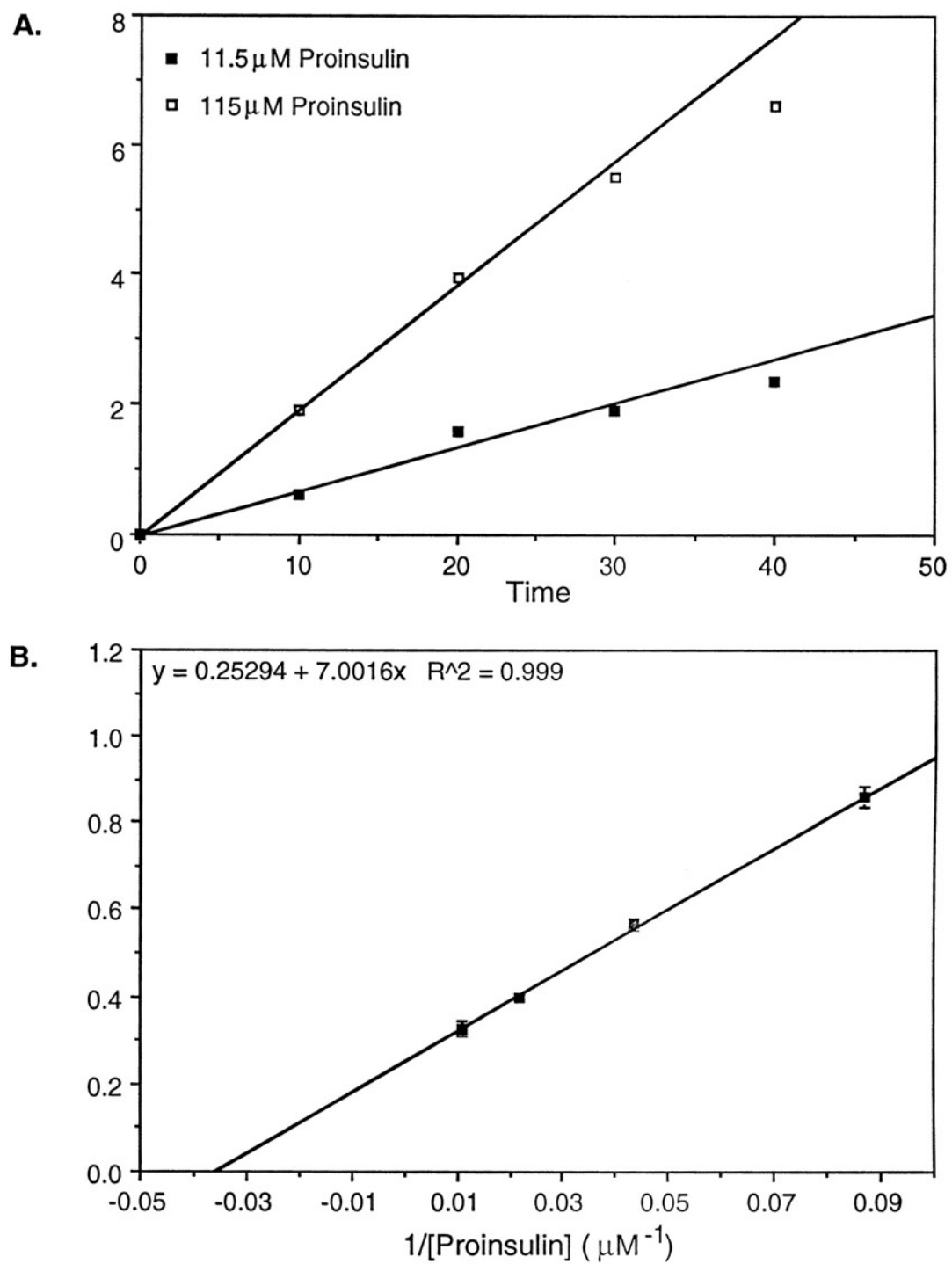


Figure 48. Initial rate (A) and Lineweaver-Burk (B) plots for the cleavage of proinsulin by YAP3p

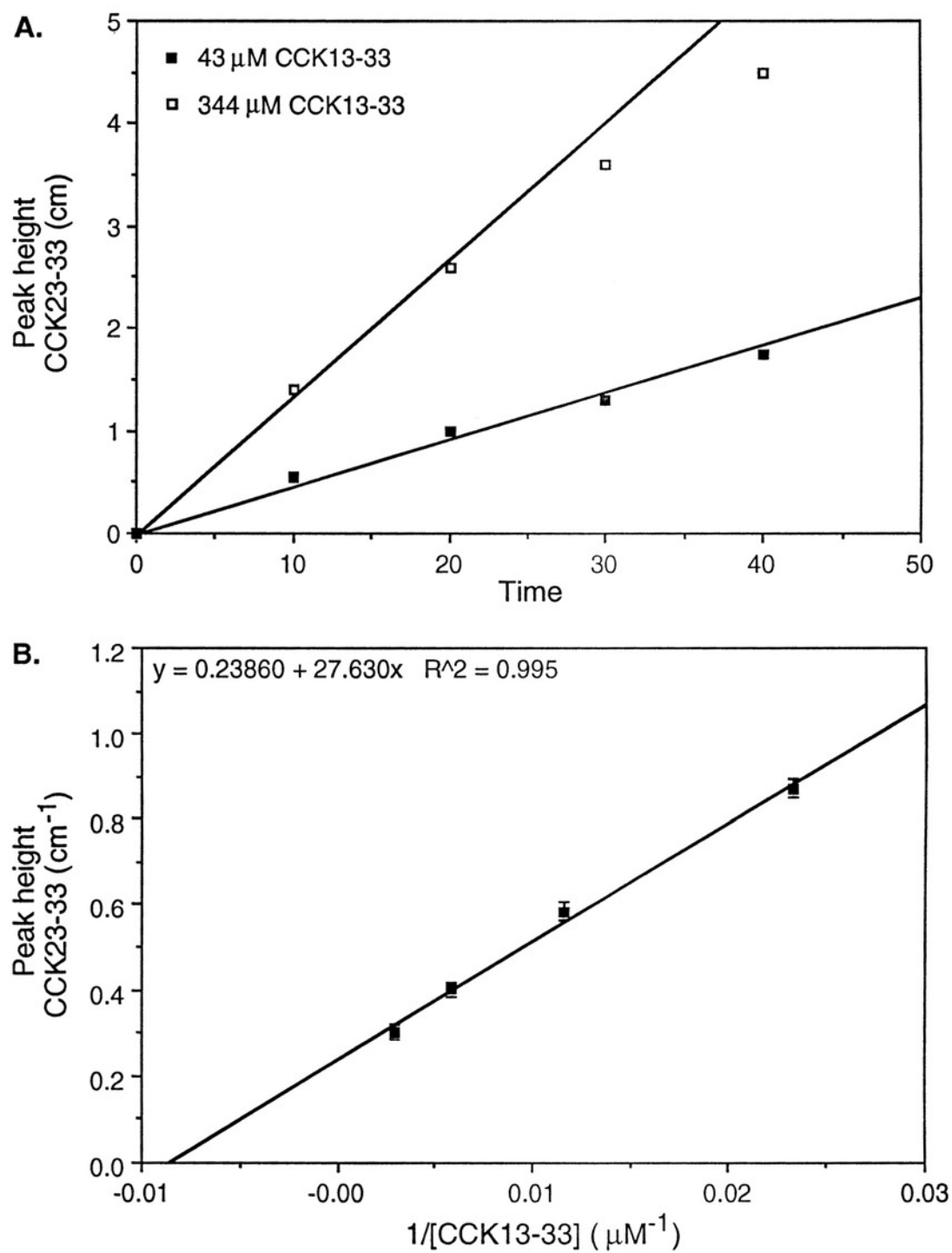


Figure 49. Initial rate (A) and Lineweaver-Burk (B) plots for the cleavage of CCK13-33 by YAP3p

Protein assay

The procedure of Biorad was used to quantitate total protein in a given sample. Initially, an aliquot of the sample was diluted with water to 800 μ l to which 200 μ l of the color reagent was added and vortexed. Depending on the intensity of the color obtained, an appropriate dilution of the sample was then made to give an absorbance at 595nm of about 0.2. The appropriate blank utilized the same volume of the buffer that the protein was in diluted to 800 μ l with water. The absorbance response of 0.2 was within the linear part of a standard curve that was generated with bovine serum albumin (BSA). Standard BSA solutions of 2 mg/ml obtained from Pierce Co., allowed the generation of accurate and consistent standard curves.

Sectioning and indirect immunofluorescence of mouse and bovine tissue

Mice, that had been kept at 20°C in a 12hr light/dark cycle, were anesthetized with chloral hydrate (400 mg/Kg, ip), and the brain and pituitary were carefully dissected out and rapidly frozen on dry ice. Serial sections (6-12 μ m) were cut throughout the whole brain and pituitary in sagittal or coronal planes on a cryostat, thaw-mounted onto gelatin-coated microscope slides and stored at -70°C until further processing. For immunofluorescence, serial sections were incubated in 3% normal goat serum (NGS) in 1X PBS for 30 min at room temperature. The sections were then incubated with MW283 antiserum (1:500) in 1X PBS containing 3% NGS and 0.3% triton X-100 for 48 hr at 4°C. Following this incubation, the sections were washed in 1X PBS six times over a 2 hr period and subsequently incubated with fluorescein isothiocyanate (FITC)-conjugated goat

anti-rabbit IgG (1:100) or rhodamine (TRITC)-conjugated goat anti-rabbit IgG (1:100) for 1 hr at room temperature. The sections were then washed and mounted in glycerin:PBS (1:3) and examined under a Nikon fluorescence microscope and photographed. Control experiments were performed with the primary antiserum replaced by normal serum or the primary or secondary antiserum omitted, one at a time.

PUBLICATIONS

1. Azaryan, A.V, Wong, M., Friedman, T.C., Cawley, N.X., Estivariz, F.E., Chen, H-C., and Loh, Y.P. (1993) Purification and Characterization of a yeast, paired basic residue-specific aspartic protease encoded by the YAP3 gene: Similarity to the mammalian pro-opiomelanocortin converting enzyme. *J. Biol. Chem.* **268**:11968-11975
2. Cawley, N.X., Noe, B.D., and Loh, Y.P. (1993) Purified yeast aspartic protease 3 cleaves anglerfish pro-somatostatin I and II at di- and monobasic sites to generate somatostatin-14 and -28. *FEBS Lett* **332**:273-276
3. Loh, Y.P., and Cawley, N.X. (1994) Strategies and techniques for endoproteolytic processing enzyme purification and characterization. In *Neuroprotocols: A Companion to Methods in Neurosciences*, Beinfeld, M.C. (ed) Academic Press, San Diego, CA, **5**:122-129.
4. Loh, Y.P., Cawley, N.X., Friedman, T.C., and Pu, L-P. (1995) "Yeast and mammalian, basic residue-specific aspartic proteases in prohormone conversion." In: *Aspartic Proteinases*, Takahashi, K. (ed) Plenum Press, New York, p519-527.
5. Azaryan, A.V., Friedman, T.C., Cawley, N.X., and Loh, Y.P. (1995) "Characteristics of YAP3, a new prohormone processing aspartic protease from *S. cerevisiae*." In: *Aspartic Proteinases*, Takahashi, K. (ed) Plenum Press, New York, p569-572.

6. Loh, Y.P., and Cawley, N.X. (1995) Processing enzymes of the aspartic protease family: Yeast aspartic protease 3 and pro-opiomelanocortin converting enzyme. In: *Proteolytic Enzymes: Aspartic and Metallo Peptidases, Methods in Enzymology*, Barrett, A.J. (ed), Academic Press, Orlando, FL, **248**.
7. Cawley, N.X., Wong, M., Pu, L-P., Tam, W., and Loh, Y.P. (1995) Secretion of Yeast Aspartic Protease 3 (YAP3p) is Regulated by its Carboxy-Terminus Tail: Characterization of Secreted YAP3p. *Biochemistry* **6**:7430-7437
8. Cawley, N.X., Chen, H-C., Beinfeld, M.C., and Loh, Y.P. (1995) Specificity and Kinetic Studies on the Cleavage of Various Prohormone Mono- and Paired Basic Residue Sites by Yeast Aspartic Protease 3. *J. Biol. Chem.* (submitted)
9. Cawley, N.X., Wong, M., Pu, L-P., Loh, Y.P. (1993) The bovine pro-opiomelanocortin converting enzyme is structurally homologous to the yeast aspartic protease, YAP3, *75th Annual Meeting of the Endocrine Society, Las Vegas, NV*, (abstract 1376).
10. Cawley, N.X., Chen, H-C., Beinfeld, M.C., and Loh, Y.P. (1995) Yeast Aspartic Protease 3 Cleaves Prohormones at Selective Paired and Mono-Basic Residues with Preference for a Lys/Arg Residue Upstream from the Cleavage Site, *24th Annual Meeting of the Society of Neuroscience, Miami, FL*, (abstract).
11. Cawley, N.X., Chen, H-C., and Loh, Y.P. (1995) Purification and Processing of Yeast Aspartic Protease 3. (in preparation).

12. Cawley, N.X., Pu, L-P., and Loh, Y.P. (1995) Distribution and Characterization of Yeast Aspartic Protease 3-like immunoreactive proteins in mammalian brain and pituitary. (in preparation)

REFERENCES

1. von Heijne, G., *Signal sequences. The limits of variation.* J. Mol. Biol., 1985. **184** p. 99-105.
2. Walter, P. and Blobel, G., *Translocation of proteins across the endoplasmic reticulum II. Signal recognition protein (SRP) mediates the selective binding to microsomal membranes of in-vitro-assembled polysomes synthesizing secretory protein.* J. Cell Biol., 1981. **91** : p. 557-561.
3. Walter, P. and Blobel, G., *Disassembly and reconstitution of signal recognition particle.* Cell, 1983. **34** : p. 525-533.
4. Walter, P. and Blobel, G., *Signal recognition particle: a ribonucleoprotein required for cotranslational translocation of proteins, isolation and properties.* Meth. Enzymol., 1982. **96** : p. 682-691.
5. Jackson, R.C. and Blobel, G., *Post-translational cleavage of presecretory proteins with an extract of rough microsomes from dog pancreas containing signal peptidase activity.* Proc. Natl. Acad. Sci. U.S.A., 1977. (74): p. 5598.
6. Lively, M.O. and Walsh, K.A., *Hen oviduct signal peptidase is an integral membrane protein.* J. Biol. Chem., 1983. **258** : p. 9488.
7. Kukuruzinska, M.A., Bergh, M.L.E., and Jackson, B.J., *Protein glycosylation in yeast.* Ann. Rev. Biochem., 1987. **56** : p. 915-944.
8. Bulenda, D. and Gratzl, M., *Matrix free Ca²⁺ in isolated chromaffin vesicles.* Biochemistry, 1985. **24** : p. 7760-7765.
9. Yoo, S.H., *Identification of the Ca²⁺ dependent calmodulin-binding region of chromogranin A.* Biochemistry, 1992. **31** : p. 6134-6140.
10. Orci, L., Ravazzola, M., Storch, M.-J., Anderson, R.G.W., Vassalli, J.-D., and Perrelet, A., *Proteolytic maturation of insulin is a post-Golgi event which occurs in acidifying clathrin-coated secretory vesicles.* Cell, 1987. **49** (6/19/87): p. 865-868.
11. Seksek, O., Biwersi, J., and Verkman, A.S., *Direct measurement of trans-Golgi pH in living cells and regulation by second messengers.* J. Biol. Chem., 1995. **270** : p. 4967-4970.
12. Loh, Y.P., Tam, W.W.H., and Russell, J.T., *Measurement of δ -pH and membrane potential in secretory vesicles isolated from bovine pituitary intermediate lobe.* J. Biol. Chem., 1984. **259** (13): p. 8238-8245.

13. Mains, R.E., Dickerson, I.M., May, V., Stoffers, D.A., Perkins, S.N., Ouafik, L.H., Husten, E.J., and Eipper, B.A., *Cellular and molecular aspects of peptide hormone biosynthesis*. Front. Neuroendocrinology, 1990. **11** : p. 52-89.
14. Lindberg, I., *The new eukaryotic precursor processing proteinases*. Molecular Endocrinology, 1991. **5** (10): p. 1361-1365.
15. Loh, Y.P., Beinfeld, M.C., and Birch, N.P., *Proteolytic processing of prohormones and pro-neuropeptides*, in *Mechanisms of intracellular trafficking and processing of proproteins*, Loh, Y.P., Editor. 1993, CRC Press: Boca Raton, FL. p. 179-224.
16. Seidah, N.G., Day, R., Marcinkiewicz, M., and Chretien, M., *Mammalian paired basic amino acid convertases of prohormones and proproteins*. Ann. N. Y. Acad. Sci., 1993. **680** (May): p. 135-146.
17. Fricker, L.D., , in *Peptide Biosynthesis and Processing*, Fricker, L.D., Editor. 1991, CRC Press: Boca Raton, FL. p. 199-229.
18. Gainer, H., Russell, J.T., and Loh, Y.P., *An amino peptidase activity in bovine pituitary secretory vesicles that cleaves the N-terminal arginine from beta-lipotropin(60-65)*. FEBS Lett., 1984. **175** : p. 135-139.
19. Steiner, D.F., Smeekens, S.P., Ohagi, S., and Chan, S.J., *The new enzymology of precursor processing endoproteases*. J. Biol. Chem., 1992. **267** (33): p. 23435-23438.
20. Van de Ven, W.J., Roebroek, A.J., and Van Duijnhoven, H.L., *Structure and function of eukaryotic proprotein processing enzymes of the subtilisin family of serine proteases*. Crit. Rev. Oncog., 1993. **4** (2): p. 115-136.
21. Nakagawa, T., Hosaka, M., Torii, S., Watanabe, T., Murakami, K., and Nakayama, K., *Identification and functional expression of a new member of the mammalian Kex2-like processing endoprotease family: its striking structural similarity to PACE4*. J. Biochem., 1993. **113** : p. 132-135.
22. Lusson, J., Vieau, D., Hamelin, J., Day, R., Chretien, M., and Seidah, N.G., *cDNA structure of the mouse and rat subtilisin/kexin-like PC5: A candidate proprotein convertase expressed in endocrine and nonendocrine cells*. Proc. Natl. Acad. Sci. U.S.A., 1993. **90** : p. 6691-6695.
23. Egel-Mitani, M., Flygenring, H.P., and Hansen, M.T., *A novel aspartyl protease allowing KEX2-independent MF alpha propheromone processing in yeast*. Yeast, 1990. **6** : p. 127-137.

24. Chesneau, V., Pierotti, A.R., Prat, A., Gaudoux, F., Foulon, T., and P., C., *N-arginine dibasic convertase (NRD convertase): A newcomer to the family of processing endopeptidases. An overview.* Biochimie, 1994. **76** : p. 234-240.
25. Pierotti, A.R., Prat, A., Chesneau, V., Gaudoux, F., Leseney, A.-M., Foulon, T., and Cohen, P., *N-Arginine dibasic convertase, a metalloendopeptidase as a prototype of a class of processing enzymes.* Proc. Natl. Acad. Sci. USA, 1994. **91** : p. 6078-6082.
26. Julius, D., Brake, A., Blair, L., Kunisawa, R., and Thorner, J., *Isolation of the putative structural gene for the lysine-arginine cleaving endopeptidase required for processing of yeast prepro-alpha-factor.* Cell, 1984. **37** : p. 1075-1089.
27. Fuller, R., Brake, A., and Thorner, J., *The Saccharomyces cerevisiae KEX2 gene, required for processing prepro-alpha-Factor, encodes a calcium-dependent endopeptidase that cleaves after Lys-Arg and Arg-Arg sequences.* Microbiology, 1986. : p. 273-278.
28. Julius, D., Blair, L., Brake, A., Sprague, G., and Thorner, J., *Yeast alpha-factor is processed from a larger precursor polypeptide: the essential role of a membrane-bound dipeptidyl aminopeptidase.* Cell, 1983. **32** : p. 839-852.
29. Bourbonnais, Y., Germain, D., Latchinian-Sadek, L., Boileau, G., and Thomas, D.Y., *Prohormone processing by yeast proteases.* Enzyme, 1991. **45** (5-6): p. 244-256.
30. van den Ouweland, A., van Duijnhoven, H., Keizer, G., Dorssers, L., and Van de Ven, W., *Structural homology between the human fur gene product and the subtilisin-like protease encoded by yeast KEX2.* Nucleic Acids Res., 1990. **18** (3): p. 664.
31. van de Ven, W.J., Voorberg, J., Fontijn, R., Pannekoek, H., van den Ouweland, A.M., van Duijnhoven, H.L., Roebroek, A.J., and Siezen, R.J., *Furin is a subtilisin-like proprotein processing enzyme in higher eukaryotes.* Mol. Biol. Rep., 1990. **14** : p. 265-275.
32. Seidah, N., Gaspar, L., Mion, P., Marcinkiewicz, M., Mbikay, M., and Chretien, M., *cDNA sequence of two distinct pituitary proteins homologous to Kex2 and Furin gene products: tissue-specific mRNAs encoding candidates for pro-hormone processing proteinases.* DNA and Cell Biol., 1990. **9** (6): p. 415-424.
33. Seidah, N., Marcinkiewicz, M., Benjannet, S., Gaspar, L., Beaubien, G., Mattei, M., Lazure, C., Mbikay, M., and Chretien, M., *Cloning and primary sequence of a mouse candidate prohormone convertase PC1 homologous to PC2, furin, and Kex2: distinct chromosomal localization and messenger RNA distribution in brain and pituitary compared to PC2.* Molecular Endocrinology, 1991. **5** (1): p. 111-122.

34. Smeeckens, S., Avruch, A., LaMendola, J., Chan, S., and Steiner, D., *Identification of a cDNA encoding a second putative prohormone convertase related to PC2 in AtT20 cells and islets of Langerhans*. Proc. Natl. Acad. Sci., 1991. **88** (1/91): p. 340-344.
35. Nakayama, K., Hosaka, M., Hatsuzawa, K., and Murakami, K., *Cloning and functional expression of a novel endoprotease involved in prohormone processing at dibasic sites*. J. Biochem., 1991. **109** (6): p. 803-806.
36. Smeeckens, S.P. and Steiner, D.F., *Identification of a human insulinoma cDNA encoding a novel mammalian protein structurally related to the yeast dibasic processing protease Kex2*. J. Biol. Chem., 1990. **265** (6): p. 2997-3000.
37. Kiefer, M.C., Tucker, J.E., Joh, R., Landsberg, K.E., Saltman, D., and Barr, P.J., *Identification of a second human subtilisin-like protease gene in the fes/fps region of chromosome 15*. DNA and Cell. Biol., 1991. **10** (10): p. 757-769.
38. Nakayama, K., Kim, W., Torii, S., Hosaka, M., Nakagawa, T., Ikemizu, J., Baba, T., and Murakami, K., *Identification of the fourth member of the mammalian endoprotease family homologous to the yeast Kex2 protease*. J. Biol. Chem., 1992. **267** (9): p. 5897-5900.
39. Seidah, N., Day, R., Hamelin, J., Gaspar, A., Collard, M., and Chretien, M., *Testicular expression of PC4 in the rat: molecular diversity of a novel germ cell-specific Kex2/Subtilisin-like proprotein convertase*. Molecular Endocrinology, 1992. **6** (10): p. 1559-1570.
40. Nakagawa, T., Murakami, K., and Nakayama, K., *Identification of an isoform with an extremely large Cys-rich region of PC6, a Kex2-like processing endoprotease*. FEBS Lett., 1993. **327** : p. 165-171.
41. Day, R., Schafer, M.K.-H., Watson, S.J., Chretien, M., and Seidah, N.G., *Distribution and regulation of the prohormone convertases PC1 and PC2 in the rat pituitary*. Molecular Endocrinology, 1992. **6** (3): p. 485-497.
42. Hakes, D.J., Birch, N.P., Mezey, A., and Dixon, J.E., *Isolation of two complementary deoxyribonucleic acid clones from a rat insulinoma cell line based on similarities to Kex2 and Furin sequences and the specific localization of each transcript to endocrine and neuroendocrine tissues in rats*. Endocrinology, 1991. **129** (6): p. 3053-3063.
43. Hatsuzawa, K., Hosaka, M., Nakagawa, T., Nagase, M., Shoda, A., Murakami, K., and Nakayama, K., *Structure and expression of mouse furin, a yeast Kex2-related protease*. J. Biol. Chem., 1990. **265** : p. 22075-22078.

44. Benjannet, S., Rondeau, N., Paquet, L., Boudreault, A., Lazure, C., Cretien, M., and Seidah, N.G., *Comparative biosynthesis, covalent post-translational modifications and efficiency of prosegment cleavage of the prohormone convertases PC1 and PC2: glycosylation, sulphation and identification of the intracellular site of prosegment cleavage of PC1 and PC2*. *Biochem. J.*, 1993. **294** : p. 735-743.
45. Zhou, Y. and Lindberg, I., *Enzymatic properties of carboxyl-terminally truncated prohormone convertase 1 (PC1/SPC3) and evidence for autocatalytic Conversion*. *J. Biol. Chem.*, 1994. **269** (28): p. 18408-18413.
46. Benjannet, S., Rondeau, N., Day, R., Chretien, M., and Seidah, N.G., *PC1 and PC2 are proprotein convertases capable of cleaving proopiomelanocortin at distinct pairs of basic residues*. *Proc Natl Acad Sci USA*, 1991. **88** : p. 3564-3568.
47. Seidah, N.G., Fournier, H., Boileau, G., Benjannet, S., Rondeau, N., and Chretien, M., *The cDNA structure of the porcine pro-hormone convertase PC2 and the comparative processing by PC1 and PC2 of the N-terminal glycopeptide segment of porcine POMC*. *FEBS Lett*, 1992. **310** (3): p. 235-9.
48. Birch, N.P., Tracer, H.L., Hakes, D.J., and Loh, Y.P., *Coordinate regulation of mRNA levels of pro-opiomelanocortin and the candidate processing enzymes PC2 and PC3, but not furin, in rat pituitary intermediate lobe*. *Biochem. Biophys. Res. Commun.*, 1991. **179** (3): p. 1311-9.
49. Bennett, D.L., Bailyes, E.M., Nielsen, E., Guest, P.C., Rutherford, N.G., Arden, S.D., and Hutton, J.C., *Identification of the type 2 proinsulin processing endopeptidase as PC2, a member of the eukaryote subtilisin family*. *J. Biol. Chem.*, 1992. **267** (21): p. 15229-15236.
50. Breslin, M.B., Lindberg, I., Benjannet, S., Mathis, J.P., Lazure, C., and Seidah, N.G., *Differential processing of proenkephalin by prohormone convertases 1(3) and 2 and furin*. *J. Biol. Chem.*, 1993. **268** (Dec. 25): p. 27084-27093.
51. Rehemtulla, A., Barr, P.J., Rhodes, C.J., and Kaufman, R.J., *PACE4 is a member of the mammalian propeptidase family that has overlapping but not identical substrate specificity to PACE*. *Biochemistry*, 1993. **32** : p. 11586-11590.
52. Decroly, E., Vandenbranden, M., Ruyschaert, J.-M., Cogniaux, J., Jacob, G.S., Howard, S.C., Marshall, G., Kompelli, A., Basak, A., Jean, F., Lazure, C., Benjannet, S., Chretien, M., Day, R., and Seidah, N.G., *The convertases furin and PC1 can both cleave the human immunodeficiency virus (HIV)-1 envelope glycoprotein gp160 into gp120 (HIV-1 SU) and gp41 (HIV-1 TM)*. *J. Biol. Chem.*, 1994. **269** (#16, April): p. 12240-12247.

53. Dupuy, A., Lindberg, I., Zhou, Y., Akil, H., Lazure, C., Chretien, M., Seidah, N.G., and Day, R., *Processing of prodynorphin by the prohormone convertase PC1 results in high molecular weight intermediate forms. Cleavage at a single arginine residue.* FEBS Lett., 1994. **337** : p. 60-65.
54. Friedman, T.C., Loh, Y.P., and Birch, N.P., *In vitro processing of proopiomelanocortin by recombinant PC1 (SPC3).* Endocrinology, 1994. **135** (3): p. 854-862.
55. MacKay, V.L., Armstrong, J., Yip, C., Welch, S., Walker, K., Osborn, S., Sheppard, P., and Forstrom, J., *Characterization of the BAR proteinase, an extracellular enzyme from the yeast Saccharomyces cerevisiae,* in *Structure and Function of the Aspartic Proteinases*, Dunn, B.M., Editor. 1991, Plenum Press: New York. p. 161-172.
56. Dickson, C., Eisenman, R., Fan, H., Hunter, E., and Teich, N., *RNA Tumor Viruses* . 2nd ed. Cold Spring Harbor Lab., ed. Weiss, R., Teich, N., Varmus, H., and Coffin, J. 1984, New York: p513-648.
57. James, M.N.G. and Sielecki, A.R., *Structure and refinement of penicillopepsin at 1.8 Å resolution.* J. Mol. Biol., 1983. **163** : p. 3701-3713.
58. Suguna, K., Bott, R.R., Padlan, E.A., Subramanian, E., and Sherif, S., *Structure and refinement at 1.8 Å resolution of the aspartic proteinase from Rhizopus chinensis.* J. Mol. Biol., 1987. **196** : p. 877-900.
59. Pearl, L.H. and Blundell, T., *The active site of aspartic proteinases.* FEBS Lett., 1984. **174** : p. 96-101.
60. Andreeva, N.S., Zdanov, A.S., Gustchina, A.E., and Fedorov, A.A., *Structure of ethanol-inhibited porcine pepsin at 2-Å resolution and binding of the methyl ester of phenylalanyl-diiodotyrosine to the enzyme.* J. Biol. Chem., 1985. **259** : p. 11353-11365.
61. James, M.N.G. and Sielecki, A.R., *Molecular structure of an aspartic proteinase zymogen, porcine pepsinogen, at 1.8 Å resolution.* Nature, 1986. **319** : p. 33-38.
62. Pearl, L.H. and Taylor, W.R., *Sequence specificity of retroviral proteases [letter].* Nature, 1987. **328** : p. 482.
63. Tang, J. and Wong, R.N.S., *Evolution in the structure and function of aspartic proteases.* J. Cell. Biochem., 1987. **33** : p. 53-63.
64. Davies, D.R., *The structure and function of the aspartic proteinases.* Annu. Rev. Biophys. Chem., 1990. **19** : p. 189-215.

65. Loh, Y.P., Parish, D.C., and Tuteja, R., *Purification and characterization of a paired basic residue-specific pro-opiomelanocortin converting enzyme from bovine pituitary intermediate lobe secretory vesicles*. J. Biol. Chem., 1985. **260** (12): p. 7194-7205.
66. Parish, D.C., Tuteja, R., Altstein, M., Gainer, H., and Loh, Y.P., *Purification and characterization of a paired basic residue-specific prohormone-converting enzyme from bovine pituitary neural lobe secretory vesicles*. J. Biol. Chem., 1986. **261** (31): p. 14392-14397.
67. Mackin, R.B., Noe, B.D., and Spiess, J., *The anglerfish somatostatin-28-generating propeptide converting enzyme is an aspartyl protease*. Endocrinology, 1991. **129** (4): p. 1951-1957.
68. Krieger, T.J. and Hook, V.Y.H., *Purification and characterization of a cathepsin D protease from bovine chromaffin granules*. Biochem., 1992. **31** (#17): p. 4223-4231.
69. Bourbonnais, Y., Ash, J., Daigle, M., and Thomas, D.Y., *Isolation and characterization of S.cerevisiae mutants defective in somatostatin expression: cloning and functional role of a yeast gene encoding an aspartyl protease in precursor processing at monobasic cleavage sites*. EMBO J., 1993. **12** (1): p. 285-294.
70. Inagami, T., Chang, J.J., Dykes, C.W., Takii, Y., Kisaragi, M., and Misono, K.S., *Renin: structural features of active enzyme and inactive precursor*. Fed. Proc., 1983. **42** : p. 2729-2734.
71. Nouffer, C., Jenö, P., Conzelmann, A., and Riezman, H., *Determinants for glycosylphospholipid anchoring of the Saccharomyces cerevisiae GSI1 protein to the plasma membrane*. Mol. Cell. Biol., 1991. **11** (1): p. 27-37.
72. Olsen, V., Masters Thesis, *A putative prohormone convertase from Saccharomyces cerevisiae. Characterization of biosynthesis and cellular localization of the YAP3 gene product*. 1994, University of Copenhagen, Denmark:
73. Bourbonnais, Y., Germain, D., Ash, J., and Thomas, D.Y., *Cleavage of prosomatostatins by the yeast YAP3 and KEX2 endoproteases*. Biochimie, 1994. **76** : p. 226-233.
74. Nussey, S.S., Soo, S.-C., Gibson, S., Gout, I., White, A., Bain, M., and Johnstone, A.P., *Isolated congenital ACTH deficiency: a cleavage enzyme defect?* Clinical Endocrinology, 1993. **39** : p. 381-385.
75. Molloy, S.S., Bresnahan, P.A., Leppla, S.H., Klimpel, K.R., and Thomas, G., *Human furin is a calcium-dependent serine endoprotease that recognizes the sequence*

- Arg-X-X-Arg and efficiently cleaves anthrax toxin protective antigen.* J. Biol. Chem., 1992. **267** (23): p. 16396-16402.
76. Brenner, C. and Fuller, R.S., *Structural and enzymatic characterization of a purified prohormone-processing enzyme: Secreted, soluble Kex2 protease.* Proc. Natl. Acad. Sci. U.S.A., 1992. **89** (February): p. 922-926.
77. Fricker, L., Das, B., and Angeletti, R., *Identification of the pH-dependent membrane anchor of carboxypeptidase E (EC 3.4.17.10).* J. Biol. Chem., 1990. **265** (5): p. 2476-2482.
78. Baldari, C., Murray, J.A., Ghiara, P., Cesareni, G., and Galeotti, C.L., *A novel leader peptide which allows efficient secretion of a fragment of human interleukin 1 beta in Saccharomyces cerevisiae.* EMBO J., 1987. **6** (1): p. 229-234.
79. Becker, D.M. and Lundblad, V., *Introduction of DNA into yeast cells.* Curr. Protocols Mol. Biol., 1992. **18** : p. 13.7.1-13.7.2.
80. Azaryan, A.V., Wong, M., Friedman, T.C., Cawley, N.X., Estivariz, F.E., Chen, H.C., and Loh, Y.P., *Purification and characterization of a paired basic residue-specific yeast aspartic protease encoded by the YAP3 gene. Similarity to the mammalian pro-opiomelanocortin-converting enzyme.* J. Biol. Chem., 1993. **268** (16): p. 11968-11975.
81. Verbalis, J.G., Hoffman, G.E., Rosenbaum, L.C., Nilaver, G., and Loh, Y.P., *Generation and characterization of antiserum directed against neurohypophyseal prohormones.* J. Neuroendocrinology, 1991. **3** : p. 267-272.
82. Pringle, J.R. and Hartwell, L.H., *The Saccharomyces cerevisiae cell cycle*, in *The Molecular Biology of the Yeast Saccharomyces: Life Cycle and Inheritance*, Strathern, J.N., Jones, E.W., and Broach, J.R., Editor. 1981, Cold Spring Harbour, New York. p. 97-142.
83. Doering, T.L., Masterson, W.J., Hart, G.W., and Englund, P.T., *Biosynthesis of glycosyl phosphatidylinositol membrane anchors.* J. Biol. Chem., 1990. **258** : p. 15261-15273.
84. Mackin, R.B. and Noe, B.D., *Characterization of an islet carboxypeptidase B activity involved in prohormone processing.* Endocrinology, 1987. **120** : p. 457-468.
85. Noe, B.D., Fletcher, D.J., Bauer, G.E., Weir, G.C., and Patel, Y., *Somatostatin biosynthesis occurs in pancreatic islets.* Endocrinology, 1978. **102** : p. 1675-1685.
86. Mackin, R.B. and Noe, B.D., *Direct evidence for two distinct prosomatostatin converting enzymes.* J. Biol. Chem., 1987. **262** (14): p. 6453-6456.

87. Mackin, R., Noe, B., and Spiess, J., *Identification of a somatostatin-14-generating propeptide converting enzyme as a member of the Kex2/furin/PC family*. *Endocrinology*, 1991. **129** (4): p. 2263-2265.
88. Nakayama, K., Watanabe, T., Nakagawa, T., Kim, W.S., Nagahama, M., Hosaka, M., Hatsuzawa, K., Kondoh-Hashiba, K., and Murakami, K., *Consensus sequence for precursor processing at mono-arginyl sites. Evidence for the involvement of a Kex2-like endoprotease in precursor cleavages at both dibasic and mono-arginyl sites*. *J. Biol. Chem.*, 1992. **267** (23): p. 16335-16340.
89. Gomez, S., Boileau, G., Zollinger, L., Nault, C., Rholam, M., and Cohen, P., *Site-specific mutagenesis identifies amino acid residues critical in prohormone processing*. *EMBO J.*, 1989. **8** : p. 2911-2916.
90. Beinfeld, M.C., Meyer, D.K., Eskay, R.L., Jensen, R.T., and Brownstein, M.J., *The distribution of cholecystokinin immunoreactivity in the central nervous system of the rat as determined by radioimmunoassay*. *Brain Res.*, 1981. **212** (1): p. 51-57.
91. Lineweaver, H. and Burk, D., *The determination of enzyme dissociation constants*. *J Am Chem Soc*, 1934. **56** : p. 658-666.
92. Beinfeld, M.C., Jensen, R.T., and Brownstein, M.J., *HPLC separation of cholecystokinin peptides- two systems*. *J. Liq. Chrom.*, 1980. **3** : p. 1367-1371.
93. Smeekens, S., Montag, A., Thomas, G., Albiges-Rizo, C., Carroll, R., Benig, M., Phillips, L., Martin, S., Ohagi, S., Gardner, P., Swift, H., and Steiner, D., *Proinsulin processing by the subtilisin-related proprotein convertases furin, PC2, and PC3*. *Proc. Natl. Acad. Sci.*, 1992. **89** (9/92): p. 8822-8826.
94. Bailyes, E.M., Shennan, K.I., Seal, A.J., Smeekens, S.P., Steiner, D.F., Hutton, J.C., and Docherty, K., *A member of the eukaryotic subtilisin family (PC3) has the enzymic properties of the type 1 proinsulin-converting endopeptidase*. *Biochem. J.*, 1992. **285** (Pt 2): p. 391-394.
95. Cawley, N.X., Noe, B.D., and Loh, Y.P., *Purified yeast aspartic protease 3 cleaves anglerfish pro-somatostatin I and II at di- and monobasic sites to generate somatostatin-14 and -28*. *FEBS Lett.*, 1993. **332** (3): p. 273-276.
96. McCaman, M.T. and Cummings, D.B., *A mutated bovine prochymosin zymogen can be activated without proteolytic processing at low pH*. *J. Biol. Chem.*, 1986. **261** : p. 15345-15348.
97. Richo, G.R. and Conner, G.E., *Structural requirements of procathepsin D activation and maturation*. *J. Biol. Chem.*, 1994. **269** (#20, May): p. 14806-14812.

98. Viereck, J.C. and Beinfeld, M.C., *Characterization of a cholecystokinin 8-generating endoprotease purified from rat brain synaptosomes*. J. Biol. Chem., 1992. **267** (27): p. 19475-19481.
99. Estivariz, F.E., Birch, N.P., and Loh, Y.P., *Generation of Lys- γ 3-melanotropin from pro-opiomelanocortin by a bovine intermediate lobe secretory vesicle membrane-associated aspartic protease and purified pro-opiomelanocortin converting enzyme*. J. Biol. Chem., 1989. **264** (30): p. 17796-17801.
100. Loh, Y.P., *Kinetic studies on the processing of human B-lipotropin by bovine pituitary intermediate lobe pro-opiomelanocortin-converting enzyme*. J. Biol. Chem., 1986. **261** (#26, Sept.): p. 11949-11955.
101. *Biochemistry [Textbook]*, Voet, D. and Voet, J.G., Editor. Wiley: p. 337.
102. Zhou, Y. and Lindberg, I., *Purification and characterization of the prohormone convertase PC1(PC3)*. J. Biol. Chem., 1993. **268** (8): p. 5615-5623.
103. Rufaut, N.W., Brennan, S.O., Hakes, D.J., Dixon, J.E., and Birch, N.P., *Purification and characterization of the candidate prohormone-processing enzyme SPC3 produced in a mouse L cell line*. J. Biol. Chem., 1993. **268** (#27, Sept. 25): p. 20291-20298.
104. Thomas, L., Leduc, R., Thorne, B., Smeekens, S., Steiner, D., and Thomas, G., *Kex2-like endoproteases PC2 and PC3 accurately cleave a model prohormone in mammalian cells: evidence for a common core of neuroendocrine processing enzymes*. Proc Natl Acad Sci, 1991. **88** (6/91): p. 5297-5301.
105. Rouille, Y., Westermarck, G., Martin, S.K., and Steiner, D.F., *Proglucagon is processed to glucagon by prohormone convertase PC2 in alphaTC1-6 cells*. Proc. Natl. Acad. Sci., 1994. **91** (April): p. 3242-3246.
106. Hosaka, M., Nagahama, M., Kim, W., Watanabe, T., Hatsuzawa, K., Ikemizu, J., Murakami, K., and Nakayama, K., *Arg-X-Lys/Arg-Arg motif as a signal for precursor cleavage catalyzed by furin within the constitutive secretory pathway*. J. Biol. Chem., 1991. **266** (19): p. 12127-12130.
107. Bresnahan, P.A., Leduc, R., Thomas, L., Thorne, J., Gibson, H.L., Brake, A.J., Barr, P.J., and Thomas, G., *Human fur gene encodes a yeast Kex2-like endoprotease that cleaves pro-beta-NGF in vivo*. J. Cell Biol., 1990. **111** : p. 2851-2859.
108. Hatsuzawa, K., Nagahama, M., Takahashi, S., Takada, K., Murakami, K., and Nakayama, K., *Purification and characterization of furin, a Kex2-like processing endoprotease, produced in chinese hamster ovary cells*. J. Biol. Chem., 1992. **267** (#23, August 15): p. 16094-16099.

109. Guthrie, C. and Fink, G.R., ed. *Guide to Yeast Genetics and Molecular Biology . Methods in Enzymology*, Vol. 194. 1991, Academic Press, Inc.: San Diego, CA.
110. Martens, G.J.M., Braks, J.A.M., Eib, D.W., Zhou, Y., and Lindberg, I., *The neuroendocrine polypeptide 7B2 is an endogenous inhibitor of prohormone convertase PC2*. Proc. Natl. Acad. Sci., 1994. **91** (June): p. 5784-5787.
111. Hook, V.Y.H., Purviance, R.T., Azaryan, A.V., Hubbard, G., and Krieger, T.J., *Purification and characterization of alpha1-antichymotrypsin-like protease inhibitor that regulates prohormone thiol protease involved in enkaphalin precursor processing*. J. Biol. Chem., 1993. **268** (#27, Sept.): p. 20570-20577.
112. Hook, V.Y.H., Azaryan, A.V., Hwang, S.-H., and Tezapsidis, N., *Proteases and the emerging role of protease inhibitors in prohormone processing*. FASEB J., 1994. **8** : p. 1269-1278.
113. Dunn, B.M., *Determination of protease mechanism*, in *Proteolytic Enzymes: a practical approach*, Beynon, R.J. and Bond, J.S., Editor. 1989, IRL Press: Oxford University Press. p. 57-81.
114. Salvesen, G. and Nagase, H., *Inhibition of proteolytic enzymes*, in *Proteolytic Enzymes: a practical approach*, Beynon, R.J. and Bond, J.S., Editor. 1989, IRL Press: Oxford University Press. p. 83-104.
115. Umezawa, H., Aoyagi, T., Morishima, H., Matzusaki, M., Hamada, H., and Tekeucki, T., *Pepstatin, a new pepsin inhibitor produced by actinomycetes*. J. Antibiot., 1970. **23** : p. 259.
116. Marciniyszyn, J., Jr., Hartsuck, J.A., and Tang, J., *Mechanism of intramolecular activation of pepsinogen. Evidence for an intermediate delta and the involvement of the active site of pepsin in the intramolecular activation of pepsinogen*. J. Biol. Chem., 1976. **251** : p. 7088-7094.
117. Valler, M.J. and Kay, J., *The interaction of aspartic proteinases with naturally-occurring inhibitors from actinomycetes and ascaris lumbricoides*. J. Enzyme Inhibition, 1985. **1** : p. 77-82.
118. Fuller, R.S., Brake, A., and Thorner, J., *Yeast prohormone processing enzyme (Kex2 gene product) is a Ca²⁺ dependent serine protease*. Proc. Natl. Acad. Sci., 1989. **86** : p. 1434-1438.
119. Fuller, R.S., Sterne, R.E., and Thorner, J., *Enzymes required for yeast prohormone processing*. Ann. Rev. Physiol., 1988. **50** : p. 345-362.

120. Thomas, G., Thorne, B.A., Thomas, L., Allen, R.G., Hruby, D.E., Fuller, R., and Thorner, J., *Yeast KEX2 endopeptidase correctly cleaves a neuroendocrine prohormone in mammalian cells*. Science, 1988. **241** : p. 226-228.